Effects of SEA0400 on Mutant NCX1.1 Na^+-Ca^{2+} Exchangers with Altered Ionic Regulation

A Thesis Presented to the University of Manitoba
In Partial Fulfillment of the Requirement
For the Degree of:

MASTERS OF SCIENCE IN PHYSIOLOGY

By
Markian Platon Choptiany

Department of Physiology
Faculty of Medicine

THE UNIVERSITY OF MANITOBA

FACULTY OF GRADUATE STUDIES

*****

COPYRIGHT PERMISSION PAGE

Effects of SEA0400 on Mutant NCX1.1 Na^+-Ca^{2+} Exchangers with Altered Ionic Regulation

BY

Markian Platon Choptiany

A Thesis/Practicum submitted to the Faculty of Graduate Studies of The University of Manitoba in partial fulfillment of the requirements of the degree of

MASTER OF SCIENCE

TABLE OF CONTENTS

TABLES AND FIGURES.....5

LIST OF ABBREVIATIONS.....8

I. ABSTRACT.....11

II. LITERATURE REVIEW.....14

1. Role of Na^+-Ca^{2+} Exchanger.....14

1.1. Excitation Contraction Coupling.....14

1.2. Forward Mode Na^+-Ca^{2+} Exchange.....19

1.3. Reverse Mode Na^+-Ca^{2+} Exchange.....21

2. Molecular Biology of the Na^+-Ca^{2+} Exchanger.....23

2.1. The Exchanger Superfamily.....23

2.2. Gene Structure.....26

2.3. Topology of the Na^+-Ca^{2+} Exchanger.....28

3. Transport Properties of Na^+-Ca^{2+} Exchange.....40

3.1. Electrogenicity and Stoichiometry.....40

3.2. Turnover Rates and Density.....44

3.3. Transport Mechanism.....46

4. Regulation of Na^+-Ca^{2+} Exchange.....52

4.1. Na^+-dependent Regulation (I_1).....52

4.2. Ca^{2+}-dependent Regulation (I_2).....54

4.3. pH.....57

4.4. Phosphorylation.....58

4.5. Further Regulators of Na^+-Ca^{2+} exchange.....63

5. Pharmacology of Na^+-Ca^{2+} Exchange.....64

5.1. Di-and Trivalent Cations.....65

5.2. Peptides.....67

5.3. Organic Inhibitors.....70

6. Na^+-Ca^{2+} Exchange and Cardiac Pathophysiology.....85

III. METHODS.....89

1. Preparation of *Xenopus laevis* Oocytes.....89

2. Synthesis of NCX1.1 cRNAs.....90

3. Preparation of Mutant NCX1.1 Exchangers.....90

4. Measurement of Exchange Activity.....92

IV. RESULTS.....100

1. SEA0400 and Na^+-Ca^{2+} Exchange Currents.....100

2. SEA0400 and Na^+-Ca^{2+} Exchange Regulatory Mechanisms (I_1 and I_2).....105

3. Effect of SEA0400 with Increasing Regulatory Ca^{2+}.....107

4. SEA0400 and Exchanger Recovery.....110

5. Effect of SEA0400 on Inward Na^{+}-Ca^{2+} Exchange.....112

6. NCX1.1 Mutant Exchangers.....114

7. Group 1 NCX1.1 Mutants (Outward Current).....116

8. Group 2 NCX1.1 Mutants (Outward Current).....119

9. Group 3 NCX1.1 Mutants (Outward Current).....122

10. F_{ss} and λ.....124

11. Group 1 NCX1.1 Mutants (Inward Exchange).....125

12. Group 2 and 3 Mutants (Inward Exchange).....129

V. DISCUSSION.....134

1. Transport Mode Selectivity.....134

2. SEA0400 and Ionic Regulatory Mechanisms.....136

3. SEA0400 and Mutant Na^{+}-Ca^{2+} exchangers.....139

4. Mutant Na^{+}-Ca^{2+} exchangers with altered I_1 (Outward Exchange).....140

5. Mutant Na^{+}-Ca^{2+} exchangers with altered I_2 (Outward Exchange).....141

6. Inward Mutant Na^{+}-Ca^{2+} Exchange (Group 1-3).....142

7. Peak vs. Steady State Inhibition.....143

8. Pathophysiological Implications.....143

VI. REFERENCES.....146

LIST OF TABLES AND FIGURES

Tables

1. The Exchanger Superfamily.....27
2. Effect of 0.1 μM SEA0400 on Peak and Steady State Outward Current in NCX1.1 and Mutant Na^+-Ca^{2+} Exchangers.....132
3. Effect of 0.1 μM SEA0400 on F_{ss} in NCX1.1 and Mutant Na^+-Ca^{2+} Exchangers.....132
4. Effect of 0.1 μM SEA0400 on λ in NCX1.1 and Mutant Na^+-Ca^{2+} Exchangers.....133
5. Effect of 0.1 μM SEA0400 on Steady State Inward Current in NCX1.1 and Mutant Na^+-Ca^{2+} Exchangers.....133

Figures

1. The role of the Na^+-Ca^{2+} exchanger in Excitation-Contraction Coupling.....16
2. Putative 3-Dimensional Arrangement of the Na^+-Ca^{2+} Exchanger.....33
3. Topology of the Na^+-Ca^{2+} Exchanger.....39
4. The Consecutive Eight-State Model for Na^+-Ca^{2+} Exchange.....48
5. Na^+-Dependent Inactivation (I_1).....51
6. Ca^{2+}-Dependent Regulation (I_2).....56
7. Chemical Structure of KB-R7943.....73

8. Chemical Structure of SEA0400.....82

9. The Giant, Excised Patch Technique.....94

10. Initiation of a Typical Outward (*i.e.*, Reverse Mode) Na^+-Ca^{2+} Exchange Current.....96

11. Initiation of a Typical Inward (*i.e.*, Forward Mode) Na^+-Ca^{2+} Exchange Current.....98

12. The Inhibitory Effects of SEA0400 on Combined Inward-Outward Na^+-Ca^{2+} Exchange Activity.....101

13. Concentration-Dependent Inhibition of Wild-Type NCX1.1 Outward Exchange Current with SEA0400.....104

14. Effects of SEA0400 on Outward Exchange Currents Following Proteolytic Treatment.....106

15. Effects of SEA0400 with Increasing Regulatory Ca^{2+} Concentrations.....109

16. Effects of SEA0400 on Exchanger Recovery.....111

17. Effects of SEA0400 on Inward Exchange Currents Following Proteolytic Treatment.....113

18. Electrophysiological Profiles of Wild-Type and NCX1.1 Mutants.....115

19. Effects of SEA0400 on Outward Na^+-Ca^{2+} Exchange Currents of Mutant NCX1.1 Exchangers Exhibiting Enhanced I_1 Inactivation.....118

20. Effects of SEA0400 on Outward Na^+-Ca^{2+} Exchange Currents of Mutant NCX1.1 Exchangers Exhibiting Suppressed I_1 Activity.....121

21. Effects of SEA0400 on Outward Na^+-Ca^{2+} Exchange Currents of a Mutant NCX1.1 Exchanger Exhibiting Altered I_1 and I_2 Regulation.....123

22. Effects of SEA0400 on Inward Na^+-Ca^{2+} Exchange Currents of Wild-Type NCX1.1 Exchangers.....126

23. Effects of SEA0400 on Inward Na^+-Ca^{2+} Exchange Currents of Mutant NCX1.1 Exchangers Exhibiting Enhanced I_1 Inactivation.....128

24. Effects of SEA0400 on Inward Na^+-Ca^{2+} Exchange Currents of Mutant NCX1.1 Exchangers Exhibiting Suppressed I_1 Inactivation.....130

25. Effects of SEA0400 on Inward Na^+-Ca^{2+} Exchange Currents of Mutant NCX1.1 Exchangers Exhibiting Altered I_1 and I_2 Regulation.....131

LIST OF ABBREVIATIONS

λ, rate of current decay

ARF, acute renal failure

BSA, bovine serum albumin

C, Cysteine

$Ca(NO_3)_2$, calcium nitrate

$CaCl_2$ calcium chloride

$CaCO_3$, calcium carbonate

CALX, *Drosophila melanogaster* Na^+-Ca^{2+} exchanger

CCCP, carbonyl cyanide m-chrolophenylhydrazone

CHX, Ca^{2+}-H^+ exchanger

CICR, Ca^{2+}-induced-Ca^{2+}-release

cRNA, complementary ribonucleic acid

cDNA, complementary deoxyribonucleic acid

CsOH, cesium hydroxide

DAD(s), delayed afterdepolarization(s)

DCB, (3',4'-dichlorobenzamil)

DPC, days post coitus

DMSO, dimethyl sulfoxide

E, Glutamic acid

EAD(s), early afterdepolarization(s)

EGTA, ethylene glycol-bis(β-aminoethyl ether)-N,N,N',N'-tetra-acetic acid

F, Phenylalanine

FMRF-amide, molluscan cardioexcitatory peptide

FRCRCF-amide, analogue of molluscan cardioexcitatory peptide

F_{SS}, fraction of steady state current remaining

G, Glycine

HEPES, (N-[2-hydroxyethyl]piperazine-N'-[2-ethanesulfonic acid])

I_1, Na^+-dependent inactivation

I_2, Ca^{2+}-dependent regulation

I_{K1}, inward rectifying potassium current

I_{TI}, transient inward current

I-V, current-voltage relationship

K, Lysine

K_2HPO_4, potassium phosphate

KB-R7943, (2-[2-[4-(4-nitrobenzyloxy)-phenyl]ethyl]isothiourea methesulfonate)

KCl, potassium chloride

KOH, potassium hydroxide

L, Leucine

LiOH, lithium hydroxide

MES, (2-[N-morpholino]ethanesulfonic acid

$Mg(OH)_2$, magnesium hydroxide

$MgSO_4$, magnesium sulfate

MOPS, (3-[N-morpholino]propanesulfonic acid)

myristyl-FRCRCF-amide, analogue of molluscan cardioexcitatory peptide

N, Asparagine

NaCl, sodium chloride

$NaHCO_3$, sodium bicarbonate

NCKX, Na^+-Ca^{2+}/K^+ exchanger

NCX, Na^+-Ca^{2+} exchanger

NMG-MES, N-methyl-D-glucamine-(2-[N-morpholino]ethanesulfonic acid

PI, phosphatidylinositol

PIP_2, phosphatidylinositol 4,5-bisphosphate

PKA, protein kinase A

PKC, protein kinase C

PMA, phorbol 12-myristate 13-acetate

Q, Glutamine

R, Arginine

RT, room temperature

SEA0400, (2-4[-[(2,5-difluorophenyl)methoxy]phenoxy]-5-ethoxyaniline)

SL, Sarcolemma(l)

SR, Sarcoplasmic Reticulum

T, Threonine

TEA-OH, tetraethylammonium hydroxide

TMS, transmembrane segment(s)

V, Valine

XIP, e*x*change *i*nhibitory *p*eptide

Y, Tyrosine

I. ABSTRACT

The plasmalemmal Na^+-Ca^{2+} exchanger protein plays an integral role in cardiac Ca^{2+} homeostasis. This unique protein allows for transsarcolemmal transport of Ca^{2+} across the cell membrane, in exchange for Na^+. Removal of virtually all Ca^{2+} entering through L-type Ca^{2+} channels occurs on a beat-to-beat basis, allowing for the maintenance of a proper resting $Ca^{2+}{}_i$ level. Calcium efflux occurs by removing Ca^{2+} in exchange for Na^+ and is known as forward mode exchange. As the direction of exchange transport is based on both electrical and chemical gradients, there exists the potential for drawing Ca^{2+} into the cell. Calcium entry via the exchanger is labelled reverse mode exchange and is implicated in both cardiac injury and disease. Both exchanger modes are the subjects of intense investigation, as their precise physiological roles are controversial.

Although the physiological role of Na^+-Ca^{2+} exchange in cardiac muscle is unclear, the current body of knowledge suggests it contributes to cellular relaxation (*i.e.,* forward mode) and cardiac pathophysiology (*i.e.,* reverse mode). Under various pathological settings, reverse mode exchange (*i.e.,* an elevated $Na^+{}_i$, promoting Ca^{2+} entry) may be favoured. Thus, the exchanger may participate in cellular "Ca^{2+} overload", creating a toxic intracellular environment. Toxicity via Ca^{2+} can eventually kill the cell through a variety of mechanisms (*i.e.,* protease activation). Having a selective, reverse mode exchange inhibitor (leaving forward mode (*i.e.,* Ca^{2+} removal) exchange unaffected) could prove most useful in the therapeutic setting. Hindering a detailed understanding of Na^+-Ca^{2+} exchange is the general lack of

selective and potent pharmacological agents. A few functional inhibitors, which were by-in-large weak, non-selective and potentially toxic (millimolar requirements for desired action) were described in the early 1990's. In 1996, a potent and reverse mode selective Na^+-Ca^{2+} exchange inhibitor, KB-R7943 (formerly No.7943) was described. However, as the results of KB-R7943 were presented, discrepancies over mode selectivity, site of action, and potency became apparent. In 2000, a new Na^+-Ca^{2+} exchange inhibitor was developed. SEA0400 was released as a the most potent and mode selective (preferential for reverse mode) inhibitor of Na^+-Ca^{2+} exchange ever produced. SEA0400 significantly inhibited reverse mode exchange and was without effect on forward mode exchange. This effect led to the search for its potential mechanism(s) of action. Previous work from our lab suggested that SEA0400 stabilizes or promotes the entry of Na^+-Ca^{2+} exchangers into a Na^+_i-dependent inactive state (I_1). Upon deregulation of the Na^+-Ca^{2+} exchanger with α-chymotrypsin, SEA0400's action was substantially reduced, suggesting an interaction/requirement of intact regulatory mechanisms for proper function. The two main regulatory mechanisms proposed to control the exchanger, are Na^+_i-dependent inactivation (I_1) and Ca^{2+}-dependent regulation (I_2). When deregulated (*i.e.*, α-chymotrypsin), the exchanger no longer exhibited I_1 and I_2 regulation. To differentiate between the regulatory mechanisms that guide SEA0400's inhibition, previously characterized Na^+-Ca^{2+} exchanger mutants with defined alterations in their ionic regulatory properties were implemented. Mutants were categorized into three groups; those with accelerated I_1 (F223E, K225Q), lacking I_1 (K229Q, Δ229-232), and lacking I_2 (Δ680-685). We then applied the giant, excised patch clamp technique

on *Xenopus laevis* oocytes expressing the cloned canine cardiac exchanger NCX1.1, and measured resulting inward and outward currents. To these currents, we applied SEA0400 and measured its effects. Using F223E, a mutant displaying strongly accelerated I_1 (Na^+_i-dependent inactivation), inhibition with SEA0400 was substantially increased. However, the second Group 1 mutant, K225Q, showed I_1 similar to that of wild-type. While, inhibition of K225Q with SEA0400 was comparable to that of wild-type. The first Group 2 mutant, K229Q, initially lacked I_1, yet upon SEA0400 application an I_1-like inactive state appeared. Conversely, with the larger Δ229-232 mutant, which lacked I_1, SEA0400 was virtually without effect. Lastly, Δ680-685 (the sole Group 3 mutant), lacked I_2 (Ca^{2+}_i-dependent regulation) and inhibition with SEA0400 paralleled that of wild-type (WT). These results suggest that I_1 plays an integral, if not essential role in SEA0400's inhibitory nature. As such, when I_1 is accelerated, SEA0400's effects are increased. Conversely, when I_1 is absent, SEA0400 appears ineffective. These results may provide an explanation for SEA0400's mode selectivity.

II. LITERATURE REVIEW

1. Role of Na^+-Ca^{2+} Exchanger

1.1. Excitation-Contraction Coupling

With every contraction and relaxation of the heart, intracellular Ca^{2+} concentration changes dramatically yet, for the most part, proper cardiac function is maintained. Through a series of pumps, channels, exchangers, and various signalling proteins, this order is upheld. Many factors that are so vital to internal cellular processes can ironically lead to organelle failure and eventually, cell death. For instance, in cardiac myocytes, Ca^{2+} is essential for cardiac contraction, yet at high levels it can become toxic to the cell's internal environment, thereby interrupting cellular processes and/or killing the cell. Roughly, per beat, the internal Ca^{2+} concentration increases ~ 100 fold (0.1-10 μM). Calcium must be removed in order to preserve proper cellular function and allow for complete myocyte relaxation. The cell has several well-documented methods of maintaining Ca^{2+} homeostasis.

A primary mechanism for removing Ca^{2+} from cardiac tissue is the Na^+-Ca^{2+} exchanger. In 1968, this ion transporter was initially identified in cardiac muscle (275). The exchanger's role is prominent in Calcium-Induced-Calcium-Release (CICR), a term used to describe the cellular process allowing for cardiac contraction (91; 92). During contraction initiation, Ca^{2+} travels down its favoured concentration gradient (into the cytoplasm), signals a further Ca^{2+} release, and thereby increases

Ca^{2+} levels high enough to activate myofilament interaction (29; 43; 55; 221). From here, various cellular processes allow for: i) resequestering of Ca^{2+} and ii) transsarcolemmal Ca^{2+} removal. In doing so, this allows for proper cellular relaxation and diastolic filling, in preparation for the next consecutive beat. Although this process may seem initially simple, it is quite intricate.

Excitation-Contraction Coupling

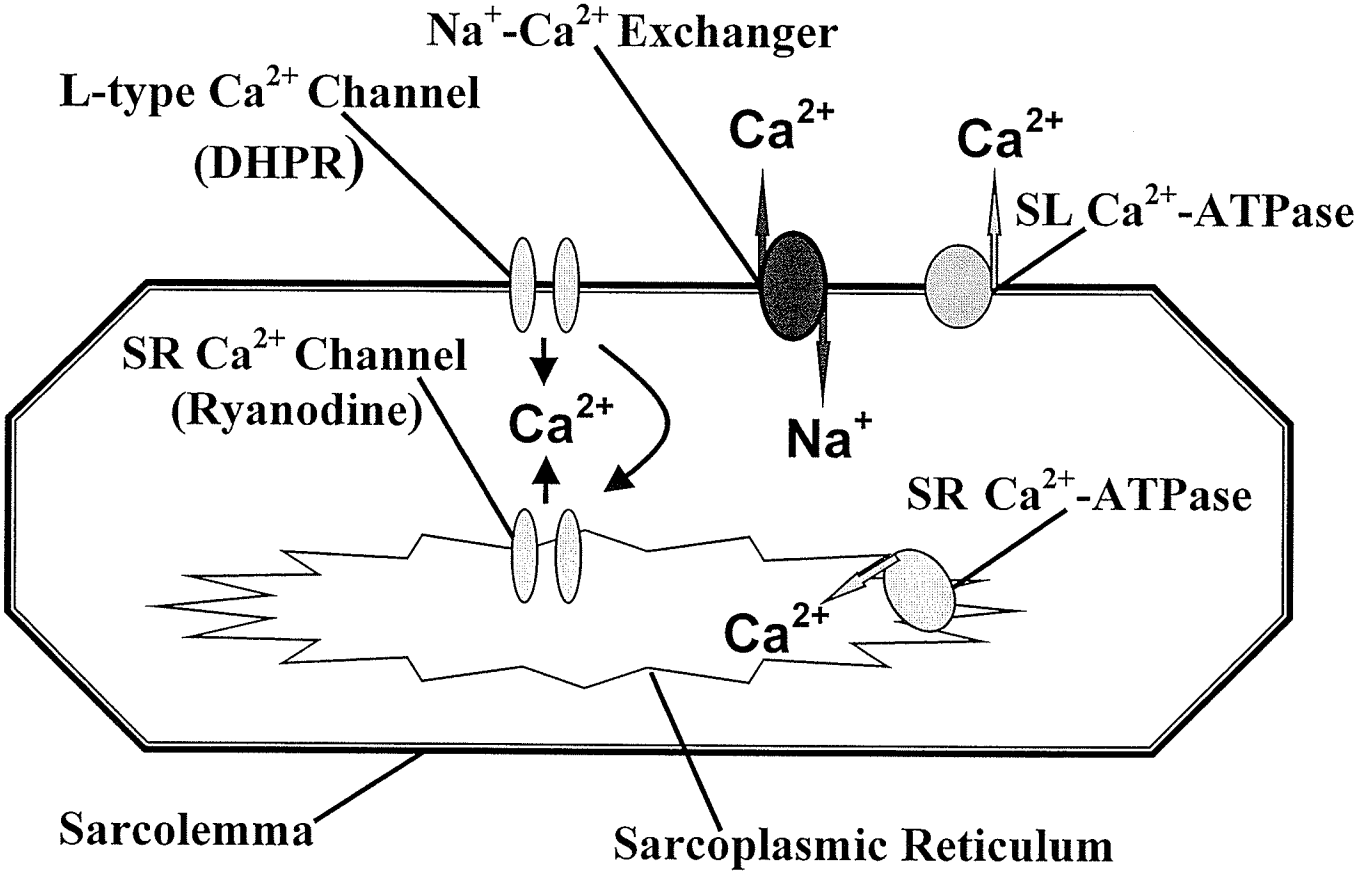

Figure 1. ***Excitation-Contraction Coupling of the Na^+-Ca^{2+} exchanger.*** This figure represents the interplay among Ca^{2+} transporters involved in regulating cardiac contraction and Calcium-Induced-Calcium-Release (CICR).

For every cardiac beat to occur, a wave of depolarization is deployed, stimulating a cascade of events. First, the depolarizing wave travels along the sarcolemma reaching voltage-gated L-type Ca^{2+} channels and in turn activates them. These channels open and Ca^{2+} flows into the cell. This quantity of Ca^{2+} is appropriately termed "trigger Ca^{2+}", for it binds to the nearby sarcoplasmic reticular (SR) ryanodine receptors, and "triggers" the SR to release its internal Ca^{2+} stores (29; 43; 55; 221). This large intracellular Ca^{2+} increase initiates contraction through cardiac myofilament interaction (29; 43; 55; 92). The location of various cellular proteins and structures (L-type Ca^{2+} channels, SR ryanodine receptors, and Na^{+}-Ca^{2+} exchangers) are biologically organized to allow maximum efficiency. For example, a close association between L-type Ca^{2+} channels (on T-tubule invaginations) and ryanodine receptors has been shown (50; 51; 279; 306). However, diseases such as hypertrophy and heart failure may occur when these receptors and channels are no longer in close proximity, hinting at the importance of cellular location (103). As cardiac contraction requires specific machinery, so does relaxation.

After contraction, myocyte internal Ca^{2+} is high (~10 μM) and must be restored to resting diastolic levels (100 nM) (18). This decrease in Ca^{2+} is crucial for maintaining healthy cells, allowing them to relax, and promote diastolic filling. There are three primary components involved in cytosolic Ca^{2+} removal: the SR Ca^{2+}-ATPase, Na^{+}-Ca^{2+} exchanger and the Sarcolemmal (SL) Ca^{2+}-ATPase. These mechanisms of Ca^{2+} extrusion have all been thoroughly reviewed (11; 19; 21; 36; 130; 237; 250). To start, the SR Ca^{2+}-ATPase is responsible for resequestering Ca^{2+} (activator Ca^{2+}) initially released from the SR upon stimulation. It is the primary

mechanism of intracellular Ca^{2+} removal, with reports on rabbit myocytes (133) and rabbit ventricular muscle (22), suggesting that it contributes to ~ 75 % of the relaxation process. The ATPase utilizes energy derived from ATP hydrolysis, in order to pump Ca^{2+} back into the SR, against a large concentration gradient (135). In addition, results of transgenic mice over expressing SR Ca^{2+}-ATPase show an alteration in myocardial contractility with an increase in relaxation (6). Conversely, from experiments where SR Ca^{2+}-ATPase was functionally removed (245), a defect in relaxation was shown. Both over expression and functional SR Ca^{2+}-ATPase removal show this protein's significance in contributing to proper cardiac relaxation.

The second ATPase involved in Ca^{2+} removal is the sarcolemmal (SL) Ca^{2+}-ATPase. Although a transmembrane Ca^{2+} removal mechanism, its role in cardiac relaxation remains quite ambiguous. It is thought to contribute minimally to Ca^{2+} removal (18; 330). For example, experiments having SL Ca^{2+}-ATPase as the single Ca^{2+} extrusion mechanism, demonstrated a massive decrease in relaxation rate (~ 1200%) compared to cells with intact mechanisms (22). Yet, there are increasing reports suggesting otherwise (13; 14; 54). Studies implementing carboxeosin, a SL Ca^{2+}-ATPase inhibitor, show the Ca^{2+}-ATPase to contribute 24%-45% of total membrane Ca^{2+} efflux (54; 237; 320). Furthermore, in 1999, a report demonstrated in rat ventricular myocytes lacking SR Ca^{2+}-ATPase, that Ca^{2+} efflux via the SL Ca^{2+}-ATPase was higher than previously reported (54). However, even a two-fold over-expression of SL Ca^{2+}-ATPase in transgenic rats, showed no substantial effect on cardiac function (106). Lastly, findings with the plasmalemmal Ca^{2+} pump absent, reported no change in cytoplasmic Ca^{2+} levels, further suggesting this pumps effects

are negligible (46). Functional importance of the Ca^{2+} pump has been suggested as a species dependent characteristic, wherein ferret ventricular muscle, the SL Ca^{2+}-ATPase was shown to have comparative level of importance to the Na^{+}-Ca^{2+} exchanger (14; 19). Although a specific physiological role of SL Ca^{2+}-ATPase is not yet established, it is generally agreed upon that its contribution during relaxation is minimal and may only serve to perform minute alterations of resting Ca^{2+} levels. Even if the SL Ca^{2+}-ATPase does contribute to Ca^{2+} efflux to a greater degree than currently reported, its transport rate is much too slow to be effective (*i.e.,* 15-30 times slower than Na^{+}-Ca^{2+} exchange) (21). This leaves Na^{+}-Ca^{2+} exchange as the major pathway for plasmalemmal Ca^{2+} extrusion, contributing to cardiac relaxation.

1.2. Forward Mode Na^{+}-Ca^{2+} Exchange

Effective Ca^{2+} homeostasis is paramount for cardiac function. In short, any Ca^{2+} that enters a cell must be removed. If this delicate balance is not met over time, numerous cardiac dysfunctions will result. As stated previously, during contraction, Ca^{2+} enters through L-type Ca^{2+} channels and further stimulates Ca^{2+} release from the SR (CICR). SR Ca^{2+} is then resequestered via the SR Ca^{2+}-ATPase, leaving the Na^{+}-Ca^{2+} exchanger to deal with the remaining Ca^{2+} (initially brought in through the L-type Ca^{2+} channels). Thus, Ca^{2+} removed by the Na^{+}-Ca^{2+} exchanger must precisely balance L-type Ca^{2+} channel Ca^{2+} brought in. Removing Ca^{2+} in exchange for Na^{+} is known as forward mode exchange (*i.e.,* Ca^{2+} efflux) (11; 19; 21; 36; 44; 130; 237; 250). It is essential that Ca^{2+} influx and efflux be matched. While the SR and the

mitochondria (sites of Ca^{2+} storage) can uptake Ca^{2+}, they only have limited capacities for storage, leaving the Na^{+}-Ca^{2+} exchanger as the last mechanism to withdraw any residual Ca^{2+}. Several studies have shown the Na^{+}-Ca^{2+} exchanger to play a powerful role in maintaining this balance between Ca^{2+} influx and efflux. An example of such was the 1975 study by Bridge *et al.*, that measured Ca^{2+} efflux via the Na^{+}-Ca^{2+} exchanger matching that of the inward L-type Ca^{2+} current (assuming a 3:1 stoichiometry) (41). Further studies by Niggli and Lederer, using flash photolysis and "caged Ca^{2+}", found a significant parallel between current amplitudes from Na^{+}-Ca^{2+} exchange and L-type Ca^{2+} channels (233). Lastly, caffeine-induced and rapid cooling contractions were used to quantify SR Ca^{2+} and showed a significant role for Na^{+}-Ca^{2+} exchange in Ca^{2+} removal (23; 40; 133). Ca^{2+} entry can be quite varied physiologically (*i.e.,* by changes in frequency, Ca^{2+} levels, and adrenergic stimulation) and pharmacologically (*i.e.,* dyhydropyridines (negative), and adrenergic compounds (positive)) (20; 26; 246). This is a crucial function of the Na^{+}-Ca^{2+} exchanger, for cardiac myocytes have a low tolerance to Ca^{2+} imbalance. However, as with other cellular proteins, different species and stages of development may vary exchanger function (36).

Compared to adult rat and rabbit hearts, newborn rat and fetal rabbit hearts appeared to have a six to eight-fold greater expression in Na^{+}-Ca^{2+} exchangers (38). It was proposed that Na^{+}-Ca^{2+} exchange constitutes the majority of Ca^{2+} removal in these underdeveloped hearts. These hearts lack plasmalemmal invaginations, known as T-tubules, and a fully formed SR. Although results are derived from an underdeveloped organism, they strengthen the significance of Na^{+}-

Ca^{2+} exchange, whether in fetal development or in mature adults. Since the exchanger's transport mode depends on electrical and chemical gradients, it has the potential to reverse directions. Thus, in theory, the Na^{+}-Ca^{2+} exchanger could contribute to systole as it does in diastole (11; 44; 237). This topic is currently contentious and has serious implications regarding the physiological and pathophysiological role(s) of the Na^{+}-Ca^{2+} exchanger.

1.3. Reverse Mode Na^{+}-Ca^{2+} Exchange

Understanding a physiological role for Ca^{2+} entry (*i.e.*, reverse mode) via the Na^{+}-Ca^{2+} exchanger has been an ongoing process. It is suggested that Ca^{2+} entry through this protein can parallel the effects of "trigger Ca^{2+}" from the L-type Ca^{2+} channels, and initiate Calcium-Induced-Calcium-Release from the SR (24; 128) but there are also those that see no such result (39; 90). During the action potential upstroke, submembrane Na^{+} levels could initiate reverse mode Na^{+}-Ca^{2+} exchange but Ca^{2+} from the L-type Ca^{2+} channels increase cytoplasmic Ca^{2+} and reduces the drive for Ca^{2+} entry (11; 36). Not only is the drive for reverse mode exchange (Ca^{2+} influx) reduced, but the amount of Ca^{2+} entering through the Na^{+}-Ca^{2+} exchanger is marginal compared to that of L-type Ca^{2+} channels (292; 299). Nonetheless, reverse mode Na^{+}-Ca^{2+} exchange has been used to explain the positive inotropic effects of cardiac glycosides (34; 35; 187).

The positive inotropic effects of cardiac glycosides (digoxin, digitoxin, and ouabain) are well known. They block the Na^{+}-K^{+}-ATPase (enzymatic portion of the Na^{+} pump), allowing for an elevation of intracellular Na^{+} levels (~ 1-2 mM) (268).

This intracellular Na^+ increase promotes reverse mode Na^+-Ca^{2+} exchange, bringing Ca^{2+} into the cell, thereby stimulating SR Ca^{2+} release channels. The elevated levels of cytoplasmic Ca^{2+}, leads to greater SR Ca^{2+} loading, Ca^{2+} release and contraction. Yet, unlike the rapid increase of intracellular Ca^{2+} due to L-type Ca^{2+} channels, influx through reverse mode Na^+-Ca^{2+} exchange is slow (200). On a beat-to-beat basis, reverse mode Ca^{2+} influx, activating Ca^{2+}-induced-Ca^{2+}-release (CICR), is thought by some to be unlikely (39; 45).

It has also been proposed that the influx of Na^+ upon depolarization may be enough to accumulate near the membrane and stimulate reverse mode exchange. This would bring Ca^{2+} into the cell and stimulate Ca^{2+}-induced-Ca^{2+}-release (CICR) (181). There are several reasons why this idea may be problematic. First, an intracellular Na^+ concentration required to initiate reverse mode exchange does not occur under physiological conditions (but does in the experimental setting) (130). Secondly, this would imply that the SR was over-sensitive and spontaneously releases Ca^{2+} every instance Ca^{2+} concentration fluxed (39; 90; 221; 292; 293; 298; 299). However, certain adrenergic interactions with the voltage-dependent Na^+ channels may result in a phenomenon termed "Slip Mode conductance". Here, Ca^{2+} and Na^+ enter via voltage-gated Na^+ channels upon depolarization. Ca^{2+} entry here *is* sufficient to initiate Ca^{2+}-induced-Ca^{2+}-release (CICR).

If we consider the location of membrane proteins once more, we continue to find discrepancies. Ideally, for CICR, Na^+-Ca^{2+} exchangers should be in close proximity to the SR, such that they can act on ryanodine receptors efficiently. Certain reports localize the exchanger along T-tubules (96), while others describe exchanger

positioning as being uniformly placed along the sarcolemma (48; 160). If a uniform distribution of the exchanger exists, then the probability of reverse mode Na^+-Ca^{2+} exchange having an effect on the SR would be low. Reverse mode Na^+-Ca^{2+} exchange has been proposed to modify the efficacy of L-type Ca^{2+} channels with respect to CICR (12; 17). This mechanism, if possible, implies the Na^+-Ca^{2+} exchanger could increase SR Ca^{2+} release and thereby, increase SR Ca^{2+} content (load) (198; 335). Most recently, a report by Thomas *et al.*, using a novel Na^+-Ca^{2+} exchange antibody, combined with confocal microscopy (CLSM), found that immunoreactivity is strongly expressed throughout the SL surface and intercalated disk regions with sporadic labelling of the vertical transverse T-tubules but not the longitudinal T-tubules (313). Using normal and detubulated rat cardiomyocytes they suggested that the exchanger has multiple functions depending upon membrane location such as; CICR modulation, SR Ca^{2+} load, and resting Ca^{2+} levels (313).

2. Molecular Biology of the Na^+-Ca^{2+} Exchanger

2.1. The Exchanger Superfamily

From the initial cloning of the canine cardiac Na^+-Ca^{2+} exchanger NCX1.1 (cDNA) in 1990 by the Philipson group, a large group of related proteins have emerged (227). This is now collectively known as the exchanger superfamily. It is a group of Na^+-Ca^{2+} exchangers and related proteins (227). Most of these proteins have been identified through BLAST and PSI-BLAST searches of the GenBank database (2). Many of these isolated proteins' function and significance are not known.

However, based on the sequence homology of other well-documented proteins, many of these homologous proteins are predicted to be membrane transporters. Based on hydrophobicity plots, every exchanger superfamily protein is found to have a conserved Calx-α motif and contain membrane-spanning regions (36; 130; 250). As reviewed by Philipson and Nicoll in 2000 (250), the exchanger superfamily has been divided into four categories: (1) NCKX family; (2) Bacterial family; (3) CHX family; (4) NCX family (Table 1).

2.1.1. The NCKX Family

The NCKX, has a similar homology to the Na^+-Ca^{2+}-K^+ exchanger cloned from bovine rod photoreceptors. It is also however, found in neural tissue (316). The family consists of three mammalian NCKX exchangers, NCKX1 (273), NCKX2 (316), NCKX3 (174), six from *Caenoorhabditis elegans*, one from *Schizosaccharomyces pombe*, and one from *Arabidopsis thaliana*. The cloned mammalian exchanger NCKX1 has a stoichiometry of 4 Na^+: 1 Ca^{2+}: 1 K^+, with a requirement of K^+ co-transport for all members (285; 286). This is the primary feature that separates them functionally from the NCX exchangers. Each exchanger has sequence similarity, a pair of Calx-α motifs, and a large intracellular loop.

2.1.2. The Bacterial Family

Although they constitute nine members of the superfamily, very little is actually known about this unique group. This exchanger family lacks the large intracellular loop and therefore, has a dramatically reduced exchanger size (~ 400

residues compared to those of NCX and NCKX; ~ 900 residues). Their primary point of homology is through the Calx-α motifs of each family member (263).

2.1.3. The CHX Family

This family consists of only a few members presently. CHX antiporters are believed to transport Ca^{2+} in exchange for H^{+}. *Escherichia coli* (136), *Sacchraomyces cerevisiae* (63), and *Arabidopsis thaliana* (126) all produce CHX exchangers.

2.1.4. The NCX Family

The most extensively studied and documented exchangers are found in this family. This is primarily due to cloning of the canine cardiac isoform NCX1.1 by Nicoll *et al.* (227). There are three mammalian exchangers: NCX1 (227), NCX2 (192), and NCX3 (230). The NCX1 gene is widely expressed in a variety of cells (*i.e.,* cardiac muscle, skeletal muscle, smooth muscle, neurons, astrocytes, kidney, lung and spleen (265). NCX2 and NCX3 are only found in brain and skeletal muscle (192; 265). These genes have similar hydropathy analysis results, suggesting a similar structure. They also appear to have functional similarity (36; 194). Genes sharing homology with NCX1 have been characterized by comparing to various mammalian species such as: humans (168; 170), rabbit (169), bovine tissue (1), guinea pig (317), mouse (163), and rat (100). In addition, there are exchangers isolated from non-mammalian species such as *Loligo opalescens*, squid exchanger NCX-SQ1 (114) and from the fruit fly, *Drosophila melanogaster*, CALX (131; 277;

290). These exchangers all have tight sequence similarity and analogous function. Other non-mammalian species include two proteins isolated from *Caenorhabditis elegans* (nematode) that share homology to various NCX proteins (331) and one from *Xenopus* species (146).

2.2. Gene Structure

NCX1, NCX2, and NCX3 are located on human chromosomes 2p21-23 (295), 19q13.2 (192), and 14q21-31 (230), respectively. The intron/exon structure of NCX1 has been characterized with respect to its organization on the gene (169; 173). The NCX1 gene runs more than 200 kb (169; 172; 173) and contains 12 exons, with the majority of the gene being coded in one exon of 1.8 kb. Also, each gene has a 5`-end alternatively spliced region prior to the open reading frame (184), which most likely contributes to regulating the expression of different isoforms. These regions are labelled as "tissue-specific" promoters. Recently, in 1999, the Philipson and Menick groups revealed that cardiac specific expression is regulated by a promoter region of roughly 200 bp (containing a GATA transcriptional element), a CarG element and by an E-box (49; 224). The gene is also regulated by β-adrenergic stimulation (102).

Table 1. ***The Exchanger Superfamily.*** The Exchanger Superfamily consists of four families: (1) the Na^+-Ca^{2+} exchanger (NCX) family, (2) the Na^+-Ca^{2+}/K^+ exchanger (NCKX) family, (3) the Bacterial family, and (4) the Ca^{2+}-H^+ exchanger (CHX) family. Listed below are known genes and the species from which the gene originated (Adapted from Philipson and Nicoll (10)).

FAMILY	SPECIES	GENE
NCX	*Canis* sp.	NCX1
	Rattus norvegicus	NCX2
	R. norvegicus	NCX3
	Drosophila melanogaster	Calx
	Loligo opalescens	NCX-SQ1
	Caenorhabditis elegans	CEJ001181
	C. elegans	CENACAEX
	Arabidopsis thaliana	ATAC002535
NCKX	*Bos Taurus*	NCKX1
	Rattus norvegicus	NCKX2
	R. norvegicus	NCKX3
	Caenorhabditis elegans	CEF35C12
	C. elegans	CEC35A5
	Schizosaccharmoyces pombe	SPZC3A12.06c
	Arabidopsis thaliana	AC0001061
	Caenorhabditis elegans	C13D9.7
	C. elegans	C13D9.8
	C. elegans	C07A9.11
	C. elegans	C07A9.4
Bacterial	*Esherichia coli*	YRBG ECOLI
	Treponema pallidum	TP1034
	Synechosystis sp.	
	Aquifex aeolicus	aq 066
	Borrelia burgdorferi	BB0164
	Pyrococcus horikoshii	PH0473
	Methanococcus jannaschii	MJ0091
	M. thermoautotrophicum	MTH1155
	M. thermoautotrophicum	MTH1073
CHX	*Saccharomyces cerevisiae*	VCX1
	Arabidopsis thaliana	AF049236

2.3. *Topology of the Na^+-Ca^{2+} Exchanger NCX1.1*

Since the cloning of NCX1.1 from canine cardiac cDNA, there have been many advances in the Na^+-Ca^{2+} exchange field (227). Initially, studies from mammalian cardiac sarcolemmal vesicles, measuring Na^+-Ca^{2+} exchange transport revealed electrogenic movement of Na^+ and Ca^{2+} with a 3:1 stoichiometry (27; 47; 257; 271; 272). These results were followed by protein purification work (249) that allowed for the initiation of NCX1.1 cloning (227). Nicoll *et al.* (227) reported polypeptides with molecular masses of 70, 120, and 160 kDa (249). Upon establishing polyclonal antibodies for these peptides, they were used to screen a cardiac expression library. Continuing, Nicoll *et al.* then cloned a sequence for a peptide that reacted with the polyclonal antibodies, and this was used to further identify the entire clone. From here, cRNA was produced and injected into the *Xenopus* oocyte expression system. Proper Na^+-Ca^{2+} exchanger expression was measured *via* giant, excised patch clamping and compared to a control of water-injected oocytes. Na^+_i-dependent Ca^{2+} influx could be measured in cRNA injected oocytes but not in the control oocytes (water-injected) (227). This demonstrated that the exchanger clone was complete, reliable, and displayed proper exchanger functions.

Initial molecular weight estimates for NCX1.1 ranged between 33 kD – 82 kD (105; 199). However, once the exchanger was cloned in 1990 (227), it revealed a full length NCX1.1 cDNA, with a reading frame of 2910 nucleotides. These nucleotides ultimately create a 970 amino acid protein weighing approximately 108 kD (227). Initially, the Philipson group modeled the exchanger as having twelve membrane

spanning segments with a large hydrophobic loop between segment 6 and 7 (labelled loop f) (227).

Essentially this cytoplasmic loop broke the exchanger into two segments. One segment contained TMS 1-6, and the other contained the remaining TMS 7-12. These results were based on hydropathy analysis (133). They also noted 6 potential N-linked glycosylation sites, and a potential phosphorylation site (227). However, in the native canine exchanger, only a single site at position 9 of the N-terminus (Asn-9) is glycosylated (81; 132; 229). Glycosylation of the exchanger appears to have no effect on the exchanger's functionality (132). Identification of potential glycosylation sites helps determine the exchanger's orientation, because amino acid glycosylation implies an extracellular location for that particular residue (36; 130). Furthermore, a would-be cleavable NH_2-terminal signal (171) and an amino acid segment resembling a calmodulin-binding domain (later known as the XIP region (193)) were reported (227). This potential cleavage site (between amino acid 32 and 33) was of interest for several reasons. Firstly, it appeared to be the start of the protein sequence and secondly, most membrane exchangers lack these sites (81). However, removing the cleavage site or deleting the signal sequence did not prevent proper membrane insertion (99; 278). A similar site was shown in both brain (192) and rod photoreceptors (273). Upon discovery of the signal sequence and through glycosylation studies, the exchanger was labelled to have 11 TMS: TMS 1-5 on the N-terminus and TMS 6-11 on the C-terminus. Later, more refined protocols, such as cysteine substitution, mutagenesis, and epitope tagging (61; 139; 228) narrowed down the TMS number to 9 (139; 228). After refining the number of TMS's, further changes were made in the exchanger's topology. For instance,

the large hydrophobic intracellular loop (loop f) was now situated between TMS 5 and 6 (228). In addition, short amino acid sequences known as Calx-α motifs (α-1 and α-2 repeats) were found to exist between TMS 2-3 (α-1) and TMS 7-8 (α-2) (139; 228). Moreover, they appeared on opposite sides of the membrane (228). TMS 6 was moved into the cytoplasmic loop f, while TMS 9 (part of α-2) was found to form a "P-loop", or re-entrant loop that terminated in the cytoplasm.

The Na^+-Ca^{2+} exchanger works as a monomer and can function properly when in a heterologous expression system (*i.e., Xenopus*) (115; 117; 122). Conversely, it has been suggested that the exchanger can function in a shortened form (lacking six C-terminal TMS) (101; 191). This gave rise to the idea that the exchanger becomes functional through dimerization. Another truncated exchanger, lacking 30 amino acids from the C-terminus, was isolated from the BALB/c mouse heart (294). The deletion is thought to occur through an early termination site. However, Ottolia *et al.* demonstrated compelling data on evenly divided exchangers ("split exchanger") expressed individually or together. They found that co-expression of both domains is required for membrane targeting and functional exchange activity (243).

Although attempts are being made to crystallize the Na^+-Ca^{2+} exchanger, an exact 3-D model is not yet available. Using cysteine susceptibility analysis and epitope tagging, Iwamoto *et al.* attempted to further characterize exchanger topology (139). This technique revealed that TMS 3 and 7 are in close proximity intracellularly, while TMS 2 and 8 are associated on the extracellular surface. These results suggest a role for TMS's and Calx-α motifs in ion translocation.

2.3.1. The Calx-α Motifs (α-1 and α-2)

In 1997, the fruit fly (*Drosophila melanogaster*) Na^+-Ca^{2+} exchanger was cloned and termed CALX (277; 290). This gene shares a >50% structural homology with the NCX family (NCX1, NCX2 and NCX3) and has a similar transport function (82; 131; 240). The CALX protein contains two motifs comprised of ~ 40 amino acids each. They are termed Calx-α motifs and are conserved in every member of the NCX family (290) and in the mammalian and *Drosophila* NCKX exchangers (110; 316). These motifs, also known as α-1 and α-2 repeats, are suggested to reside in close proximity but with opposite orientations.

When site-specific mutations were made to residues in the Calx-α repeats, the result was a significant alteration in exchanger transport properties (226). The degree of change ranged from a subtle variation to complete transport alleviation (226). For example, a study that substituted carboxyl/hydroxyl containing amino acids in TMS 2, 3, and 7 (part of the Calx-α motifs), found a decrease or elimination of $^{45}Ca^{2+}$ uptake in a *Xenopus* expression system (226). Mutations of conserved glycine residues; Gly138 (between TMS 2-3) and Gly837 (between TMS 7-8), shifted the exchanger I-V relationship. Further experiments were conducted in the hopes of tying Calx-α motifs to ion translocation. The Philipson group showed that in TMS 2, mutation of Asp101 to cysteine (N101C) removed the exchanger's cytoplasmic Na^+ regulation, while mutating threonine (T103C or T103V), increased the exchanger's affinity for cytoplasmic Na^+ (also allowing Li^+ transport) (78). Iwamoto *et al.* further strengthened the role of Calx-α motifs through the use of chimeric exchangers between NCX1 and NCX3 (143). Using a

Ni^{2+} sensitive property of wild-type Na^{+}-Ca^{2+} exchange, they were able to mimic and compare to native exchanger function using chimeras containing amino acid mutations (substitutions) in the α-1 and α-2 repeats (143). This suggested the importance of these regions in exchange properties. The same group, a year later, examined the properties of a proposed selective Na^{+}-Ca^{2+} exchange inhibitor, KB-R7943 (discussed later on). Their findings suggested that drug selectivity between the exchanger NCX family may be a result of several residues in the α-2 repeat (138). Specifically, it was shown through cysteine-scanning mutagenesis of the NCX1 α-2 repeat, a single residue, Gly833, resulted in a ≥ 30-fold *reduction* in KB-R7943 sensitivity (143). These results offer solid evidence indicating the motifs play a primary role in the ion translocation pathway and may be involved in drug inhibition (α-2 repeat) (138).

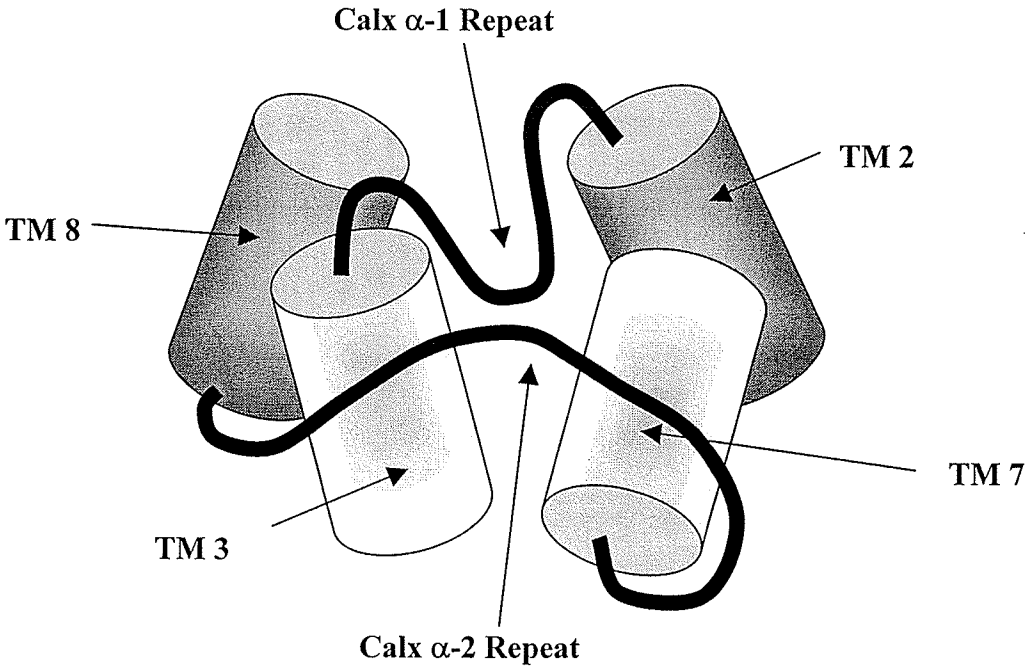

Figure 3. ***Putative 3-Dimensional Arrangement of the Na^{+}-Ca^{2+} Exchanger.*** The 3-dimensional topology of the transmembrane segments (TMS) comprising the Calx α-motifs currently are modeled to be oppositely oriented, possibly forming the ion translocation pathway (Adapted from Qui *et al.* (264)).

2.3.2. The Intracellular Loop

The large hydrophilic loop (initially termed loop f) is localized in the cytoplasm (227). It lies between TMS 5 and 6, and contains approximately 550 amino acids, most of which are not required for transport function (211). For instance, a mutant exchanger that lacked nearly the entire loop (Δ240-679) displayed normal transport/exchange activity (211). However, the intracellular loop is thought to be involved in exchanger regulation (210; 211) through intracellular Na^+, Ca^{2+}, H^+, and various kinases (76; 140; 211). This suggests that either the entire loop or a portion of it is necessary for regulation. Furthermore, exchangers subjected to proteolytic enzyme treatment (α-chymotrypsin), displayed similar results to that of the mutant (Δ240-679) exchanger lacking an intracellular loop. As with the previous regulatory experiments, the exchanger maintains proper exchange function but lacks regulation (211). The long intracellular loop comprises more than 50% of the exchanger's mass and is therefore, most likely to contribute to exchanger function and maintenance. There are to date, several key regions within the intracellular loop, and these are discussed below.

2.3.2.1. The Exchange Inhibitory Peptide Region (XIP)

A small 20 amino acid sequence of dispersed basic (positively charged) and hydrophobic residues (XIP; RRLLFYKYVYKRYRAGKQRG) occurring just off TMS 5 in the intracellular loop is called the XIP region (193; 227). It is also known as the endogenous XIP region. This unique sequence of amino acids was initially identified for

having homology to a calmodulin-binding domain (227). Li *et al.* later characterized this segment as the XIP peptide (193). It is postulated that the XIP region contributes to exchanger regulation (autoregulation or autoinhibition) (193; 227). Several groups tested the hypothesis through the use of site-directed mutagenesis (deletion and substitution) and revealed that a form of Na^+-dependent regulation could be removed (Δ229-232) or accelerated (F223E) upon residue alteration (209). Another group found that by mutating this region (XIP-4YW), they could remove Na^+-dependent regulation (244). More so, mutants lacking Na^+-dependent regulation were also insensitive to the effects of known regulators such as ATP, PIP_2, and PIP_2 antibody (112). A study by Pan *et al.* showed that these XIP mutants were insensitive to the removal of ATP (removal normally inhibits the exchanger) or to activation via phorbol esters (244). Although these exchangers maintained transport function, they could not be regulated. Just as the endogenous XIP region can exert regulatory effects, so can an exogenous form of XIP, otherwise known as the XIP peptide (193). Philipson and collaborators used a fabricated peptide with the exact 20 amino acid sequence of the original endogenous XIP region. When applied cytoplasmically to giant, excised patches from *Xenopus* oocytes, the XIP peptide completely inhibited reverse mode Na^+-Ca^{2+} exchange (IC_{50} ~ 0.1 μM) (193). The Philipson group also measured the effects of modified XIP peptides on $^{45}Ca^{2+}$ uptake in Na^+ loaded cardiac sarcolemmal vesicles. Ultimately, it was found that a fully intact XIP peptide was required for maximum potency. Furthermore, this study revealed that the major inhibitory region of XIP occurs between amino acids 5 and 16, with basic and aromatic residues constituting the most important inhibitory components (113). Changes in these amino acids drastically alter the inhibitory effects of XIP peptide (113). Current

results, using a novel Na^+-Ca^{2+} exchange inhibitor (SEA0400), are presented in the following pages and stress the importance of this small but vital region.

2.3.2.2. Regulatory Ca^{2+} Binding Region

The large intracellular loop is associated with regulation (ionic regulation via the XIP region) but other regions have been probed in the hopes of isolating further regulatory segments (193; 209). A technique known as $^{45}Ca^{2+}$ overlay was implemented on canine NCX1.1. Using fusion proteins representing various portions of the intracellular loop, they measured binding of radioactive $^{45}Ca^{2+}$. Ultimately, a 138 amino acid stretch (371-508) was isolated and characterized as the Ca^{2+} binding domain (188). In this region, there are two highly conserved portions, each containing three consecutive aspartic residues (188). Normal co-operative binding of Ca^{2+} with a range of 0.3 to 3 μM, was significantly diminished when these aspartic acid residues were mutated (188). Applying a giant, excised patch clamp identified four specific aspartic acid residues (447, 448, 498, and 500) that are responsible for a decrease in the domain's affinity for regulatory Ca^{2+}. Interestingly, this high affinity Ca^{2+} binding region is highly conserved among Na^+-Ca^{2+} exchangers, and functional Ca^{2+} regulation has been shown for NCX1, NCX2, and NCX3 (194). However, in the *Drosophila* exchanger, CALX, Ca^{2+} regulation is opposite to that of NCX1. In NCX1, Ca^{2+} stimulates exchange, whereas in CALX, Ca^{2+} inhibits exchange. The internal characteristics of these two exchangers prove to be interesting, for their Ca^{2+} regulatory regions appear to have an analogous

function (179). Further investigation into this regulatory mechanism could provide a better understanding of this important component.

2.3.2.3. Calx-β Motifs

On the intracellular loop is a pair of Calx-β motifs that were first identified on the *Drosophila* exchanger, like the Calx-α motifs (290). These highly conserved segments span ~ 70 amino acids. The first Calx-β motif is closely associated with the regulatory Ca^{2+} binding site, near the loop's N-terminus. The second Calx-β motif, located near the C-terminus of the Ca^{2+} regulatory site, is thought to fold and interact with the regulatory Ca^{2+} region. Levitsky *et al.* ran an SDS-PAGE gel and found that Ca^{2+} binding to fusion proteins stimulated a large mobility shift (188). A potential folding and protecting of the regulatory Ca^{2+} binding domain could be a possible explanation for this result.

2.3.2.4. The Alternative Splice Site

The Na^{+}-Ca^{2+} exchanger is located in various tissues, but is particularily prominent in heart, nerve and kidney cells (96; 160; 202). However, as shown by Omelchenko *et al.*, Ca^{2+} signaling and handling are different in each (83; 241). Their primary differences occur because they are tissue-specific isoforms of NCX1. These isoforms arise from an alternative splice site situated near the C-terminus of the large intracellular loop. In NCX1, this region is encoded by six cassette exons; A-F, of which

exon A and B never appear together in the same isoform. The last 4 exons can appear in different combinations for remaining splice variants. Variants containing exon A are usually located in excitable tissues, such as brain, skeletal and cardiac muscle (265). Variants containing the B exon are found in the remaining tissues (*e.g.,* kidney, lung, and smooth muscle. There are 32 potential splice variants, however only 12 have been identified (162; 169; 184; 265; 324). The existence of these tissue specific variants may imply specific roles in varying cellular systems. For example, NCX1.4 (AD exon; Brain) is regulated by protein kinase A (PKA) whereas NCX1.3 (AB exon; Kidney) is not (111; 276). As mentioned previously, Ca^{2+} signaling and ionic regulation is varied with different isoforms, especially in cardiac (NCX1.1), kidney (NCX1.3), and brain (NCX1.4) when tested via giant, excised patch clamping (83). Through these experiments, it appears that the presence of either exon A or B contributes to these differences. The *Drosophila* exchanger, CALX, contains two splice variants (CALX1.1 and CALX1.2), in a region consistent with the mammalian NCX (240; 277). A deeper investigation of the properties that govern regulation of Na^{+}-Ca^{2+} exchanger splice variants must be conducted.

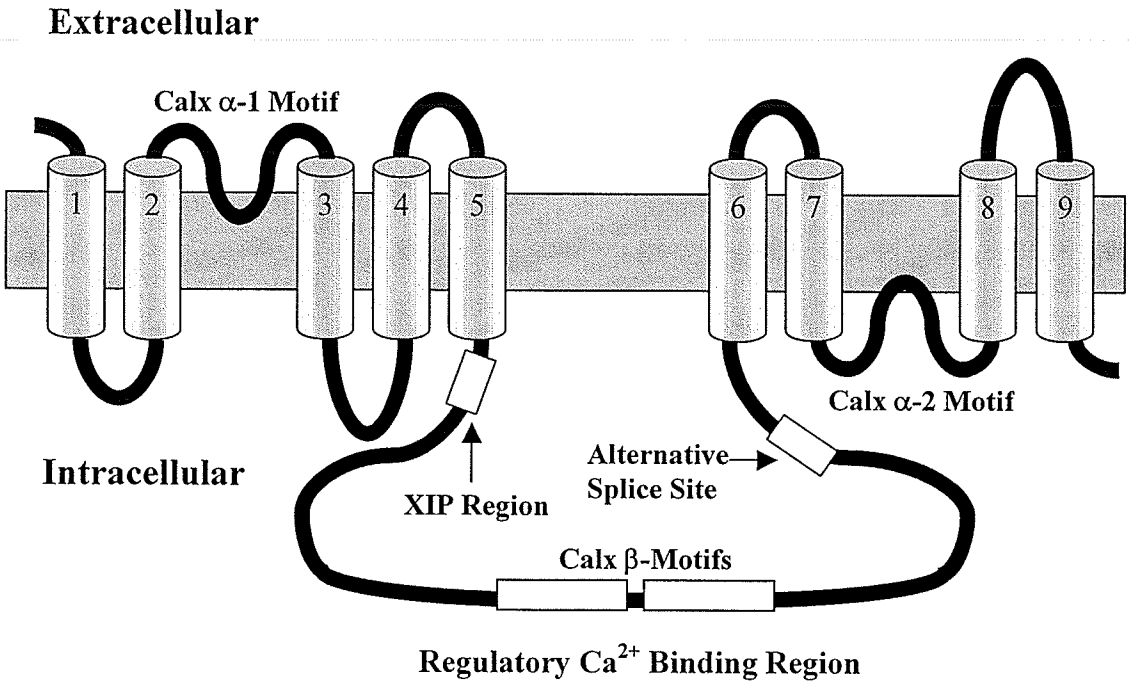

Figure 3. ***Topology of the Na^+-Ca^{2+} Exchanger.*** The Na^+-Ca^{2+} exchanger is currently modeled to span the membrane 9 times, with a large intracellular loop between transmembrane segments (TMS) 5 and 6 that houses the XIP region. There are 2 re-entrant loops, called Calx-α motifs, located between TMS 2 and 3, and TMS 7 and 8. There are two Calx-β motifs located in the central part of the intracellular loop (Adapted from Philipson and Nicoll (250)).

3. Transport Properties of the Na^+-Ca^{2+} Exchanger

3.1. Electrogenicity and Stoichiometry

Since the late 1960's, Na^+-Ca^{2+} exchange stoichiometry has been a challenging topic and therefore, subject to debate. Initial evaluations of cardiac tissue and squid axons (7) suggested that Na^+-Ca^{2+} exchange was electrogenic. This would imply a stoichiometry > 2 Na^+: 1 Ca^{2+}, for electroneutral exchange would not produce current (*i.e.,* 2:1). Many initial studies only measured unidirectional ionic movement and employed indirect methods for stoichiometric estimation (7). Currently, the Na^+-Ca^{2+} exchanger is considered an electrogenic ion countertransporter, with a well-documented stoichiometry of 3 Na^+: 1 Ca^{2+} (40; 42; 62; 144; 164; 165; 179; 205; 207). However, new progress may suggest otherwise.

Initial studies following identification of the squid Na^+-Ca^{2+} exchanger (7), measured unidirectional ion movement (Na^+-dependent-Ca^{2+} efflux and Ca^{2+}-dependent Na^+-influx), and suggested exchange was coupled at a 3 Na^+: 1 Ca^{2+} ratio (the initial stochiometry proposed for Na^+-Ca^{2+} exchange) (7). Measuring Na^+-Ca^{2+} exchange activity, on any level, can be difficult. To date, it is impossible to isolate a single Na^+-Ca^{2+} exchanger and measure the resulting current. Even so, if a single exchanger were indeed isolated, the resulting current would be too small for accurate detection (unlike ion channels that allow the movement of large amount of ions, producing large elementary currents). It is understandable, therefore, that there are so many discrepancies among Na^+-Ca^{2+} exchange results, especially in the case of stoichiometry. Earlier investigations

measured voltage-dependencies, thermodynamics, and ionic competition as stoichiometric indicators. Through these results investigators concluded exchanger electrogenicity (87; 182; 183; 257; 269; 275). These results were based on the assumption that electrogenic systems must be voltage-sensitive, however the reciprocal statement does not always hold true. This was noted, and a new experiment was performed with results concluding that both electrogenic and electroneutral Na^+-Ca^{2+} exchange are altered by membrane potential (mV) (87). In 1987, Kimura *et al.* (164) documented the first measurement of Na^+-Ca^{2+} exchange current in whole cell patches, solidifying the exchanger's electrogenicity. In 1984, Reeves and Hale re-evaluated the exchanger's stoichiometry. Using a novel method involving inside-out bovine sarcolemmal vesicles, they measured $^{45}Ca^{2+}$ flux (269). By balancing ionic concentrations they essentially removed the net driving force of both Ca^{2+} and Na^+. This allowed them to manipulate the exchanger and measure stoichiometry based on a response to changes in membrane potential (mV). Membrane potential was altered using an ionophore (valinomycin: K^+ channel former), which could generate positive or negative potentials. The result was a stoichiometry of 2.97 Na^+ to 1 Ca^{2+}. The Reeves and Hale experiment (269) complimented a less convincing study completed five years prior (257). It is imperative that a correct stoichiometry be determined for Na^+-Ca^{2+} coupled exchange, as many bodies of work have based their results on an assumption of 3 Na^+: 1 Ca^{2+} coupled exchange. Measurements of Ca^{2+} entry, efflux, transport rates (number of ions transported per unit time) and kinetics are all affected by stoichiometric designation. Once electrophysiological techniques became readily available, more attempts at identifying a correct stoichiometry were made. Certain studies chose to

measure the Na^+-Ca^{2+} exchanger reversal (E_{rev}) potential using formulaic predictions made at various stoichiometric ratios. Using whole-cell voltage clamping and measuring reversal potentials, several groups reported a consistent stoichiometry of 3:1, which has remained the popular convention (30; 86).

Recently, there have been several reports that challenge the classic 3:1 stoichiometry. Reports suggesting a 4:1 ratio have appeared over the last few years (15; 79). This ratio was initially proposed in 1977 by Mullins (219), and then later in 1983 by Ledovra and Hegyvary (182). In 2000, Fujioka et al, re-introduced the notion of a 4:1 Na^+-Ca^{2+} stoichiometry, using inside-out "macro" patches excised from guinea-pig ventricular myocytes (98). They concluded that the stoichiometry was 4:1 but had the ability to shift with changing ionic conditions (98). Measuring Na^+-Ca^{2+} exchange stoichiometry accurately in native cell systems is difficult, primarily due to confounding variables such as: 1) ionic channels and 2) various pumps. Both can affect Na^+ and Ca^{2+} movement and concentration. Therefore, Dong *et al.* suggested that the cell systems and techniques used in previous stoichiometric studies could have had confounding variables thereby, altering final results (79). They chose to express NCX1 in a system devoid of potential contaminating ionic transport pathways. Using a heterologous cell system (allowing high levels of recombinant exchange) of HEK-293 cells, they expressed NCX1.1 from rat hearts. Applying electrophysiology they measured the thermodynamic equilibrium for Na^+-Ca^{2+} exchange under varied ionic conditions. As was mentioned, only one other group, Szerencsei *et al.*, reported using this system to measure stoichiometry (309). In addition to minimizing confounding variables, they noted that HEK cells were electrically quiet, with small amounts of resting membrane current (79).

By applying various voltage steps (ramps), they set out to establish a Na^+-Ca^{2+} exchange reversal potential (E_{rev}). Through this, they found a charge ratio of 2 to 1, making the stoichiometry (if Na^+ has one charge and Ca^{2+} has two charges) 4:1.

A report from the Matsuoka group also suggested a 4:1 stoichiometry. Using inside-out macropatches excised from guinea-pig sarcolemma, XIP-sensitive currents revealed that stoichiometry was primarily 4:1. However, this ratio fluxed to that of 3:1 upon lowering cytoplasmic Na^+ concentrations (206). Kimura (125) contested these recent 4:1 findings. In their experiment, guinea pig ventricular myocytes were used to assess stoichiometry. Both the Na^+-Ca^{2+} exchanger's reversal potential and intracellular Ca^{2+} concentration (via confocal microscopy) were measured. Placing the cell at a holding potential (HP) that coincided with the theoretical reversal potentials (for different stoichiometries), they found that the E_{NCX} measured coincided with the $E_{holding}$ (HP) and the theoretical E_{rev} (same as HP in this case). Also, when measuring at a HP equal to the predicted E_{rev} for a 3:1 ratio, the membrane potential remained constant. At a holding potential (HP) equal to a 4:1 stoichiometry, however, the membrane potential initially began as a 4:1 value, but soon shifted to a 3:1 value. Based on these results, a conclusion of 3:1 was given (125).

Establishing an accurate stoichiometry is crucial to further Na^+-Ca^{2+} exchange study. Future studies require an accurate determination of stoichiometry to assess other various exchange functions. It has been suggested that if a 4:1 ratio existed, then a serious re-evaluation of previous literature would be required (130). Properties such as transport and turnover rates (98; 118; 124; 150), probability of mode occurrence under physiological conditions (*i.e.,* forward vs. reverse), resting ionic concentrations, and even

the exchanger's level of physiological importance would change. Although not globally accepted, the idea of a 4:1 stoichiometry is not entirely illogical. It is reported that a related exchanger, the NCKX (Na^+-Ca^{2+}/K^+ exchanger), has a similar 4:1 stoichiometry (261; 316). The NCKX family are found in photoreceptor cells (273) and neural tissue (261; 316), and are functionally related but hold little structural similarity to the NCX family. However, both families are ion counter-transporters that move Ca^{2+} across the membrane. With the NCKX family, a Ca^{2+}-dependent regulatory mechanism was reported, preventing a sub-nanomolar Ca^{2+} range from occurring (287; 288). This said, the potential of a 4:1 stoichiometry existing, may be more realistic then initially considered.

3.2. Turnover Rates and Exchanger Density

A transport/turnover rate refers to the number of ions transported by a single exchanger/channel per unit time. However, an ion channel allows a large number of ions to pass, making it easier to measure elementary current (the magnitude of current passing through a single channel) and to detect turnover rates. Considering the difficulty of isolating single exchangers and that resulting current is very small, direct measurements cannot be made. Therefore, most Na^+-Ca^{2+} exchanger turnover rates have been made through indirect approaches. As in the case of stoichiometry, there remains significant disparity regarding correct turnover rates. Reports estimating values from $<75 s^{-1}$ (262), to 5000 s^{-1} (118; 124) have appeared in the literature. Such a diverse range of turnover rates largely occurs because of indirect and different methods applied by investigators. In

1996, Hilgemann *et al.* implemented a new, more direct technique equating current noise associated with exchanger inactivation to transport rate measurements (124). Maximum unitary exchange currents were estimated at 0.6 - 1.3 fA (10-15 A), with a charge movement rate of 5000 s^{-1} (124).

Lacking experimental tools (*i.e.,* radioligands) and unable to accurately assess elementary current (no way to determine an exchanger count), investigators turned to measuring exchanger densities. Combined results of exchanger densities and turnover rates could provide insight into the protein's physiological and pathophysiological importance. Nevertheless, exchanger densities proved equally ambiguous. Density values range from 250 (232), 300-400 (in giant, excised patches) (118; 124), to 1235 (262) exchangers per μm^2. Equally indefinite to exchanger density is exchanger location. Understanding the exchanger density in various cellular regions (*i.e.,* T-tubules or other membrane invaginations) would be valuable in characterizing exchanger function. However, most recent evidence shows the Na^+-Ca^{2+} exchange to be located on the surface of the SL, intercalated disc region and vertical T-tubule region. Furthermore, using the rat model, Thomas *et al.* implemented double labelling studies and found that the Na^+-Ca^{2+} exchanger is as close to the SR Ca^{2+} release channels as the L-type Ca^{2+} channels are. This may provide additional support for the Na^+-Ca^{2+} exchanger having more than a Ca^{2+} removal role in the cell. Such that, under certain circumstances (increased $[Na^+]_i$ and diseased states) reverse mode exchange could play an important role in E-C coupling.

3.3. Transport Mechanism

The Na^+-Ca^{2+} exchanger has two proposed transport mechanisms. The first mechanism, dubbed "Consecutive" or "Ping-Pong" transport, has ion binding sites that shift between intracellular or extracellular positions (124; 151; 155; 190; 242). Essentially, the process can be broken down into two-steps. First, Na^+ binds and is translocated across the membrane. Next, Ca^{2+} binds and is carried through the membrane. This process is considered analogous to that of the Na^+ pump (Na^+-K^+-ATPase) (36; 214). During the translocation of these ions, they pass through several occluded states. The process is reversible and occurs at a very rapid rate. The second mechanism is known as "simultaneous" transport. Basically, ionic transport only occurs if both external and internal sites become occupied (*i.e.,* Na^+ binds extracellularly and Ca^{2+} binds intracellularly), and are transported at the same time. There is, however, a third mechanism termed "sequential" transport, initially proposed by Milanick and Frame (214), stating that an exchanger requires both ions to be bound on the same side, in order for an ion to dissociate (214). Consecutive transport is largely agreed upon. In 1977, Blaustein produced results consistent with the simultaneous model (37). This analysis was based on two results. First, there was no increase in Ca^{2+} efflux upon an increase of intracellular Ca^{2+}. Secondly, the exchanger mediated both Na^+-Ca^{2+} exchange and Ca^{2+}-Ca^{2+} exchange (alkali metal ion-activated), implying that both exchanger sides must be occupied for transport to occur (36; 37). If this were not the case, they would have noticed unidirectional or uncoupled transport occurring, but they did not. Perhaps the assumption that uncoupled exchangers are still functional and that recordings were not

performed under "zero-trans conditions" (*i.e.,* concentration of counter ion on the opposite side should be zero) lead to these conclusions (36). However, in 1990 and 1991, Khananshvili and Kimura respectively, repeated the Blaustein experiment under "zero-trans conditions" and generated results that were in agreement with the consecutive transport mechanism (155; 189).

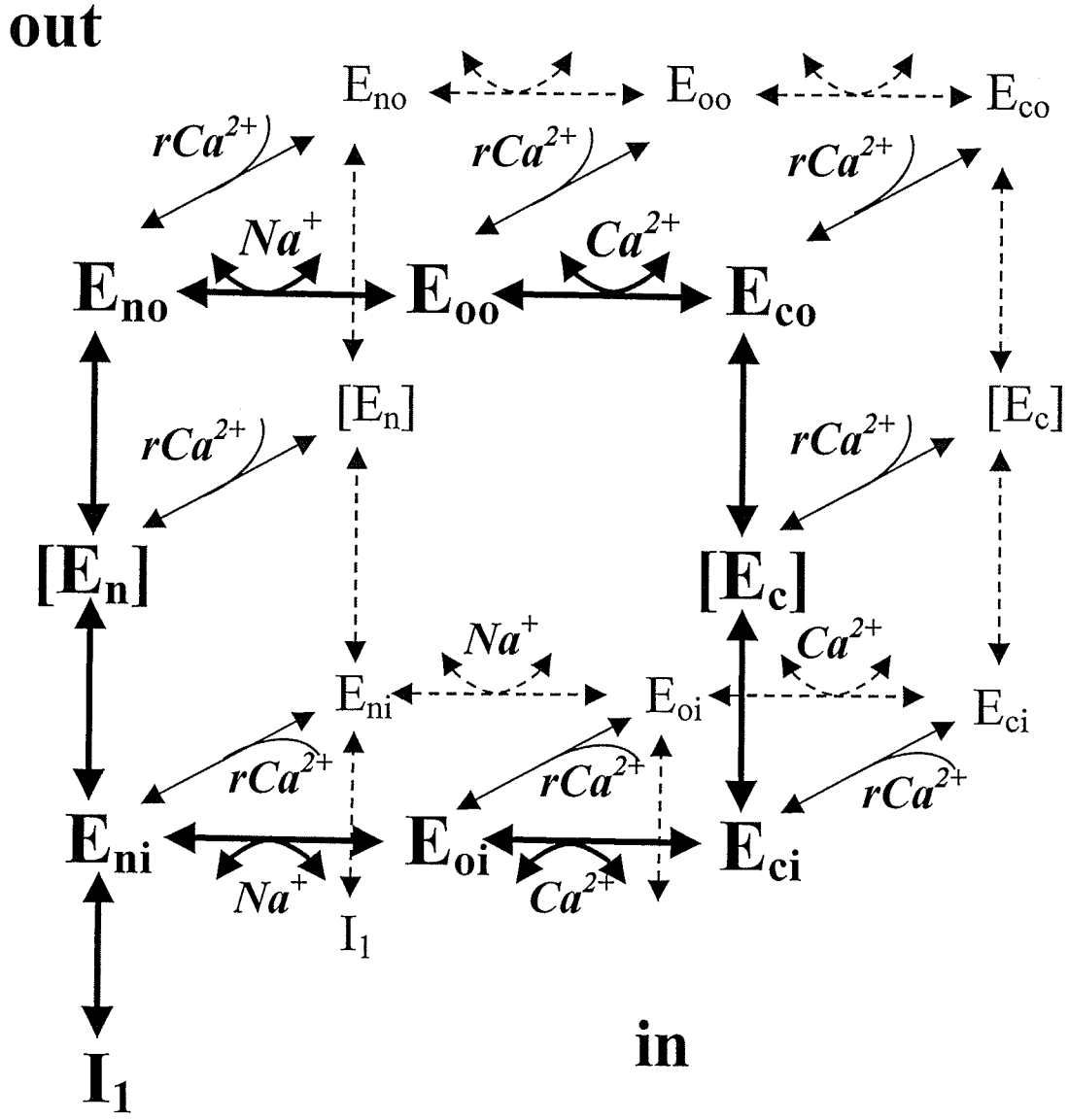

Figure 4. ***The Consecutive Eight-State Model for Na^+-Ca^{2+} Exchange.*** Eight kinetic states and one inactive state (I_1) are represented in this transport model. E_{oi} and E_{oo} represent empty states, E_n and E_c are Na^+ and Ca^{2+} occluded states, E_{no} and E_{co} correspond to extracellular Na^+ and Ca^{2+} bound states, while E_{ni} and E_{ci} stand for intracellular Na^+ and Ca^{2+} bound states. The representation is shown with both slow (front) and fast (back) transport configurations. Clockwise cycling represents reverse mode (*i.e., Ca^{2+} influx*) exchange and counter-clockwise cycling represents forward mode (*i.e., Ca^{2+} efflux*) exchange.

In 1991, Hilgemann *et al.* applied an electrophysiological approach to the measurement of transport {124}. Using the giant, excised patch technique, they measured Na^+ and Ca^{2+} partial transport reactions and suggested a consecutive mechanism of transport. Low extracellular (pipette) concentrations of either Na^+ (5 mM) or Ca^{2+} (10 μM) were applied initially in the absence of intracellular Na^+ or Ca^{2+}. With only one type of ion in the pipette at a time (either Na^+ or Ca^{2+}), the exchanger would bind the ion and translocate it. At this point, the exchanger-binding site is facing the cytoplasmic side, devoid of any ions. In a consecutive model, all the ion-binding sites orient themselves facing the cytoplasmic side, and therefore, all the exchangers were facing the cytoplasm prior to experiment initiation. A positive charge movement was measured with cytoplasmic Na^+ application, but not with Ca^{2+} (150). Thus, Na^+ translocation and/or unbinding were considered to be the electrogenic step(s) (150).

Using flash photolysis (releasing "caged Ca^{2+}" upon stimulation), Niggli and Lederer reported unidirectional charge movements termed "conformational currents", in voltage-clamped myocytes. These currents were reportedly different compared to Na^+-Ca^{2+} exchange current (232). Also using photoreleased "caged Ca^{2+}", Kappl and Hartung found that a negative charge movement was observed during Ca^{2+} translocation (under specific pipette ion concentrations) (151). Partial reaction charge movements examined in the squid Na^+-Ca^{2+} exchanger (NCX-SQ1), were found using either transport substrate (Na^+ or Ca^{2+}), suggesting that ion translocation is electrogenic (114). Overall, the most recent evidence suggests that the exchanger operates via a consecutive transport mechanism.

Initial transport cycle analysis described the exchanger as having eight kinetic states (124) (Figure 4). The E_{oo} and E_{oi} states are exchangers when their binding sites are empty and ready to bind ions. The E_{no} and E_{co} are extracellular states when the ions (either Na^+ or Ca^{2+}) are bound, while the E_n and E_c are the occluded ion bound states. The E_{ni} and E_{ci} are the bound states on the intracellular side of the exchanger (124). There is also an inactive state known as the I_1, which is entered through the E_{ni} state, also known as E_{3ni} (for it binds 3 Na^+ ions) (123). Not only does the exchanger transport Na^+ and Ca^{2+} ions, it is regulated by them (121; 123). Specifically, Na^+ regulates the exchanger by activating it and then brings it into an inactive state known as I_1. Initially described by Hilgemann in 1990 (116), this process is known as Na^+-dependent inactivation (I_1) and occurs only during reverse mode (clockwise cycling) exchange (where cytoplasmic Na^+ is present). It is termed Na^+-dependent inactivation (I_1), because as Na^+ concentration increases, there is a corresponding increase in current decay to a steady state level (123). In addition, the eight state model presented includes the hypothetical "fast" and "slow" cycles. It was proposed by Omelchenko *et al.* that the exchanger could transition between "slow" and "fast" cycles depending on the presence or absence of regulatory Ca^{2+} (242). It is believed that recovery from the I_1 inactive state is accelerated by increasing cytoplasmic Ca^{2+} and this promotes the exchanger to transition into a "fast" cycle, in which the likelihood of entry into I_1 is decreased, while exit from I_1 is increased. This may explain why less I_1 is observed upon increasing regulatory Ca^{2+} concentrations.

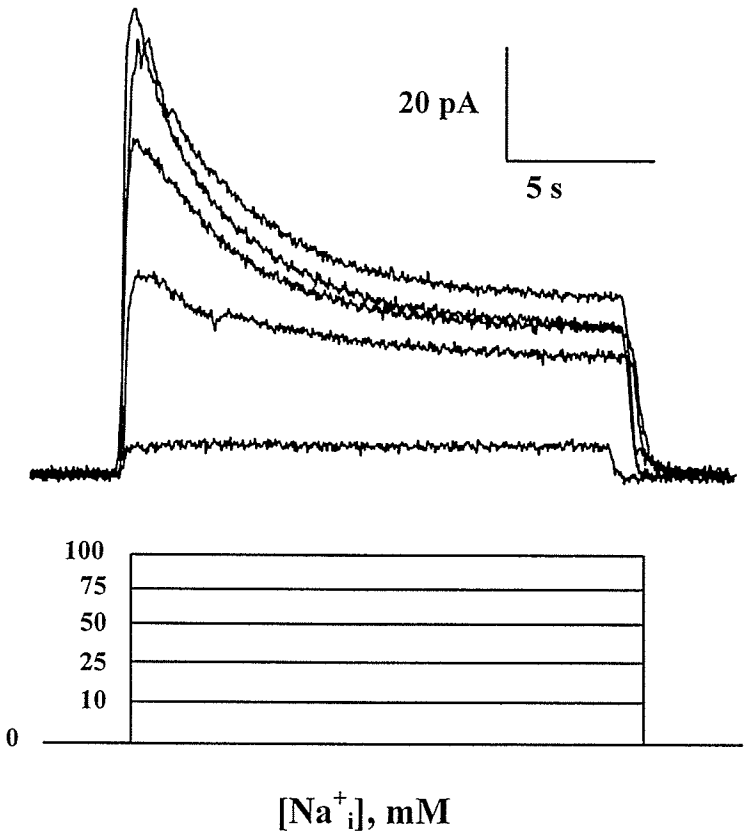

Figure 5. ***Na^+-Dependent Inactivation (I_1).*** The above figure shows a typical outward (*i.e.,* reverse mode) Na^+-Ca^{2+} exchange current trace obtained using the giant, excised patch technique. Current decay (*i.e.,* inactivation) increases as the cytoplasmic Na^+ concentration is raised.

4. Regulation of Na^+-Ca^{2+} Exchange

4.1. Na^+-Dependent Regulation (I_1)

Currently, it is unclear whether Na^+-dependent regulation (I_1) plays an important role in the physiological setting. Since we do not know for certain when and where reverse mode exchange occurs, it is difficult to determine this mechanism's importance. In a whole cell system of intact cardiac guinea-pig myocytes, Na^+-dependent inactivation was reported (208). However, like many other experimental procedures, this study was conducted under atypical physiological conditions. Specifically, intracellular Na^+ concentrations used were > 30 mM, nearly three times that of physiological levels (~ 10 mM) (208). Most experimental settings measuring Na^+-dependent inactivation use concentrations of 25-100 mM Na^+_i to achieve significant exchange current and inactivation (current decay; I_1). Otherwise, such results are unlikely under normal physiological Na^+ concentrations. Na^+ pooling (during an action potential) near the sarcolemma is suggested to be sufficient for the initiation of reverse mode exchange (5; 185; 328; 329). Like many other cellular phenomenon, this may be physiologically possible but highly unlikely. At very high (positive) membrane potentials, the reverse mode exchange is favoured. This is due to the positive repulsion of intracellular Na^+, which would favour exiting the cell, thereby stimulating outward Na^+-Ca^{2+} exchange (reverse mode). Weber *et al.* demonstrated exchange activity at membrane potentials well above physiological levels (+50 mV) (329). This study showed that a very high potential must be reached to achieve reverse mode exchange. However, there are times

when normal physiological conditions are exceeded and could produce the "unlikely" reverse mode exchange. Specifically, in the case of a positive inotropic increase, where frequency of stimulation is increased, augmenting local Na^+ levels with every depolarization. These Na^+ levels would rapidly accumulate and contribute to the positive inotropic response seen under such circumstances (*i.e.,* increasing CICR and resting Ca^{2+} levels).

Understanding Na^+-Ca^{2+} exchange function pathophysiologically is equally important as understanding it physiologically. Insight into the regulatory role of Na^+-dependent inactivation remains a key research interest, as I_1 regulation is reverse mode specific, which in turn, is primarily associated with pathophysiology. An explanation into the I_1 mechanism and its implications in cardiac pathophysiology could lead to novel therapeutic approaches (ideally pharmaceutical). When α-chymotrypsin-induced proteolysis of the Na^+-Ca^{2+} exchanger is analysed, the I_1 mechanism is apparently removed, while the resulting exchanger appears deregulated (116). It is suggested that cleavage occurs along the large intracellular loop, because a loop-less exchanger lacks I_1 (211). The XIP region has been implicated in the development of I_1, for mutagenesis experiments reveal significant alterations in Na^+-dependent inactivation (113; 209; 244). Usually mutants targeting Na^+-dependent inactivation also affected Ca^{2+} regulation (209). Moreover, it has been shown that both regulatory Ca^{2+} and mutations in the regulatory Ca^{2+} binding domain, affect I_1 suggesting an interaction between these two mechanisms (in the intact exchanger) (121; 209; 210). Recent studies using a novel reverse mode specific Na^+-Ca^{2+} exchange inhibitor, SEA0400, suggest a mechanism of action requiring I_1 (data currently in review).

4.2. *Ca^{2+}-Dependent Regulation (I_2)*

Intracellular Ca^{2+} contributes to the Na^+-Ca^{2+} exchanger's regulatory profile. Intracellular Na^+ inactivates Na^+-Ca^{2+} exchange. Cytoplasmic Ca^{2+} stimulates it. This regulatory Ca^{2+} remains non-transported and is essential for Ca^{2+}-dependent regulation, otherwise known as I_2 (116; 123; 208). DiPolo, who found that in the absence of intracellular Ca^{2+} no Na^+-dependent Ca^{2+} influx occurs (67), initially reported Ca^{2+}-dependent regulation in the giant squid axon. Furthermore, Ca^{2+}-dependent regulation, or I_2, alleviates Na^+-dependent inhibition (121) and stimulates exchange activity thereby, increasing current. This has been shown in several different exchanger types (such as SQ1-NCX (114), NCX1, NCX2, and NCX3 (194)) and in varying experimental settings (52; 93; 210; 215). Comparing techniques, the electrophysiological approach of giant, excised patch clamping provided the most detailed characterization of Ca^{2+}-dependent regulation (I_2) (116; 121; 210). These data suggest regulatory Ca^{2+} is not transported and is primarily an activator of Na^+-Ca^{2+} exchange. The Ca^{2+} affinity (K_m) for the regulatory Ca^{2+} binding domain ranges from nanomolar to micromolar values. Various experimental settings from guinea-pig myocytes to *Xenopus* giant, excised patches have reported K_m values ranging from 22 nM – 0.4 μM (97; 121; 209; 210; 215). With such a broad spectrum of K_m values, it is difficult to assess the proper physiological role of Ca^{2+}-dependent activation. For example, if a low K_m value is correct (*i.e.,* nanomolar affinity), then even at resting diastolic Ca^{2+} values, this regulatory site would be saturated, implying that it has no modulatory role. However, if the K_m value were in the low micromolar range, then this would be more responsive to the physiological environment (activating at systolic Ca^{2+} values and inactivating at lower diastolic Ca^{2+} values). Bers *et*

al. gave a projected physiological Ca^{2+} range (during systole and diastole) of ~ 0.1 - 1.0 μM (19). Part of this K_m discrepancy may be a result of different experimental conditions. In the case of whole cell patches versus giant, excised patches, the former has limited capabilities for intracellular Ca^{2+} change. Cells cannot tolerate high Ca^{2+} as they become toxic. This toxicity could either produce incorrect results and/or kill the cell. Therefore, results at higher Ca^{2+} concentrations may be overlooked due to these concentration borders. In contrast, giant, excised patches can be subjected to a wide range of cytoplasmic Ca^{2+} concentrations (10-30 μM range), and allows for a broader analysis (130).

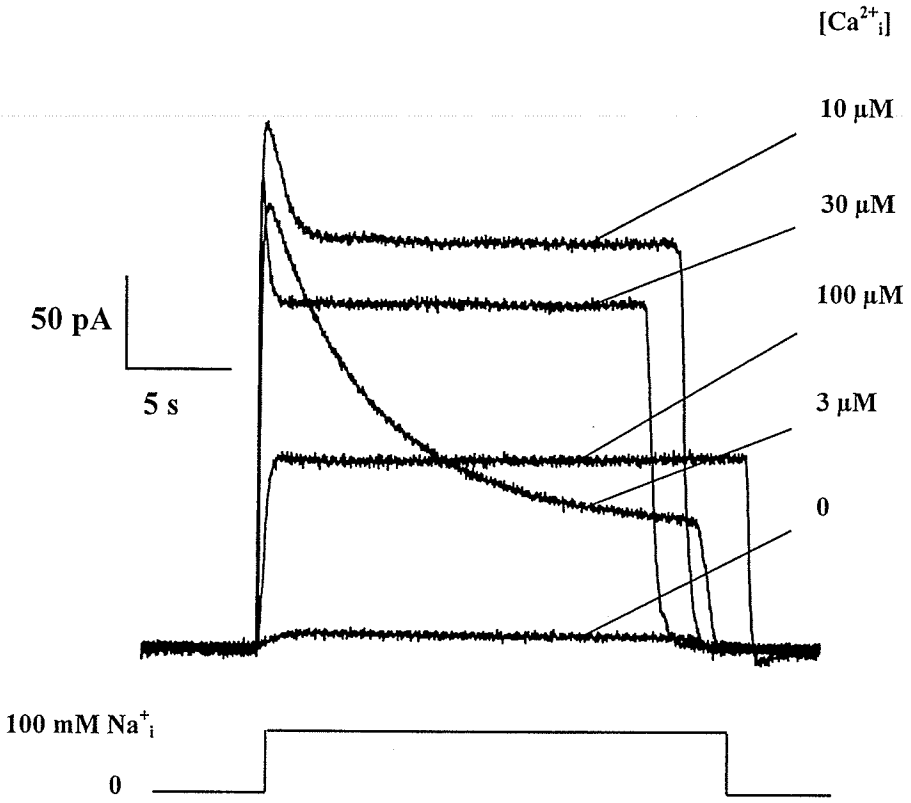

Figure 6. ***Ca^{2+}-Dependent Regulation (I_2).*** Illustrated above is a typical outward (*i.e.*, reverse mode) Na^+-Ca^{2+} exchange current trace obtained from giant, excised patch clamp experiments. Increasing cytoplasmic Ca^{2+}, or regulatory Ca^{2+}, stimulates Na^+-Ca^{2+} exchange current and alleviates I_1 inactivation. At concentrations > 10 µM regulatory Ca^{2+}, Na^+-Ca^{2+} exchange activity decreases presumably due to competition between transport Ca^{2+} and Na^+.

As mentioned earlier, there appears to be substantial interaction between these two regulatory mechanisms. It has been demonstrated by Hilgemann *et al.*, that upon increasing regulatory Ca^{2+}, the exchanger is stimulated while Na^+-dependent inactivation is attenuated (121). If the regulatory Ca^{2+} levels are high enough, I_1 can appear abolished. Furthermore, mutations in the regulatory Ca^{2+} binding region performed by Matsuoka *et al.*, decreased relative cytoplasmic Ca^{2+} affinities and altered Na^+-dependent inactivation (210). This report established Ca^{2+} regulation for both forward (Ca^{2+} efflux) and reverse mode (Ca^{2+} influx) exchange (210). Conversely, mutations specific for Na^+-dependent inactivation altered Ca^{2+} regulation (209). Continuing, α-chymotrypsin treatments eliminated Ca^{2+}-dependent regulation as well as Na^+-dependent inactivation (116; 151; 211). There is a significant body of literature suggesting these two mechanisms interact with one another and play important roles in reciprocal regulation. Investigations of both I_1 and I_2 may provide further insight as to how the exchanger regulates itself as a global and/or single unit.

4.3. Regulation of Na^+-Ca^{2+} Exchange by pH

When the cell is exposed to varying pH levels, a corresponding change in Na^+-Ca^{2+} exchange activity occurs. It has been shown that the Na^+-Ca^{2+} exchanger is highly sensitive to slight variances in resting cellular pH (~ 7.2) (75-77; 159; 247). In general, it appears that an alkalinization of the environment increases exchange activity, while an acidification inhibits. The cytoplasmic surface of the exchanger looks to be affected to a greater extent than the extracellular surface. Take for example, a study by DiPolo *et al.*,

which displayed a ~ four-fold increase in exchanger activity upon *intracellular* alkalinization to pH 8.8, yet no effect was seen with an *extracellular* alkalinization up to pH 9.0 (68). Upon acidification, exchanger inhibition by way of proton block is suggested to occur through two separate components (76). The first inhibitory component is slow forming and dependent on the presence of cytoplasmic Na^+. The second component was noted as rapid and Na^+-independent. In giant, excised patches exposed to α-chymotrypsin, the proteolyzed exchanger appears unaffected by acidification, which would normally result in inactivation. Considering that the proteolyzed exchanger lacks ionic regulation and that a component of proton block required the presence of Na^+ (cytoplasmic), it is possible that the effects of pH on the exchanger involve I_1, I_2, and/or the intracellular loop (77).

4.4. Phosphorylation

4.4.1. Protein Kinase C (PKC) and Protein Kinase A (PKA)

Na^+-Ca^{2+} exchange phosphorylation has been studied for nearly 30 years, yet still remains a controversial subject. Initially characterized on the squid axon exchanger in 1977 by DiPolo *et al.*, phosphorylation via ATP and various analogues (with hydrolysable terminal phosphates) was shown to stimulate Na^+-Ca^{2+} exchange (Na^+-dependent Ca^{2+} efflux) (36; 66; 70; 72). Exchange activity, stimulated through ATP application, displayed an increased affinity for intracellular Ca^{2+} and extracellular Na^+, with a decreased Na^+-dependent inactivation (33). Recently, DiPolo *et al.* reported a 13

kDa peptide, isolated from the squid axon cytoplasm, which was required for MgATP-dependent exchanger activation (73). When exogenous alkaline phosphatases were injected directly into the axoplasm, the ability for ATP to activate the exchanger was reversed (73). Even in the previous experiment (73), Dipolo found that under Na^+_i-free conditions, ATP does not increase exchanger activity when measuring forward mode exchange. As a note, this mode of exchanger lacks Na^+-dependent inactivation (I_1). Later, Hilgemann used giant, excised patches from cardiac myocytes, and revealed that the exchanger was regulated and inactivated by intracellular Na^+ (123). He further examined this property (I_1) and found that it could be alleviated through cytoplasmic MgATP application (123). Perhaps this explains the lack of stimulation by ATP on forward mode exchange (in the absence of Na^+) observed in the DiPolo study (73). The Na^+-dependent inactivation process is implicated in this effect. However, Hilgemann and Ball suggested that ATP-dependent activation was the result of phosphatidylinositol 4,5-bisphosphate (PIP_2) production by phosphorylation of phosphatidylinositol (PI) (119).

Mene *et al.* proposed that vasoconstrictors (angiotensin II and/or endothelin-1) promote Na^+-Ca^{2+} exchange by a mechanism independent of Ca^{2+} and PKC, but potentially linked to Na^+ influx (213). Other investigators found that phenylephrine, endothelin 1, growth factors, and angiotensin II all stimulated Na^+-Ca^{2+} exchange activity through a G protein (G_q)-mediated mechanism (8; 9), whereas blocking PKC action prevented exchanger stimulation (9; 140; 141; 305). In mammalian exchangers, PKC mediated phosphorylation was first presented by Iwamoto on aortic smooth muscle (144), followed by its identification in cardiac muscle (141). These studies further indicated that brief exposure to phorbol esters (phorbol 12-myristate 13-acetate or PMA) allowed

PKC-dependent phosphorylation, activating the exchanger (129; 141). However, long-term exposure resulted in the removal of any excitatory response that occurred by growth factors in aortic smooth and cardiac muscle myocytes (141; 144). Another agent found to activate the exchanger through phosphorylation was the platelet-derived growth factor BB (PDGF-BB) (144). However, this effect did not occur when applied to exchangers previously subjected to PMA incubation (144). On the contrary, another study showed that 24-hour pre-treatment with PMA could prevent exchanger activation via angiotensin II (213). Prolonged exposure to both PKC (arteriole myocytes) and PMA is shown to decrease exchanger expression (302; 303). Using phosphopeptide analysis and site-specific mutagenesis, Iwamoto *et al.* identified multiple phosphorylation sites. There were three sites identified, all on serine residues (Ser-249, Ser-250, and Ser-357) (141; 144). The Shigekawa group, however, created a mutant exchanger where all identified phosphorylation residues were substituted with alanine. Following mutation, it was discovered that the exchangers retained responsiveness to PMA (phorbol ester), suggesting direct phosphorylation of the Na^+-Ca^{2+} exchanger was not required for PKC-dependent stimulation. Yet, in NCX1, PMA responsiveness was missing when the large intracellular loop was mutated (244). In this case, an NCX1 mutant, XIP-4YW was not activated by PMA and was resistant to inhibition by ATP removal. The results suggested that the XIP region is involved in exchanger regulation by protein kinase C and/or ATP (244).

Collins *et al.* used the giant, excised patch clamp technique to observe ATP-induced Na^+-Ca^{2+} exchange activation (57). Through the use of various kinase inhibitors, phosphatases, and phosphatase inhibitors they found no increase in exchange activity

(57). In a later report using bovine cardiac exchanger expressed in Chinese hamster ovary cells, Condrescu *et al.* showed that both calyculin A and okadaic acid (phosphatase inhibitors) significantly inhibited reverse mode exchange (Ca^{2+} influx). They further reported that mutant exchangers lacking their intracellular loops (central part ~ 420 amino acids) were still responsive to inhibition by calyculin A and okadaic acid, suggesting that phosphorylation exerts its effects indirectly through other cellular proteins. Forward mode exchange was slightly inhibited by calyculin A and okadaic acid (59).

Another modulator of Na^{+}-Ca^{2+} exchange is protein kinase A, or PKA. In the case of PKA-dependent stimulation, NCX1 isoform-specific results have emerged. For instance, the PKA-dependent stimulation of NCX1.4 only displayed a 40% increase in exchange activity. Conversely, NCX1.3 was not stimulated by PKA (16). The use of different cell types, recording techniques, materials, protocols, exchanger species and isoforms all contribute to varying results. A variety of proteins and enzymes may be present and/or lacking among individual experimental methods, potentially contributing to these final results. Although a complete agreement regarding exchanger phosphorylation is lacking, results suggest an involvement in exchanger function.

4.4.2. Phosphatidylinositol 4,5-bisphosphate (PIP_2)

For over 25 years, it has been shown that ATP stimulates the Na^{+}-Ca^{2+} exchanger. The giant, excised patch clamp technique has been instrumental in the recent explanation for this mechanism. In 1992, Hilgemann and Ball, using giant, excised

patches, investigated ATP-dependent stimulation on outward (Ca^{2+} influx) Na^{+}-Ca^{2+} exchange currents. They revealed that the conversion of phosphatidylinositol (PI) to phosphatidylinositol 4,5-bisphosphate (PIP_2) via phosphorylation was the primary mechanism (119). While cytoplasmic application of PIP_2 mimicked stimulatory effects of ATP, a PI-specific phospholipase C eliminated them. However, the effect could be restored once again, by direct PI application. Also, reversing the stimulatory effect of ATP were PIP_2-specific phospholipase, anti-PIP_2 antibody, and aluminium (binds PIP_2 highly) (119). In addition, Hilgemann and Ball noted that high intracellular $[Ca^{2+}]_i$ reversed the effect of ATP, possibly through the activation of a PIP_2-specific phospholipase C (119).

The stimulatory effect of ATP on the Na^{+}-Ca^{2+} exchanger is only observed during reverse mode exchange (Ca^{2+} influx) (73; 123). Na^{+}-dependent inactivation (I_1), and its attenuation by ATP, implicated the regulatory XIP region. Therefore, the Philipson group examined potential interaction(s) between PIP_2 and the XIP region (112). Exchangers containing mutated endogenous XIP regions were created. These mutants displayed altered Na^{+}-dependent inhibition (I_1). Findings revealed that regardless of the resulting changes in I_1, any functional response to PIP_2 or PIP_2 antibodies was removed (112). Furthermore, they used immobilized phospholipid vesicles (containing low concentrations of PIP_2,) to which exogenous, iodinated XIP peptide was applied and found to bind. These results further accentuate the complexity and involvement of various phospholipids in Na^{+}-Ca^{2+} exchange regulation.

4.5. *Other Modulators of Na^+-Ca^{2+} Exchange Activity*

Several reports have shown that the Na^+-Ca^{2+} exchanger can be directly and indirectly modulated by its lipid environment (56; 120; 176; 177; 251-254; 321; 322). It is known that other ion transporters, such as the Ca^{2+}-ATPase and Na^+-K^+-ATPase, are sensitive to their lipid environment (322), perhaps even to specific lipids. Therefore, it was suggested that a unique lipid group might regulate Na^+-Ca^{2+} exchange. Na^+-Ca^{2+} exchange is sensitive to charged lipid components, specifically anionic amphiphiles (248). Philipson *et al.* demonstrated in cardiac sarcolemmal vesicles that anionic phospholipids (namely phsophatidylserine and phosphitydylcholine), when incorporated, could stimulate exchange activity (252; 253; 321). Using solubilized Na^+-Ca^{2+} exchangers reformed in proteoliposomes and cardiac sarcolemmal vesicles, phospholipase C and D (which increase negatively charged lipids in the membrane) were both shown to stimulate Na^+-Ca^{2+} exchange activity (248; 251). Phospholipase D in particular, displayed at times, a 400% increase in stimulation with a paralleling 9-fold increase in membrane phosphatidic acid (251). The exchanger was shown function optimally under a certain lipid ratio (PC-30% / PS-50% / Cholesterol-20 %) (321). This 20 % component of cholesterol proved important in a previous report by Kutryk *et al.*, when the cholesterol content in ventricular dog sarcolemma was modified via incubation of phosphatidylcholine liposomes with cholesterol (in varied amounts) (177). Cholesterol-enriched vesicles displayed up to a 48% increase in exchange activity, while cholesterol-depleted vesicles decreased in activity by 15% (177). Furthermore, a study investigating the effects of fatty acids on Na^+-Ca^{2+} exchange, reported stimulation of

exchanger activity (252). In 1987, Collins *et al.* utilized giant, excised membrane patches (from cardiac sarcolemma) to study phospholipid involvement (56). By direct application of "vehicle-suspended" phospholipids onto patches, their results conferred a strong stimulatory effect of phosphatidylserine on outward exchange current and altered exchanger kinetics (56). Phosphatidylserine treated patches were deregulated by α-chymotrypsin (56) and showed no further stimulatory effect. This suggested phosphatidylserine exerts its effect on the "protease-sensitive regulatory domain". Using deregulated exchangers (not already treated with phosphatidylserine) a stimulation with phosphatidylserine was maintained. This suggested an interaction with the exchange mechanism rather than regulatory mechanisms. In general, there is an agreement that the Na^+-Ca^{2+} exchanger is affected by specific sterol/protein interactions in the cellular environment.

5. Pharmacology of the Na^+-Ca^{2+} Exchanger

Pharmacology can reveal information on specific characteristics, mechanisms, and function(s) of various proteins. Conversely, understanding exchanger function can help understand drug mechanism(s). This results in the production of newer and more effective agents. Unfortunately, tools used to manipulate the exchanger have been significantly limited, especially in the "blockers" category.

5.1. *Inorganic Cations: Di- and Trivalent Cations*

For many years, studies have revealed that certain divalent and trivalent cations can serve as substrates and inhibitors of various Ca^{2+}-dependent mechanisms. The Lanthanides, a group of trivalent cations (*e.g.*, La^{3+}, Nd^{3+}, Tm^{3+}, Y^{3+}, and Gd^{3+}) and their effects on Na^{+}-Ca^{2+} exchange have been investigated (7; 164; 267; 315). Primarily, La^{3+} is regarded as a blocker of Na^{+}-Ca^{2+} exchange, with a low apparent affinity ($\geq$ 0.5 mM) (296). Yet extracellularly applied La^{3+} was shown to enter cells through Na^{+}-Ca^{2+} exchange, substituting for Ca^{2+} (296). It is suggested that if this occurs, inhibition may act through the intracellular surface. La^{3+} also blocks voltage-gated L-type Ca^{2+} channels and the plasmalemmal Ca^{2+}-ATPase (with a higher affinity than for Na^{+}-Ca^{2+} exchange) (267; 280). This property of La^{3+} is used to isolate Na^{+}-Ca^{2+} exchange by inhibiting other forms of transport activity, when applied at a low concentration (*i.e.*,< 0.5 mM) (100; 296). Although applied in whole cell systems (164), measuring La^{3+} inhibition should be performed in a system where the exchanger is in isolation. Therefore, when high amounts of La^{3+} are added (to induce significant inhibition), no other transporter/exchange system is affected. As mentioned previously, other lanthanides such as Tm^{3+}, Nd^{3+}, Y^{3+}, were tested by Philipson in cardiac sarcolemmal vesicles (315). They were relatively poor Na^{+}-Ca^{2+} exchange inhibitors in comparison to La^{3+}. Gd^{3+} had no inhibitory effect (315).

Like trivalent cations, divalent cations can adhere to Ca^{2+} binding sites, either inhibiting or acting as transport substrates. However, Mg^{2+}, a weak inhibitor (cardiac tissue – IC_{50} ~ 12.5 mM) (164; 301), does not show transport activity with the Na^{+}-Ca^{2+}

exchanger (315). There is, however, Na^+-coupled Mg^{2+} countertransport by Na^+-Mg^{2+} exchange (69). Sr^{2+} and Ba^{2+}, two other divalent cations, have demonstrated Ca^{2+} substitution and can act as transport substrates (albeit at slower rates) (37) for the Na^+-Ca^{2+} exchanger (58; 164; 231; 314). These ions may function in a mode-dependent manner and have been shown to disrupt Ca^{2+} transport during Na^+-Ca^{2+} exchange (37; 315). For example, Trac *et al.* demonstrated in giant, excised patches virtually no inward current (forward model; Ca^{2+} extrusion), even upon application of up to 300 μM Ba^{2+} (314). Unlike Sr^{2+} and Ba^{2+}, Ni^{2+} is used as a Na^+-Ca^{2+} exchange inhibitor, with an effective range of 2-5 mM (30; 164; 232). However, the inhibitory action of Ni^{2+} is not very specific and will inhibit other cellular transporters. Yet in many electrophysiological studies, Ni^{2+} is used to block Na^+-Ca^{2+} exchange current (known as "Ni^{2+} sensitive" current), therefore isolating it (164; 232; 233). Egger *et al.* demonstrated that Ni^{2+}, like La^{3+}, could inhibit Na^+-Ca^{2+} exchange and be simultaneously transported (in a neutral manner) across the membrane (84; 85). Overall, these ions are considered non-selective and must be applied with caution. The combination of high experimental concentrations mixed with low selectivity, makes for risky tools when measuring Na^+-Ca^{2+} exchange. However, if used properly, they can provide reliable results.

5.2. *Peptides*

5.2.1. *The Exchange Inhibitory Peptide (XIP)*

Upon cloning and sequencing the cardiac Na^+-Ca^{2+} exchanger (NCX1.1) (227), the Philipson group found a unique 20 amino acid segment residing in the large intracellular loop. This sequence is presently known as the XIP peptide (193). This small peptide trails off the fifth TMS and contains a mix of hydrophobic and basic residues resembling a calmodulin-binding site (193).

The endogenous XIP sequence (RRLLFYKVYKRYRAGKQRG) spans amino acids 219-238 of the Na^+-Ca^{2+} exchanger and is highly conserved among exchanger isoforms; NCX1, NCX2, and NCX3 (194). This peptide was exogenously applied to the cytoplasmic surface and displayed potent exchange inhibition (193). Through various preparations such as cardiac sarcolemmal membrane patches (132; 193), giant, excised membrane patches (*Xenopus* oocytes) (131; 192), and other various methods (53; 113), the XIP peptide has shown strong inhibitory properties, holding an IC_{50} range of 0.15- 1.5 μM. It was speculated that the endogenous XIP region played a role in exchanger regulation, primarily through a form of autoinhibition. Through the functional comparison of NCX isoforms (NCX1, NCX2 and NCX3), it was shown that the corresponding exchanger XIP peptides could actively inhibit NCX1, however, with a slightly reduced potency (194). Carrying a high degree of inhibition and potency, the properties of the XIP peptide became of interest to investigators. Mutagenesis studies were performed to examine specific amino acids and their relative contribution to the XIP

peptide's unique characteristics (113). Studies looking at the effects of mutant XIP peptides on the sarcolemmal Ca^{2+}-ATPase are also reported (332; 333). As mentioned previously, Philipson demonstrated that the entire intact XIP peptide is required for proper inhibition, especially amino acids 5 through 16 (270). He *et al.* uncovered that basic and aromatic residues are most important for the inhibitory function of XIP (113). Substitutions of arginine 12 and arginine 14 with alanine or glutamine (neutralizing them), significantly decreased XIP's potency (113). In contrast, Xu *et al.* conferred the opposite, suggesting that arginine 12 and 14 need not be positively charged (but cannot be negative either) for proper inhibitory function (332). Furthermore, Xu *et al.* demonstrated through Sulfosuccinimidyl acetate (SNA)-modified XIP peptides (with neutralized lysine residues) that one lysine residue out of three (positions 7, 11, or 17) was essential for inhibition (332). In an alternate study, He *et al.* proposed that most aromatic residues participate in binding and do so through hydrophobic interactions (113). Results from mutagenesis suggested tyrosine-6 was required for maximal inhibition, while phenylalanine 5, tyrosine 8, tyrosine 10 and tyrosine 13 are potentially important players in XIP function (113). The XIP peptide, although a highly potent inhibitor, must be used with caution, for it can bind and interfere with endogenous calmodulin and calmodulin binding proteins (*e.g.,* Ca^{2+}-ATPase) (89). Furthermore, XIP peptide can only act on the cytoplasmic surface and does not cross the membrane readily. Therefore, XIP peptide must be internally dialyzed for certain experimental techniques (*i.e.,* whole cell preparations).

5.2.2. Other Peptides

Other than XIP peptide, there are several similar peptides that have shown to inhibit (some with significant potency) the Na^+-Ca^{2+} exchanger. In the cardiac Na^+-Ca^{2+} exchanger, there exists an opiate-like binding site (157). The molluscan cardioexcitatory peptide Phe-Met-Arg-Phe-amide (FMRF-amide) is known to bind opiate binding sequences (157). While studying the effects of opiate agonists and antagonists on Na^+-Ca^{2+} exchange, Khananshvili *et al.* found that the FMRF-amide inhibited Na^+-Ca^{2+} exchange in cardiac sarcolemmal vesicles (156; 157). The inhibitory action of the FRMF-amide has also been reported in giant squid axons (71) and pancreatic β-cells (319). Khananshvili applied a group of newly synthesized (positively charged) cyclic hexapeptides (156). These hexapeptides have different amino acid sequences, containing two arginines, two phenylalanine, and two cysteines (to form an S-S bond) (156). Altogether, seven cyclic hexapeptides inhibited $^{45}Ca^{2+}$ uptake by Na^+-Ca^{2+} exchange with different potencies and IC_{50} values (200-300 μM) (158). When tested on rabbit ventricular myocytes, the study revealed that one of the seven cyclic hexapeptides, dialyzed Phe-Arg-Cys-Arg-Cys-Phe-amide (FRCRCF-amide), showed complete inhibition of Na^+-Ca^{2+} exchange at 1 μM (127; 158). However, a subsequent study by the Philipson group, comparing all three Na^+-Ca^{2+} exchange isoforms (NCX1, NCX2 and NCX3), demonstrated FRCRCF-amide to have a reduced potency, such that 50 μM resulted in a range of 32-41 % inhibition (194). Inhibition for the FRCRCF-amide peptide occurs on the cytoplasmic surface, just as in the case of XIP peptide. Therefore a cell-permeant analogue of FRCRCF-amide was created and termed Myristyl-(Myr)-

FRCRCF-amide. When applied exogenously on isolated rabbit ventricular myocytes in the whole cell patch configuration, Myrystyl-FRCRCF-amide moderately inhibited Na^+-Ca^{2+} exchange current but at a reduced potency (60).

5.3. Organic Inhibitors

5.3.1. Amiloride Derivatives

The acylguanidine diuretic termed amiloride is a weak inhibitor ($IC_{50} \sim 1$ mM) of the Na^+-Ca^{2+} exchanger, however, its derivatives are potent (148; 149). Two examples of stronger amiloride derivatives are benzamil and 3,4-dichlorobenzamil (DCB). The first analogue, benzamil, is considered a moderately potent Na^+-Ca^{2+} exchange inhibitor with IC_{50} values ranging from 17 μM in guinea pig vesicles and papillary muscles (297), 36 μM in bovine sarcolemmal vesicles, and 100 μM in rat anterior pituitary cells (147). The second potent analogue inhibitor, DCB, has a reported IC_{50} of $\sim$ 17 and 30 μM in guinea-pig atrial myocytes (195; 327). These compounds can be difficult to work with due to their limited solubility in aqueous solutions and lack of specificity. Therefore, they can non-selectively block other membrane transport systems (Ca^{2+}-ATPase, voltage-gated Ca^{2+} channels, Na^+-H^+ exchange, Na^+-K^+-ATPase and Na^+ channels) (31; 149). These analogues can also bind to other transport systems at higher affinities than that for the Na^+-Ca^{2+} exchanger. However, if a system in which other transport mechanisms are either absent or already blocked (perhaps measuring current in whole cell voltage clamping), Na^+-Ca^{2+} exchange can be identified by its sensitivity to the chosen inhibitor.

Therefore, studies using Ni^{2+} and amiloride derivatives (*i.e.,* benzamil, DCB or benzobenzamil) are used to isolate and inhibit Na^+-Ca^{2+} exchange (232). A report from Kaczorowski *et al.* suggested that amiloride analogues mimic Na^+ ions in Na^+-transport systems and can therefore, bind and inhibit the exchanger (149). Slaughter *et al.* found that DCB could inhibit both forward (Ca^{2+} removal) and reverse (Ca^{2+} extrusion) mode exchange (300). DCB was also shown to inhibit Na^+-Na^+ exchange but not Ca^{2+}-Ca^{2+} exchange. At low concentrations, DCB preferentially binds to a specific Na^+-binding site, while at higher concentrations, the inhibitor interferes with Na^+, Ca^{2+} and K^+ binding (300).

5.3.2. Isothiourea Derivative: KB-R7943 (No.7943)

Very few pharmacological agents are available for Na^+-Ca^{2+} exchange research. Furthermore, those agents that already exist are used exhaustively and remain poor in terms of selectivity, potency and administration. An exception to this is the XIP peptide, however, it is not membrane permeable. However, in 1996 KB-R7943 (2-[2-[4-(4-nitrobenzyloxy)phenyl]ethyl]isothiourea methanesulfonate), a selective Na^+-Ca^{2+} exchange inhibitor was introduced. KB-R7943, a sulphonylurea derivative, is an amphipilic molecule containing a positively charged isothiourea group (at neutral pH) (32). To date, there are no conclusive or unanimous agreements towards the action and potency of KB-R7943. However, most investigators agree that specific pharmacological tools used to manipulate the exchanger must be derived so that we may further our understanding of this important ion countertransporter. As it stands, KB-R7943 was a

step the right direction, for no other compound resembling KB-R7943 ever existed over the past 30 years. Combined with the use of various (available) experimental tools (e.g. mutagenesis, chimeric analysis, whole cell and giant, excised patch clamping), a specific Na^+-Ca^{2+} exchange inhibitor could provide detailed analysis and insight into exchange mechanisms, kinetic properties, ion specificity, and physiological and pathophysiological functions. As mentioned above, discrepancies still persist in regards to KB-R7943's properties (*i.e.,* inhibitory mechanism, mode specificity, isoform specificity and potency).

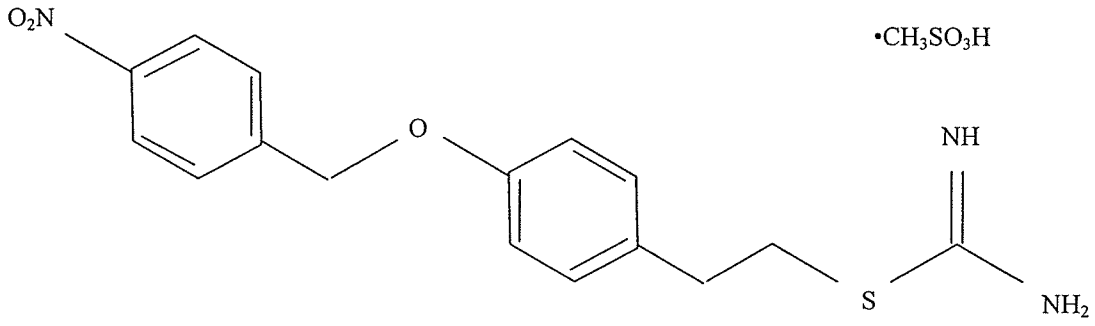

Figure 7. ***Chemical Structure of KB-R7943 (No. 7943), (2-[2-[4-(4-nitrobenzyloxy)phenyl]ethlyl]isothiourea methanesulphonate).***

The KB-R7943 inhibitor, initially described by two groups (145; 327), was evaluated as being reverse mode (Ca^{2+} influx) selective in various experimental settings such as guinea-pig ventricular myocytes (327), smooth muscle cells, and NCX1-transfected fibroblasts (145). Reported IC_{50} values ranged from 0.3-2.4 μM (reverse mode exchange) and 17-30 μM (forward mode exchange) (145; 327). However, in a report by Kimura et al, Na^+-Ca^{2+} exchange currents from guinea pig myocytes were measured using whole cell patch clamping and reported that under bi-directional conditions, KB-R7943 inhibition was mode-independent (inhibiting both modes equally with an IC_{50} ~1 μM) (166). Kimura *et al.* (167), however, potentially explained this effect in a later report. From their previous studies (327), KB-R7943 was suggested to be competitive with respect to external Ca^{2+}. Therefore, they suggested that KB-R7943's direction-dependent block was related to external Ca^{2+} concentration. They found that if Ca^{2+} was applied after KB-R7943, inhibition was ~ 90% (IC_{50} ~ 0.3 μM) and when KB-R7943 was applied following Ca^{2+}, inhibition was reduced to only ~ 50% (IC_{50} ~ 1.5 μM) (167). With Na^+ affinity for the exchanger being low and Ca^{2+} affinity being high (and that both compete with each other), when they are both present under bi-directional conditions, Ca^{2+} binds more readily. Therefore, this would explain why inhibition was equal for both modes of exchange under bi-directional conditions (167).

As mentioned above, competition between KB-R7943 and transported ions (Na^+ and Ca^{2+}) was suggested. The preliminary reports differed in their views regarding drug-ion competition. Iwamoto *et al.* proposed that KB-R7943 was non-competitive with respect to Na^+ and Ca^{2+} in cardiac myocytes, vascular smooth muscle cells and sarcolemmal vesicles (145). Watano *et al.*, using guinea pig myocytes, stated that KB-

R7943 was a competitive antagonist with external Ca^{2+}, when measuring outward Na^{+}-Ca^{2+} exchange (Ca^{2+} influx) (327). Furthermore, Iwamoto *et al.* (who initially stated that KB-R7943 was non-competitive), found while comparing NCX isoforms, that NCX1 and NCX2 showed a mixed type of competition (both competitive and non-competitive with extracellular Ca^{2+}), whereas NCX3 remained non-competitive (142). A competitive inhibition with Ca^{2+} was supported by a following report from Watano and Kimura, who showed that after-treatment of KB-R7943 inhibited outward Na^{+}-Ca^{2+} exchange current with an IC_{50} of 3 μM, a value 10 times higher that of KB-R7943 pre-treatment (326). Clearly, this component of KB-R7943 requires clarification.

When tested on different isoforms, KB-R7943 demonstrated a three fold higher level of inhibition for Na^{+}-dependent $^{45}Ca^{2+}$ uptake in CCL-39 fibroblast cells expressing NCX3, compared to those expressing NCX1 and NCX2 (IC_{50} range 1.5 – 4.9 μM) (142). However, another study by Philipson, expressing the three isoforms in BHK cells, found no differential selectivity between isoforms and only demonstrated a 35 – 45 % range of inhibition at 10 μM KB-R7943 (194). It is possible that KB-R7943 binds to regions specific to only certain isoforms, resulting in varied levels of inhibition. Currently, KB-R7943's mechanism(s) of action is still unknown. However, Iwamoto *et al.* (138) have proposed a potential binding site or region for KB-R7943. Considering Iwamoto *et al.* had shown NCX3 to be three fold more sensitive to KB-R7943 than for either NCX1 or NCX2, they chose to further examine this result (326). Using chimeras of NCX1 and NCX3, with site-directed mutagenesis, they demonstrated that the highly conserved re-entrant membrane loop, Calx-α (α-2) repeat, is responsible for differences in KB-R7943's response among isoforms (138). It was reported that the single residue

substitutions V820G, Q826V, A809V and A890I were important for drug sensitivity. Further testing through cysteine-scanning mutagenesis of the Calx-α (α-2) repeat revealed that a single residue Gly833 caused a ≥30 fold *reduction* in drug sensitivity. However, substituting Gly833 to Threonine produced an even larger difference (138). This region was proposed to form part of the receptor for KB-R7943. In addition, KB-R7943 was suggested to exert its effects from the extracellular surface, as 0.8 μM KB-R7943 significantly inhibited whole-cell outward exchange, but 30 μM applied intracellularly had minimal effect (138). Although the α-2 repeat (implicated in KB-R7943 inhibition) is accessible from the intracellular side, while inhibition is induced upon extracellular application, a conformational change of the exchanger could account for this result (138; 166). Results obtained using inside-out giant, excised patches from *Xenopus laevis* oocytes expressing NCX1.1, have demonstrated the opposite; strong inhibition with intracellular application (88). Furthermore, the initial report by Iwamoto, suggested that KB-R7943 works primarily on external sites but can inhibit the exchanger from both sides when applied intracellularly in cardiac sarcolemmal vesicles, smooth muscle cells, and CCL-39 fibroblasts (145). This was not the case in a following Iwamoto report using CCL-39 fibroblasts (138).

The capacity of KB-R7943 to inhibit Na^+-Ca^{2+} exchange in several pathophysiological models was tested. Experiments performed on both cellular and whole organ models. Firstly, several studies have shown KB-R7943 to reduce or suppress various models of cardiac arrhythmia. Mukai *et al.* found that 10 μM KB-R7943 significantly decreased the incidence of reoxygenation-induced arrhythmias and shortened the duration of arrhythmias in guinea-pig papillary muscles (218). In the case

of ouabain-induced arrhythmias, Watano *et al.* reported KB-R7943 to suppress arrhythmias in isolated guinea pig whole atria and induce changes in the measured electrocardiogram (ECG) (325). Elias *et al.* implemented re-oxygenation-induced arrhythmias on intact Langendorff-perfused whole rabbit hearts and demonstrated a suppressive effect of 3 μM KB-R7943. The result was a marked attenuation of ventricular arrhythmia (both tachycardia and fibrillation) (88). In a study presenting negative effects of KB-R7943, Lu *et al.* employed anaesthetized rats (subjected to 5 min of coronary artery occlusion followed by 10 min of reperfusion) and found that pre-treatment with KB-R7943 did not decrease ischemia/reperfusion-induced ventricular arrhythmias (201). With the dog model, mixed results have been shown. While Miyata *et al.* found KB-R7943 to prevent atrial fibrillation-induced cell shortening (217), Miyamoto *et al.* demonstrated no suppression of induced arrhythmias (216). In general, positive results have been associated with KB-R7943 treatment in various arrhythmia-inducing models.

Reperfusion injury models (*i.e.,* ischemia / reperfusion) have also been applied in the study of KB-R7943 and Na^+-Ca^{2+} exchange. In 1998, Nakamura *et al.* studied the effects of KB-R7943 in a reperfusion model using isolated rat hearts (222). In normal hearts, KB-R7943 (1 and 10 μM) did not reduce contractile function. After ischemia-reperfusion, administration of KB-R7943 resulted in a significant recovery of left ventricular developed and end-diastolic pressure, either by pre-ischemic or post-ischemic treatment (222). Later, Ladilov *et al.* measured rat cardiomyocytes with simulated ischemia. They found 20 μM KB-R7943 completely inhibited reverse mode exchange, while treatment with the same concentration during anoxia did not influence the onset of

rigor contracture but significantly reduced the cytosolic accumulation of Ca^{2+} and Na^{+}. However, upon re-oxygenation, myocytes developed hypercontracture that was significantly reduced by KB-R7943 administration (178). With the use of perfused rat hearts they found that 20 μM KB-R7943 (during anoxia) significantly attenuated reoxygenation-induced enzyme release (lactate dehydrogenase and creatine kinase) (178). Continuing, Satoh *et al.* used 5 μM KB-R7943 on rat cardiomyocytes, to selectively block Ca^{2+} entry through the Na^{+}-Ca^{2+} exchanger (~ 90%) (281). KB-R7943 did not affect steady state twitches, Ca^{2+} transients, SR Ca^{2+} load or post-rest potentiation. It did, however, prolong the action potential plateau. They concluded that Ca^{2+} entry through the exchanger is not important for normal excitation-contraction coupling but can contribute to cardiac arrhythmogenesis (281). Lastly, a recent study using KB-R7943 in whole rat hearts showed considerably suppressed intracellular Ca^{2+} levels during an ischemic period. Following reperfusion, diastolic Ca^{2+} was normalized more rapidly in KB-R7943-treated hearts (291).

Nishida *et al.* chose a model for Ca^{2+} overload, produced by metabolic inhibition (by carbonyl cyanide m-chrolophenylhydrazone (CCCP)), in isolated guinea pig myocytes (234). When applied, 10 μM KB-R7943 reduced Ca^{2+} overload, whereas other ion transport inhibitors did not (234). Using guinea pig myocytes for a Ca^{2+} paradox model (a massive Ca^{2+} influx during a Ca^{2+} repletion phase following a period of time in the absence of Ca^{2+}), Iwamoto *et al.* reported no hypercontracture on Ca^{2+} repletion, using 10 μM KB-R7943 (145). Hydroxyl-induced Ca^{2+} overload through the Na^{+}-Ca^{2+} exchanger was examined by Zeitz *et al.* (336). Their results supported a protective effect by KB-R7943, showing a preservation of diastolic function in both rabbit and rat

myocardium (336). Also, in failing human myocytes, Ca^{2+} transients and contractions exhibit an SR-related, phasic component and a slow, reverse mode Na^{+}-Ca^{2+} exchange-related tonic component (slow decay of the Ca^{2+} transient) (65). Dipla *et al.* demonstrated that KB-R7943 removed the action potential's tonic component and reduced the phasic component, in failing human ventricular myocytes (65).

In other non-cardiac related models, KB-R7943 has proven to be quite useful. For example, in CA1-neurons from rat hippocampal slices, KB-R7943 protected against hypoxic-hypoglycemic injury (289). In cultured primary osteoblasts, KB-R7943 prevented extracellular mineral deposition (304). Studies in the rat have used KB-R7943 in hepatocytes (134), forebrain neurons (28), cerebral cortex (255), and with acute renal failure (ARF) in kidney cells (175; 334).

The specificity of KB-R7943 over other ion translocation mechanisms and cellular proteins is important. Non-selective inhibitors (*i.e.,* Ni^{2+}, amiloride, and DCB) must be applied with caution, as results can be ambiguous when applied in a natural setting. KB-R7943's specificity has been assessed on several occasions. Iwamoto *et al.*, in their original report stated that KB-R7943 inhibits voltage-sensitive Na^{+} channels, L-type Ca^{2+} channels, and inward rectifying K^{+} channels with concomitant IC_{50} values of 14, 8, and 7 μM (145). Iwamoto *et al.* also reported that KB-R7943 was without effect on the Na^{+}-Ca^{2+}-K^{+} exchanger, Na^{+}-H^{+} exchanger, SR Ca^{2+}-ATPase, SL Ca^{2+}-ATPase, and the Na^{+}-K^{+}-ATPase at concentrations as high as 30 μM (145). KB-R7843 can block nicotinic acetycholine receptors (256). Most recently, KB-R7943 was proposed to directly modulate Na^{+}-Mg^{2+} exchange in a Ca^{2+}-dependent manner. Using pig carotid artery smooth muscle, the result was an increase in $Mg^{2+}{}_{i}$ (318).

Results presented on KB-R7943 are quite varied. This greasy compound has been reported as competitive, non-competitive and mixed-competative. Potency (exchanger and mode selectivity) ranged from substantially low to very high, never quite acting as an ideal inhibitor. However varied these results may be, KB-R7943 has still proven to be a useful inhibitor and has given promising insight into the future of Na^+-Ca^{2+} exchange pharmacology.

5.3.3. SEA0400

Recently, a new Na^+-Ca^{2+} exchange inhibitor, SEA0400 (2-[4-[(2,5-difluorophenyl)methoxy]phenoxy]-5-ethoxyaniline) was introduced. Currently, there are only seven reported publications involving SEA0400. SEA0400 may be the most selective and potent Na^+-Ca^{2+} exchanger inhibitor to date (137; 203; 204; 239; 310; 311). This inhibitor was isolated through the screening of a compound library, measuring Na^+-dependent Ca^{2+} uptake in cardiac sarcolemmal vesicles and astrocytes (204). The ethoxyanaline derivative was initially tested and compared to KB-R7943 using cerebral tissue and cerebral pathology models (204). In the initial SEA0400 study by Matsuda *et al.*, inhibition was measured in a cerebral ischemia-reperfusion injury (both in vitro and in vivo) model. SEA0400 showed significantly greater potency than KB-R7943 (IC_{50} ~ 2-3 μM), inhibiting Na^+-dependent Ca^{2+} uptake in neurons (IC_{50} ~ 33 nM), astrocytes (IC_{50} ~ 5.0 nM), and microglia (IC_{50} ~ 8.3 nM) (204). Conversely, KB-R7943 produced IC_{50} values of 3.8, 2.0, and 3.1 μM respectably. SEA0400 demonstrated only minor affinities for Ca^{2+} channels, Na^+ channels, K^+ channels, norepinephrine transporter, and

14 other receptors (204). In addition, SEA0400 did not alter the activities of Na^+-H^+ exchange, Na^+-K^+-ATPase, Ca^{2+}-ATPase and five enzymes (phospholipase A_2, phospholipase C, 5-lipoxygenase, iNOS and cNOS). As previously reported (4), KB-R7943 inhibited store-operated Ca^{2+} entry (SOCE) in cultured astrocytes yet SEA0400 did not until at very high concentrations (10 μM - where solubility may be questionable). SEA0400 dose-dependently attenuated; paradoxical Ca^{2+} induced reactive oxygen species (ROS) production, DNA ladder formation, and nuclear condensation in neonatal astrocytes (204). In vivo studies reported that SEA0400 reduced infarct volumes upon transient middle cerebral artery occlusion in rat cerebral cortex and striatum (204). As a result, Matsuda *et al.* concluded that SEA0400 was a specific and potent Na^+-Ca^{2+} exchange inhibitor that has protective properties for cerebral ischemia (204). SEA0400 was then employed in the cardiac setting, where Tanaka *et al.* isolated ventricular myocytes from guinea pig hearts and measured the inhibition of Na^+-Ca^{2+} exchange current (311). SEA0400 at 1 μM inhibited myocardial exchange current (~ 80%) to the same degree as 10 μM KB-R7943. At the same concentrations, KB-R7943 resulted in >50 % inhibition of Na^+ channel currents, L-type Ca^{2+} channel currents, delayed and inwardly rectifying K^+ channel currents, while SEA0400 (1 μM) had no significant effect (311). These results support SEA0400 as a potent and highly selective inhibitor of Na^+-Ca^{2+} exchange.

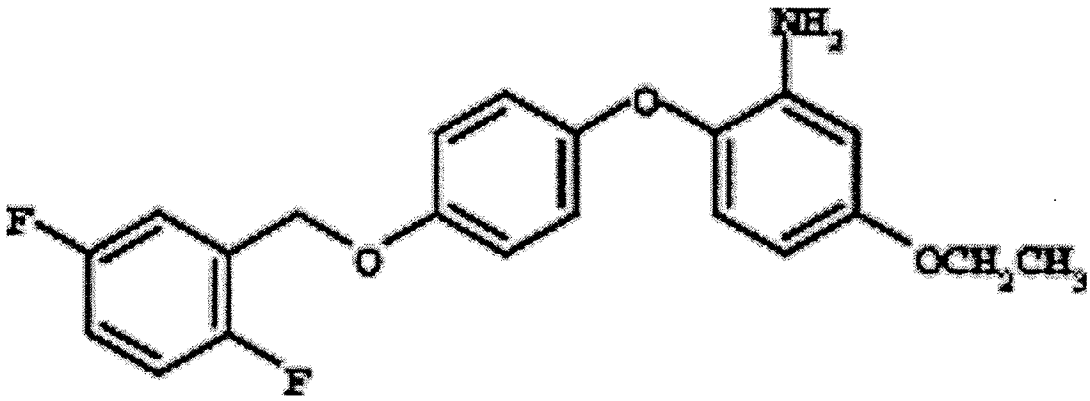

Figure 8. ***Chemical structure of SEA0400, (2-[4-[(2,5-difluorophenyl)methoxy]phenoxy]-5-ethoxyaniline (SEA0400)).***

Exchange activity is difficult to measure accurately and therefore, must be analysed from a variety of angles. Various research groups apply unique methods and models of analysis, in the hopes of improving our understanding of Na^+-Ca^{2+} exchange. One model recently published by the Philipson group implemented Na^+-Ca^{2+} exchange knockout mice ($NCX^{-/-}$) to test the specificity of KB-R7943 and SEA0400 (274). Using heart tubes from fetal mouse embryos at 9.5 days post coitus (dpc) and fura-2 loading, they were able to measure the resulting Ca^{2+} transients. The study revealed that KB-R7943 (5 μM) and SEA0400 (0.1 μM) decrease Ca^{2+} transients in both control cells and cells from knockout mice (274). Another laboratory, the Shigekawa group, used heterozygous NCX1 knockout and wild-type mice to test various inhibitors. They concluded that their model was useful, providing low NCX1 expressing mice (137).

The effects of SEA0400 were also tested in an ischemia-reperfusion setting for the rat, rabbit and dog (in vivo and in vitro) (203; 310). The first study examined isolated Langendorff-perfused rabbit hearts exposed to regional ischemia and reperfusion (203). It was found that both KB-R7943 (1 μM) and SEA0400 (0.1 μM) reduced infarct size independent of the time of administration (before or after ischemia). However, SEA0400 was more effective, reducing the infarct by ~ 75 %, whereas, KB-R7943 was only 40 % effective. At concentrations ≥ 1 μM, KB-R7943 impaired cardiac function. However, SEA0400 showed a continuous recovery of function. These data stress that SEA0400 is significantly better at cardioprotection, even at a ~10 fold lower concentration. Another ischemia-reperfusion study in canine cardiac sarcolemmal vesicles and rat cardiomyocytes prolonged the trend for SEA0400's positive results (310). Measuring Na^+-dependent $^{45}Ca^{2+}$ uptake, they reported an SEA0400 IC_{50} value of 90 nM

(sarcolemmal vesicles) and 92 nM (rat cardiomyocytes). In vivo rat coronary ligation and reperfusion experiments showed a decrease in ventricular fibrillation and mortality with SEA0400. Furthermore, Takahashi *et al.* (310) were able to reduce Ca^{2+}-paradox-induced cell death in their study. The latest evidence supporting SEA0400 as having protective effects was reported by Ogata *et al.*, using renal ischemia-reperfusion and hypoxia-reoxygenation injury in the rat model (239). It was demonstrated that SEA0400 could dose-dependently reduce ischemia-reperfusion induced renal dysfunction and tubular necrosis. Furthermore, in isolated cultured porcine tubular cells, application of SEA0400 before or after hypoxia-reoxygenation was found to protect against cellular damage (239).

It is evident that SEA0400 is an effective and useful compound. The majority of results confer that SEA0400 has great potential in the study of Na^+-Ca^{2+} exchange. A potent and mode selective inhibitor is precisely what is required in a field lacking pharmacological tools. This could prove useful in the pathophysiological studies of Na^+-Ca^{2+} exchange. Understanding its mechanism(s) of action, therefore, would be valuable information. This could lead to a better knowledge of Na^+-Ca^{2+} exchange function, but may also give rise to more potent and specific Na^+-Ca^{2+} exchange inhibitors. Therefore, presented in this thesis are results suggesting a potential mechanism of action for SEA0400.

6. Na^+-Ca^{2+} Exchange Pathophysiology

The physiological role of the cardiac Na^+-Ca^{2+} exchanger, NCX1.1, is not entirely clear. However, it is generally agreed upon that the exchanger's primarily role is transarcolemmal Ca^{2+} removal. Theoretically, Na^+-Ca^{2+} exchange should remove the exact amount of Ca^{2+} initially brought in through L-type Ca^{2+} channels thereby, balancing Ca^{2+} influx with efflux. Accurate Ca^{2+} balance is crucial for cellular and whole heart relaxation (19; 21; 36; 44; 237; 250). This process must occur on a beat-to-beat basis, otherwise Ca^{2+} overload or depletion will result. Cardiomyocytes are very sensitive to changes in intracellular Ca^{2+} and depend on the maintenance of proper Ca^{2+} homeostasis for survival. Calcium sensitivity paired with a reversible Na^+-Ca^{2+} exchanger can be dangerous for the heart and is, therefore, implicated in cardiac pathophysiology. Under a variety of conditions, the exchanger could contribute to specific types of cardiac disease and injury. Whether or not these conditions actually contribute to pathophysiology is not entirely evident. However, there is rapidly amassing evidence suggesting this possibility.

Whether Na^+-Ca^{2+} exchange function is normal, reversed, increased or decreased, there are a multitude of cellular properties that can be altered (both positive and negative). For example, cardiac action potentials (5; 61; 67; 186; 329), SR Ca^{2+} loading (153), Ca^{2+} transients and diastolic Ca^{2+} levels (30; 65; 161) are all affected by alterations in Na^+-Ca^{2+} exchange. Therefore, an understanding of Na^+-Ca^{2+} exchange activity and regulation, in both cardiac disease and injury, is essential if we wish to apply this to a clinical setting (*i.e.,* new pharmaceuticals or surgical techniques). In heart failure, it is suggested that Na^+-Ca^{2+} exchanger protein, transcript, and activity levels are altered.

Certain reports find an increase in all three (protein, transcript, and activity) (95; 107; 108; 307). Other reports demonstrate minimal change (170) or even a decrease (64; 74) in exchanger levels. In certain cases where exchanger levels are upregulated, this is considered as a mechanism compensating for a decrease in other Ca^{2+} handling proteins, such as the SR Ca^{2+}-ATPase (197; 223; 238; 238). Recently, O'Rourke *et al.*, inhibited SR function (Ca^{2+} uptake) with cyclopiazonic acid and found a greater requirement of Na^{+}-Ca^{2+} exchange for cytosolic Ca^{2+} removal. The Na^{+}-Ca^{2+} exchanger expression was increased by 104% (238). Meanwhile, Schillinger *et al.* demonstrated that poor diastolic function occurs in hearts with a decreased level of SR Ca^{2+}-ATPase but with unchanged Na^{+}-Ca^{2+} exchanger levels (109; 283). Conversely, some studies proposed that an increase in Na^{+}-Ca^{2+} exchange activity was deleterious to cardiac function (260; 266; 282).

In 2000, Schillinger *et al.* reported that overexpression of the Na^{+}-Ca^{2+} exchanger in rabbit cardiomyocytes (adenoviral gene transfer), resulted in a decrease in contractility (282). In summary, whether an increased, decreased or unchanged level of Na^{+}-Ca^{2+} exchangers actually occurs in heart failure remains to be clarified. Furthermore, understanding how the change in exchanger function effects contractile behaviour under such diseased conditions, would be important information to both the field of Na^{+}-Ca^{2+} exchange and cardiology.

Two major components of heart failure and cardiac disease are arrhythmias and reperfusion injury. Arrhythmias are an irregular heart rhythm, or an abnormality in heart beat pattern, potentially resulting in tachychardia and then fibrillation. The primary causes of arrhythmia are non-re-entrant mechanisms created by abnormal automaticity in

the heart (236; 258). This is also known as triggered arrhythmogenesis. It was shown by Blaustein *et al.* that an induced increase in intracellular Ca^{2+} could influence SR Ca^{2+} stores. A slight increase in cytosolic Ca^{2+} can lead to a substantial increase in SR uptake, allowing this Ca^{2+} to participate in the next release (35). In the heart, if the Ca^{2+} gain becomes very large, the SR can release Ca^{2+} spontaneously. This is known as SR Ca^{2+} overload (153). Ca^{2+} overload is suggested to be a result of an increase in Ca^{2+} due to reverse mode Na^{+}-Ca^{2+} exchange, and/or the reduced drive of forward mode Na^{+}-Ca^{2+} exchange (by elevated intracellular Na^{+} levels). This increase in $Ca^{2+}{}_{i}$ is still accompanied by normal Ca^{2+} influx through L-type Ca^{2+} channels. Ultimately, this leads to a "trigger sensitive" SR, instigating spontaneous release of SR Ca^{2+} stores, creating a wave of Ca^{2+}, that in turn produces a transient inward current (I_{ti}). Transient inward current occurs by two mechanisms. The first is through intracellular $Ca^{2+}{}_{i}$ activated non-selective channels (152; 154). The second mechanism is through Na^{+}-Ca^{2+} exchange (94; 195; 196; 259; 284; 337). While the non-selective channels bring ions into the cell, the Na^{+}-Ca^{2+} exchanger (forward mode) removes Ca^{2+} concomitantly bringing Na^{+} into the cell, ultimately depolarizing the membrane. Depolarization, if strong enough, can become an all-or-none response and lead to a premature contraction. This depolarizing I_{ti} is directly related to triggered arrhythmias through events called early afterdepolarizations (EAD) and delayed afterdepolarizations (DAD) (152; 154; 235). EAD's occur during a prolongation of the cardiac action potential plateau in which the resulting inward transient current is sufficient for depolarization, resulting in a contraction. A second depolarization prior to the completion of the original depolarization results in an increased Ca^{2+} load, which could produce DAD's (308; 323).

The heart is a highly aerobic muscle, requiring a constant supply of oxygen that is fed through a distinct set of vasculature. Deoxygenated blood enters the lungs, reoxygenates and returns to the heart. Ultimately, the heart's constant pumping is directly related to insuring its own oxygen supply. When blood flow is reduced or completely occluded, the heart is subjected to a period of ischemia (low or no blood flow) or anoxia (absence of oxygen). Upon reperfusion, the heart undergoes large, rapid ionic shifts. Ultimately, this has been attributed to an intracellular rise in Ca^{2+} (3; 80). As previously mentioned, injury also results from a sudden rise in Ca^{2+} when the cells are exposed to Ca^{2+} following a "Ca^{2+}-free" period. This is termed "Ca^{2+} paradox". Reverse mode Na^+-Ca^{2+} exchange contributes to the "Ca^{2+} overload" associated with ischemia-reperfusion injury (104; 220; 312). As well, during ischemia, an internal acidification occurs as a result of H^+ ion production as the cell switches to anaerobic metabolism (glycolysis) (3). ATP is degraded, resulting in the inhibition of the Na^+ pump (Na^+-K^+-ATPase). This in turn, increases intracellular Na^+ levels. Upon reperfusion, the Na^+-H^+ exchanger attempts to restore intracellular pH levels by removing H^+ ions, and therefore brings Na^+ into the cell (180). With such a large rise in intracellular Na^+, forward mode Na^+-Ca^{2+} exchange becomes less favourable. Conversely, the reverse mode becomes more favourable. This not only leads to a rise in Ca^{2+} but also a decrease in Ca^{2+} removal. Eventually, this leads to Ca^{2+} overload and may seriously damage the cell (104; 220; 312). With respect to roles for the exchanger in physiology and pathophysiology, there is sufficient disagreement to merit further investigation.

III. METHODS

1. Preparation of *Xenopus laevis* Oocytes

Xenopus laevis oocytes are large and robust single-celled biological hosts. Furthermore, they have a large membrane surface area, express the protein and localize exchangers to the membrane. As current produced by a single exchanger is small, a large exchanger population is required to create a measurable signal. Therefore, using this technique allows us to excise a large surface area and increase our experimental exchanger population. Giant, excised patch clamping also allows for rapid cytoplasmic access, which is difficult or absent in other techniques.

Xenopus laevis were anaesthetized in a solution of 250 mg/l ethyl *p*-aminobenzoate (Sigma) in deionized ice-water for 30 minutes prior to sacrificing. Oocytes were surgically removed and then washed in Solution A containing (in mM): 88 NaCl, 15 HEPES, 2.4 $NaHCO_3$, 1.0 KCl, 0.82 $MgSO_4$; pH 7.6 at room temperature (RT). Connective follicle(s) surrounding the oocytes was teased apart to assist digestion. Continuing, the oocytes were transferred into Solution A containing $\approx$ 16,000 units of collagenase (Type II; Worthington). Next, the same batch of oocytes was subjected to an incubation period accompanied by gentle agitation at RT for 1.5-2 hours. This rotating motion helps clean the egg by removing excess follicle. Following the incubation period, the oocytes were washed several times in Solution B containing (in mM): 88 NaCl, 15 HEPES, 2.4 $NaHCO_3$, 1.0 KCl, 0.82 $MgSO_4$, 0.41 $CaCl_2$, 0.3 $Ca(NO_3)_2$, 1 mg/ml BSA (Fraction V; Sigma); pH 7.6 at RT, and then transferred to a RT 100 mM K_2HPO_4 (pH

6.5) solution, containing 1 mg/ml BSA. After incubation for 12-20 minutes (with gentle agitation at RT), the oocytes were washed in Solution B. Defolliculated stage V-VI oocytes were selected and incubated in glass scintillation vials at 18 °C filled with Solution B (without BSA) until the cRNA is injected.

2. Synthesis of NCX1.1 cRNAs

Hind III (*New England* Biolabs) was used to linearize complementary DNA (cDNA encoding NCX1.1) residing in pBluescript II SK(+) (Stratagene Inc.). Complementary RNA (cRNA) was synthesized using either mCAP mRNA capping kit (Stratagene Inc.) or mMessage mMachine (Ambion) transcription kit. Oocytes were injected with ≈ 5 ng/50 nl of cRNA encoding NCX1.1, and stored in Solution B (without BSA) at 18 °C. Electrophysiological measurements of Na^+-Ca^{2+} exchange activity were obtained 3-7 days post-injection.

3. Preparation of Mutant Na^+-Ca^{2+} Exchangers

Mutations were generated using the Sculptor *in vitro* mutagenesis kit (Amersham Corp.) as previously described (82; 209; 225; 226). Both large and site-specific amino acid deletions were created for this study. The large deletions were made on the C-terminus end of the XIP region, while the site-specific amino acid mutations were created throughout. These mutations were used to determine the involvement of both I_1 and I_2 regulatory mechanisms in NCX1.1 current inhibition by SEA0400. A previous study by

He *et al.* looked at the effects of mutant, exogenous XIP peptides and their inhibitory consequences (113). They noted that a potent XIP peptide inhibitor must be intact in order to exert its full inhibitory effect. They also revealed that specific amino acids were important for proper inhibitory function. For example, they noted that basic and aromatic residues were the most important for XIP's inhibitory action. Similar results for the XIP region were found in the *Drosophila melanogaster* exchanger CALX1.1 (82). Therefore, basic and aromatic residues were the primary experimental targets, due to results from corresponding experiments involving amino acid substitutions, indicating the importance of these residues in exchanger inhibition (113). Basic residues were switched to neutral hydrophilic glutamine residues, while aromatic tyrosines were changed to threonine in order to remove the aromatic characteristic, while maintaining the residue's hydroxyl characteristic. In one case, an aromatic residue, F223, located in a strongly conserved amino NH_2-terminal of the XIP region, was mutated to glutamate so as to eliminate the aromatic group and introduce an acidic residue into a primarily basic exchanger region (209). All deletion and site-specific XIP region mutations produced functional exchangers. The mutations were categorized into three groups based on their corresponding regulatory phenotypes. Group 1, contained two site-specific mutants (K225Q, F223E) and exhibited accelerated Na^+-dependent inactivation (I_1). Group 2 mutants were comprised of one site-specific (K229Q) and one deletion mutant (Δ229-232) that exhibited suppressed Na^+-dependent inactivation (I_1). Lastly, the single Group 3 deletion mutant (Δ680-685) exhibited suppressed I_2 regulation. Although not a XIP region mutant, Δ680-685 was previously shown to have altered Ca^{2+}-dependent regulation (I_2), in both giant, excised patches from *Xenopus laevis* oocytes and whole cell

patches from mouse cardiomyocytes (212). These distinct mutant phenotypes are presented in Figure 18 and ultimately allow an assessment of SEA0400's inhibitory effect on exchanger's with altered ionic regulatory mechanisms (*i.e.*, I_1 and I_2).

4. Measurement of Exchange Activity

Na^+-Ca^{2+} exchange currents (outward and inward) were measured using the giant, excised patch clamp technique as previously described (116) (Figure 9). *Xenopus* oocytes were placed in a hypo-osmotic solution containing (in mM): 250 Sucrose, 67 KCl, 10 D-Glucose, 10 HEPES, 5 $MgCl_2$, 2.5 EGTA; pH 7.0 at RT (with KOH) for ≈ 15 minutes, to assist in removal of the vitellin layer surrounding the oocyte membrane. After vitellin layer dissection using blunt forceps, oocytes were placed in a solution containing: (values in mM): 100 KOH, 100 MES, 20 HEPES, 5 EGTA, 5 $MgCl_2$; pH 7.0 at RT (with MES). Borosilicate glass pipettes were pulled and polished to a final inner diameter of ≈ 20 - 30 μm and coated with a Parafilm™:Mineral oil mixture to enhance patch stability and reduce electrical noise. Pipettes were filled with the appropriate pipette solution for desired current, secured tightly inside the pipette holder (Axon Instruments), and positioned onto the animal pole surface (dark surface) of the oocyte by way of a micromanipulator (Narshige). Gigaohm seals were formed via gentle suction. Membrane patches (inside-out configuration) were excised through progressive horizontal and vertical pipette tip movements. Pipettes containing excised patches were then relocated to a carved divot in front of the perfusion tip. This pipette was connected

to a computer-controlled, 20-channel solution-switching machine, which allowed rapid (*i.e.*, $\approx$ 200 ms) solution changes of the bath (*i.e.*, intracellular) solution.

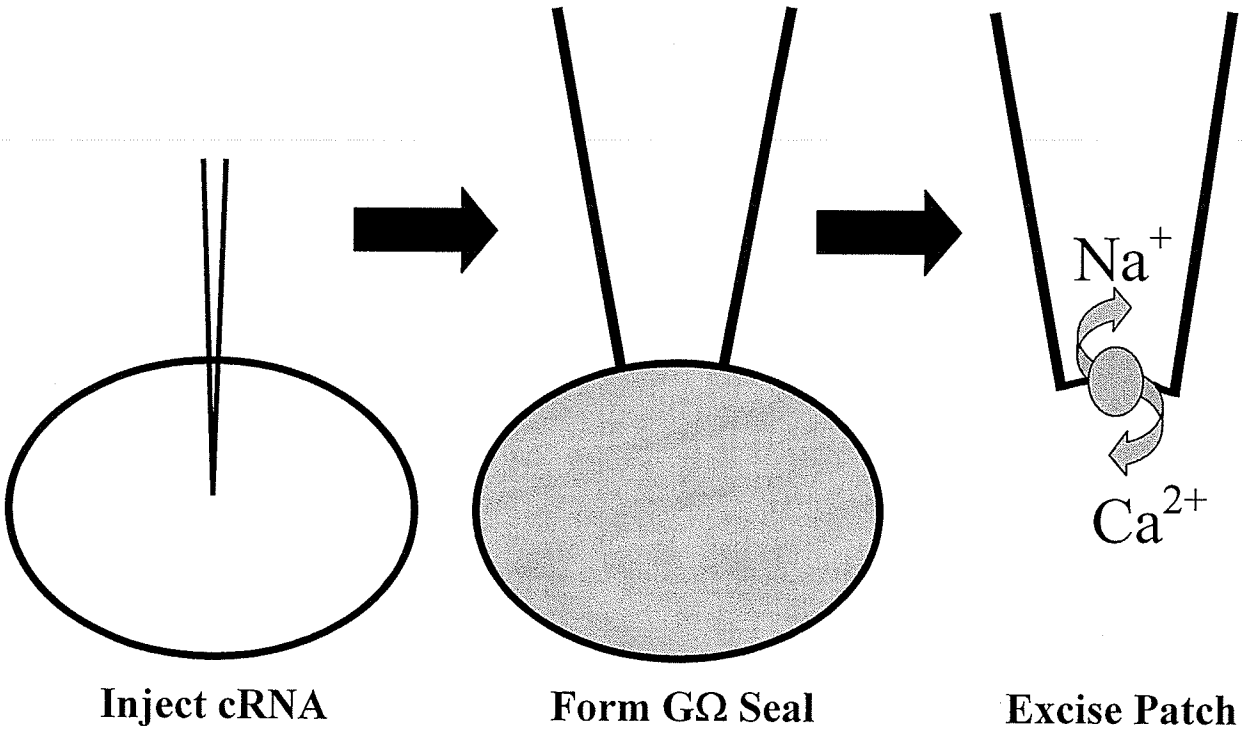

Figure 9. ***The Giant, Excised Patch Technique.*** Complimentary RNA (cRNA) encoding cardiac Na^+-Ca^{2+} exchanger protein (NCX1.1) was injected into *Xenopus laevis* oocytes (*left panel*). After 3 – 7 days, allowing time for protein expression, gigaohm (GΩ) seals were formed by gentle suction of the pipette tip onto the egg surface (*middle panel*). Excision of the membrane patch (inside-out configuration, *i.e.*, the cytoplasmic surface is exposed to the outside) was achieved by small mechanical manipulations of the pipette tip (*right panel*).

For outward (*i.e.,* reverse mode) Na^+-Ca^{2+} exchange currents, pipette (extracellular) solution contained (in mM): 100 NMG-MES, 30 HEPES, 30 TEA-OH, 16 sulfamic acid, 8.0 $CaCO_3$, 6 KOH, 0.25 ouabain, 0.1 niflumic acid, 0.1 flufenamic acid; pH 7.0 at RT with MES. Outward currents (Figure 10) were initiated by rapidly switching from a Li^+ to a Na^+-based bath solution containing (in mM): 100 [Na^+ + Li^+]-aspartate, 20 CsOH, 20 MOPS, 20 TEA-OH, 10 EGTA, 0 - 9.91 $CaCO_3$, 1.0 - 1.5 $Mg(OH)_2$; pH 7.0 at 30°C (with MES or LiOH).

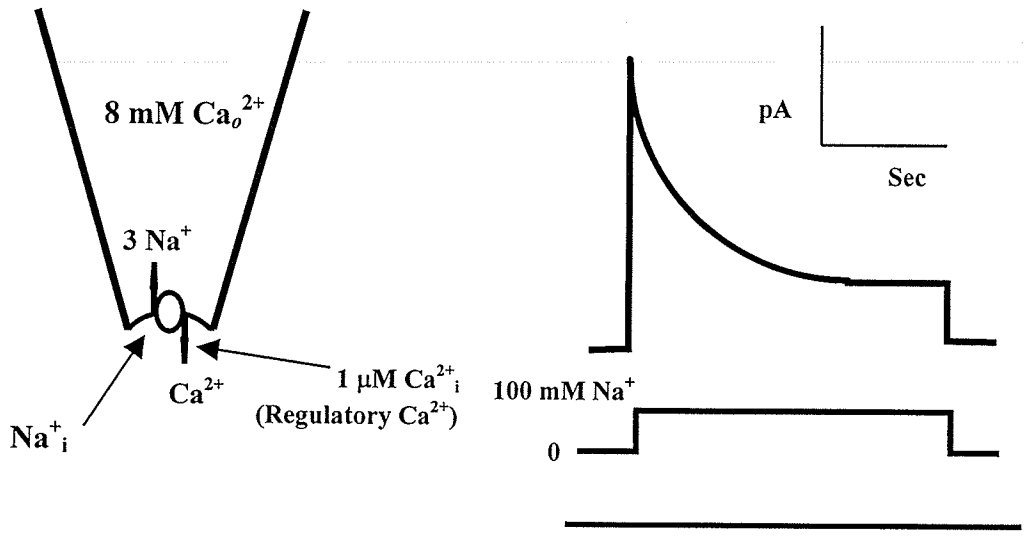

Figure 10. ***Initiation of a Typical Outward (i.e., Reverse Mode) Na^+-Ca^{2+} Exchange Current.*** For outward exchange, pipettes contain 8 mM Ca^{2+} (*left panel*). The pipette was then perfused with 100 mM Na^+ and 1 μM Ca^{2+}, initiating Na^+-Ca^{2+} exchange. As exchange occurs, 3 Na^+ ions enter the pipette in exchange for 1 Ca^{2+} ion. A net single positive charge associated with Na^+ translocation, moves across the membrane into the pipette (analogous to leaving the cell) and generates an *outward* current. The *right panel* shows a typical outward (*i.e.,* reverse mode) Na^+-Ca^{2+} exchange trace, recorded using the giant, excised patch technique.

For inward (Figure 11) Na^+-Ca^{2+} exchange current measurements, the pipette (extracellular) solution contained (in mM): 100 Na-MES, 20 CsOH, 20 TEA-OH, 10 EGTA, 10 HEPES, 8 sulfamic acid, 4 $Mg(OH)_2$, 0.25 ouabain, 0.1 niflumic acid, 0.1 flufenamic acid; pH 7.0 at R.T. with MES. Inward currents were activated by switching between Ca^{2+}-free and Ca^{2+}-containing, Li^+-based bath solutions, as described above. For combined inward-outward current measurements (on the same patch), pipettes contained (in mM): 100 Na-MES, 20 CsOH, 20 HEPES, 20 TEA-OH, 4 sulfamic acid, 2 $CaCO_3$, 0.25 ouabain, 0.1 niflumic acid, 0.1 flufenamic acid; pH 7.0 at RT (with MES). Outward and inward currents were activated using the same solutions as those used for initiating pure outward and pure inward currents, as described above.

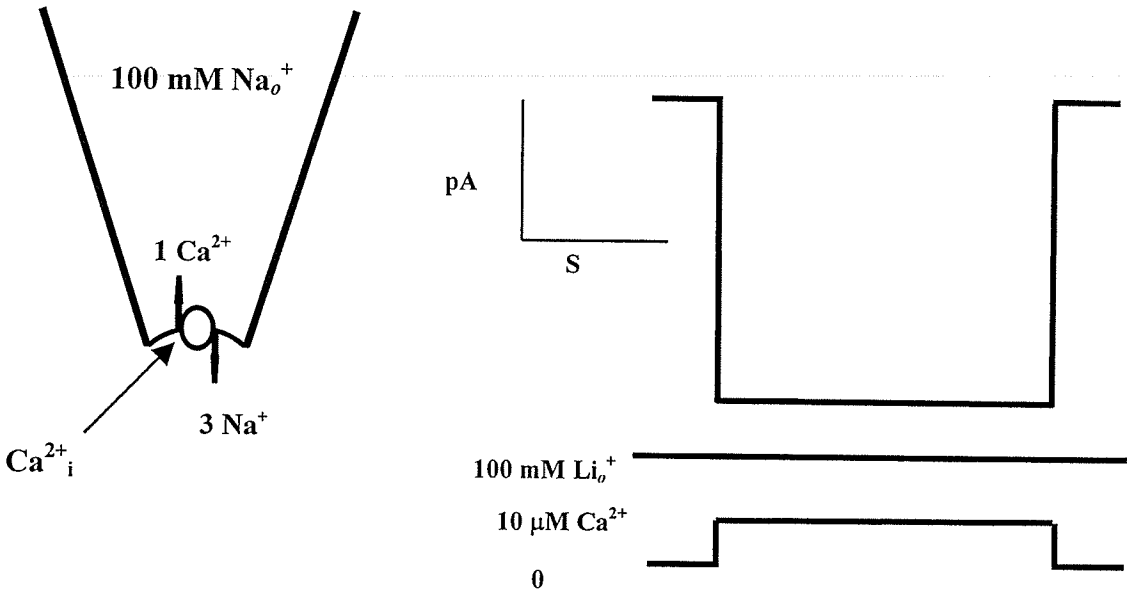

Figure 11. ***Initiation of a Typical Inward (i.e. Forward Mode) Na^+-Ca^{2+} Exchange Current.*** Here, pipettes contain 100 mM Na^+ (*left panel*). The pipettes were perfused in 100 mM Li^+ and 10 μM Ca^{2+} initiating inward Na^+-Ca^{2+} exchange. As exchange occurs 1 Ca^{2+} ion is brought into the pipette in exchange for 3 Na^+ ions. Therefore, the single positive charge associated with Na^+ translocation moves out of the pipette (analogous to entering the cell), consequently generating an *inward* current. The *right panel* shows a typical inward (*i.e.* forward mode) Na^+-Ca^{2+} exchange trace, recorded using the giant, excised patch technique.

Axon Instruments hardware (Axopatch 200a) and software (Axotape) were used for data acquisition and analysis. Origin software was used for curve-fitting (e.g. IC_{50} values) and statistical analyses. Pooled data are presented as mean ± SEM. Two-tailed Student's t-tests were used for comparison of unpaired data, and $P < 0.05$ was considered significant. Free Mg^{2+} and Ca^{2+} concentrations were calculated using MAXC software (25). Unless indicated otherwise, a holding potential of 0 mV was implemented for current measurements. All experiments were conducted at 30 ± 1°C.

SEA0400 was prepared by dissolving in DMSO as a 20-40 mM stock and further diluted directly into bath solutions. With each drug concentration change, a time period of at least 32 seconds was allowed to lapse prior to re-examining current levels. The concentration of DMSO never exceeded 0.075% and was without effect on inward or outward Na^{+}-Ca^{2+} exchange current characteristics. The solubility of SEA0400 in water is 0.03 μg/ml. In these studies however, SEA0400 was dissolved in pure DMSO, and further diluted into other experimental (buffered) solutions. The highest SEA0400 concentration used in any experimental setting was 3 μM. Taisho Pharmaceutical Co. Ltd. generously provided SEA0400.

IV. RESULTS

1. SEA0400 and Na^+-Ca^{2+} Exchange Currents

The effects of SEA0400 on both outward (reverse mode) and inward (forward mode) exchange current were measured in giant, excised membrane patches from *Xenopus laevis* oocytes expressing the canine cardiac exchanger (NCX1.1). To determine mode selectivity of SEA0400, combined outward-inward exchange currents were recorded in the absence and presence of 0.1 μM SEA0400 (Figure 12A). Both modes (inward and outward) were recorded on the same membrane patch, containing the same population of exchangers. For outward-inward current recordings, pipettes contained 2 mM Ca^{2+} and 100 mM Na^+. Outward or reverse mode exchange currents were initiated by applying 100 mM Na^+ to the cytoplasmic patch surface with 1 μM regulatory Ca^{2+}. Inward currents were activated by switching from a 100 mM Li^+ and 1 μM Ca^{2+} solution to a 100 mM Li^+ and 10 μM Ca^{2+} solution (in the absence of Na^+). Control outward and inward Na^+-Ca^{2+} exchange currents exhibited typical characteristics. That is, outward currents displayed their usual rise to a peak, followed by a progressive decay (a result of Na^+-dependent inactivation (I_1)) to a steady state level. Inward (forward mode) currents, however, showed no inactivation (I_1) and appear as square waveforms. When 0.1 μM SEA0400 was applied, the resulting effect was a substantial inhibition of outward Na^+-Ca^{2+} exchange current.

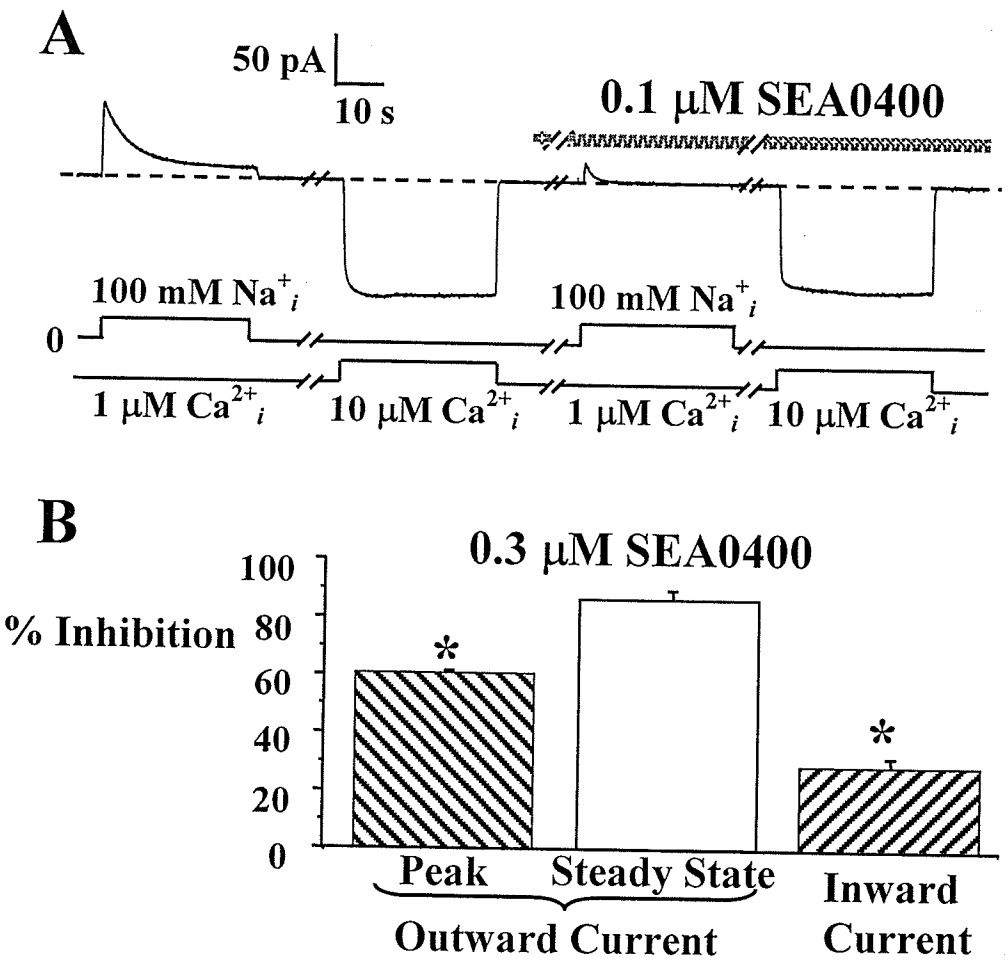

Figure 12. ***The Inhibitory Effects of SEA0400 on Combined Inward-Outward Exchange Activity.*** Figure A (*top*) shows a typical NCX1.1 mediated exchange current recording from an excised membrane patch measuring inward and outward exchange. The pipette contained 2 mM Ca^{2+} and 100 mM Na^{+}. Outward currents were initiated by applying 100 mM Na^{+} to the cytoplasmic surface of the patch with 1 μM regulatory Ca^{2+}_{i}. Inward currents were initiated by applying 100 mM Li^{+} and 10 μM Ca^{2+} to the cytoplasmic surface. Currents were recorded before and after the application of 0.1 μM SEA0400. Figure 2B shows the % inhibition of peak and steady state for both inward and outward currents, in the presence of 0.3 μM SEA0400.

Results demonstrated minimal inhibition of the inward Na^+-Ca^{2+} exchange currents, with 0.1 μM SEA0400. Shown in Figure 12B, are the pooled results of 0.3 μM SEA0400 on inhibition of peak and steady state currents for both outward and inwards currents. For outward currents, 0.3 μM SEA0400 reduced peak and steady state currents by 61 ± 1% and 87 ± 4% respectively, whereas inward currents were inhibited by 29 ± 4%. Therefore, these data show a preferential inhibition of outward (reverse mode) Na^+-Ca^{2+} exchange by SEA0400, under bi-directional conditions.

Once SEA0400's reverse mode exchange selectivity had been established, an evaluation of inhibitory potency on Na^+-Ca^{2+} exchange was performed. In this case, measurements were conducted under unidirectional conditions, where only a single transport mode could occur. Figure 13A illustrates the inhibitory effects of SEA0400 on a representative outward Na^+-Ca^{2+} exchange current. Switching from a bath solution (cytoplasmic surface) containing 100 mM Li^+ to 100 mM Na^+ activated the outward Na^+-Ca^{2+} exchange currents. As required for exchanger activation, 1 μM Ca^{2+} (regulatory Ca^{2+}) was constantly present during recording, while pipette Ca^{2+} was maintained at 8 mM (transport Ca^{2+}). Application of 0.1 and 1 μM SEA0400 to the cytoplasmic surface of the patch resulted in a dose-dependent inhibition of both peak and steady state outward Na^+-Ca^{2+} exchange currents. Figure 13B represents the pooled data of SEA0400 over a range of concentrations, further illustrating SEA0400's concentration dependent effect.

To establish this range of values, SEA0400 was applied in continuous increments and the resulting inhibition was recorded. These increments were used primarily because a satisfactory washout of SEA0400 could not be obtained. In both typical traces and pooled values, SEA0400 appeared to have a greater inhibitory potency (IC_{50}) for steady

state currents than for peak currents, with IC_{50} values of 23 ± 4 nM and 78 ± 15 nM, respectively.

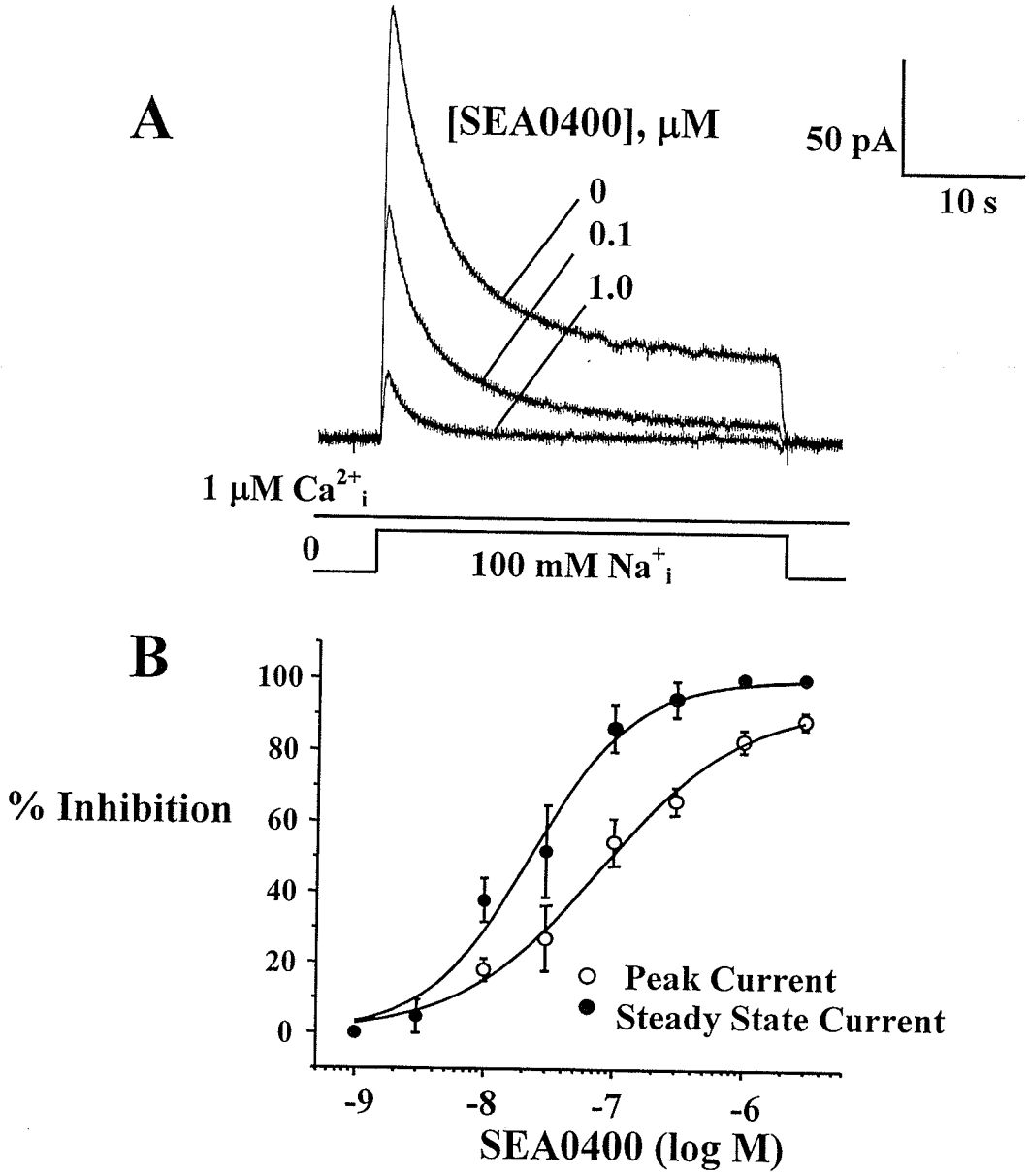

Figure 13. ***Concentration-Dependent Inhibition of Wild-Type NCX1.1 Outward Exchange Current with SEA0400.*** Panel A (*top*) shows typical outward Na^+-Ca^{2+} exchange currents from an excised membrane patch in the absence and presence of different SEA0400 (0, 0.1, 1 μM) concentrations. Panel B (*bottom*) shows the SEA0400 concentration dependency for inhibition of outward Na^+-Ca^{2+} exchange currents (peak and steady state). Pooled data show means ± S.E. obtained from 3-13 patches at each individual SEA0400 concentration.

2. SEA0400 and Na^+-Ca^{2+} Exchange Regulatory Mechanisms (I_1 and I_2)

To investigate SEA0400's inhibitory mechanism(s), experiments were conducted on outward Na^+-Ca^{2+} exchange currents in the *absence* of any primary-structure or protein based regulatory mechanisms (*i.e.*, I_1 and I_2). Membrane patches were deregulated by treatment with 1 mg/ml α-chymotrypsin for ~ 1-2 minutes. This limited proteolysis resulted in a loss of both Na^+-dependent inactivation (I_1) and Ca^{2+}-dependent regulation (I_2), leaving the exchanger in a fully activated state (116). The exchanger displayed a square waveform and no longer required cytoplasmic Ca^{2+} (regulatory Ca^{2+}) for activation. Figure 14A displays a representative outward current following α-chymotrypsin treatment, in the absence and presence of 0.1 and 1.0 μM SEA0400. Compared to intact Na^+-Ca^{2+} exchangers, the level of inhibition was notably reduced, even at a 10-fold increase in concentration. Figure 14B shows the pooled values for percent inhibition of SEA0400 following proteolytic treatment. A complete inhibitory profile of SEA0400 could not be obtained, because the compound began to precipitate out of solution at concentrations above 1-3 μM. However, an estimated IC_{50} value of 1.2 ± 0.6 μM is given. Regardless of limited solubility, these results suggested that SEA0400 requires intact regulatory mechanisms for a complete inhibitory effect.

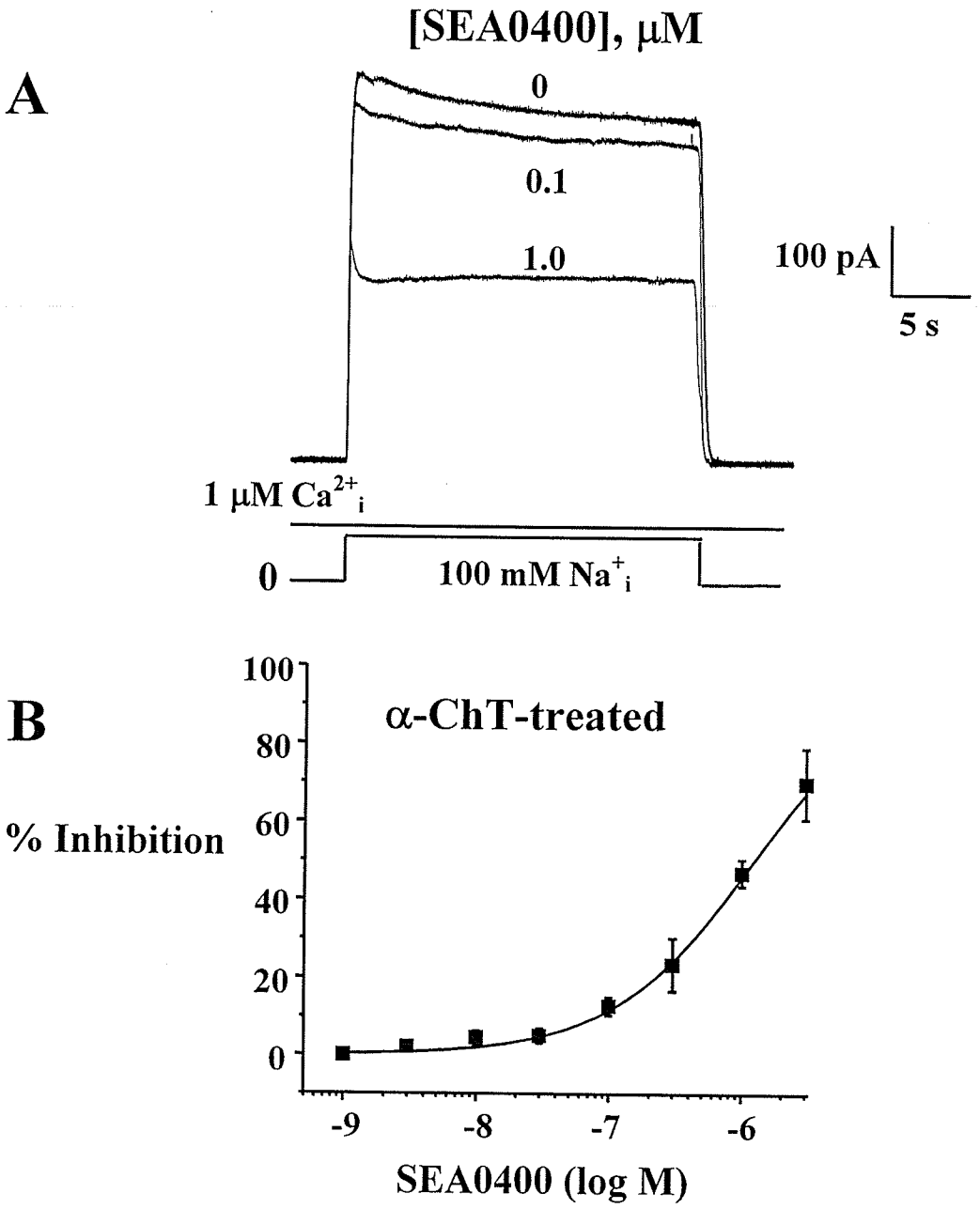

Figure 14. ***Effects of SEA0400 on Outward Exchange Currents After Proteolytic Treatment.*** Panel A (*top*) shows typical outward Na^+-Ca^{2+} exchange currents from an excised membrane patch that was deregulated by the cytoplasmic application of 1 mg/ml α-chymotrypsin for ~ 1 minute. Currents are shown in the absence and presence of 0, 0.1, and 1.0 μM SEA0400. Pooled results are shown in panel B (*bottom*), where each point represents the mean ± S.E obtained from 3-12 patches.

3. Effect of SEA0400 with Increasing Regulatory Ca^{2+}

Increases in regulatory Ca^{2+} can stimulate outward Na^{+}-Ca^{2+} exchange activity (116; 121). Activation occurs only when Ca^{2+} is applied to the cytoplasmic surface of the patch. This mechanism is referred to as Ca^{2+}-dependent regulation, or I_2 (121). Inward Na^{+}-Ca^{2+} exchange currents do not exhibit this type of behaviour for the regulatory Ca^{2+} binding site is saturated ($K_d \sim 0.3$ μM) under inward current recording conditions (210). Therefore, it was suggested that during outward (reverse mode) Na^{+}-Ca^{2+} exchange, SEA0400 might interact with varying regulatory Ca^{2+} levels. Results between SEA0400 and Ca^{2+} would be more pronounced during outward Na^{+}-Ca^{2+} exchange, as regulatory Ca^{2+} levels are low (*i.e.,* 1 μM) compared to those for inward current (*i.e.,* 10 μM). Figure 15A shows the effect of regulatory Ca^{2+} concentrations on outward Na^{+}-Ca^{2+} exchange currents, in the absence and presence of 1 μM SEA0400. Ca^{2+}-dependent regulation (I_2) is visible during the control trace, producing a square waveform and essentially eliminates Na^{+}-dependent inactivation (I_1) at 10 μM Ca^{2+}. However, at the lower regulatory Ca^{2+} concentration of 1 μM, Na^{+}-dependent inactivation (I_1) is present. Upon application of 1 μM SEA0400, Na^{+}-Ca^{2+} exchange currents are inhibited at both 1 and 10 μM Ca^{2+}. Compared to inhibition at 1 μM Ca^{2+}, SEA0400's effects are reduced at 10 μM Ca^{2+}. This result is most prominent for peak currents. Furthermore, the elimination of Na^{+}-dependent inactivation (I_1) at 10 μM Ca^{2+} is absent in the presence of SEA0400. The effects of SEA0400 and regulatory Ca^{2+} on F_{ss} values (ratio of steady state to peak currents) are shown in Figure 15B (pooled data). These data suggest that when in the presence of SEA0400, 10 μM Ca^{2+} is unable to increase F_{ss} values as it does

in control recordings. Moreover, these results suggest a potential interaction between SEA0400 and the Na^+-dependent inactivation (I_1) regulatory mechanism.

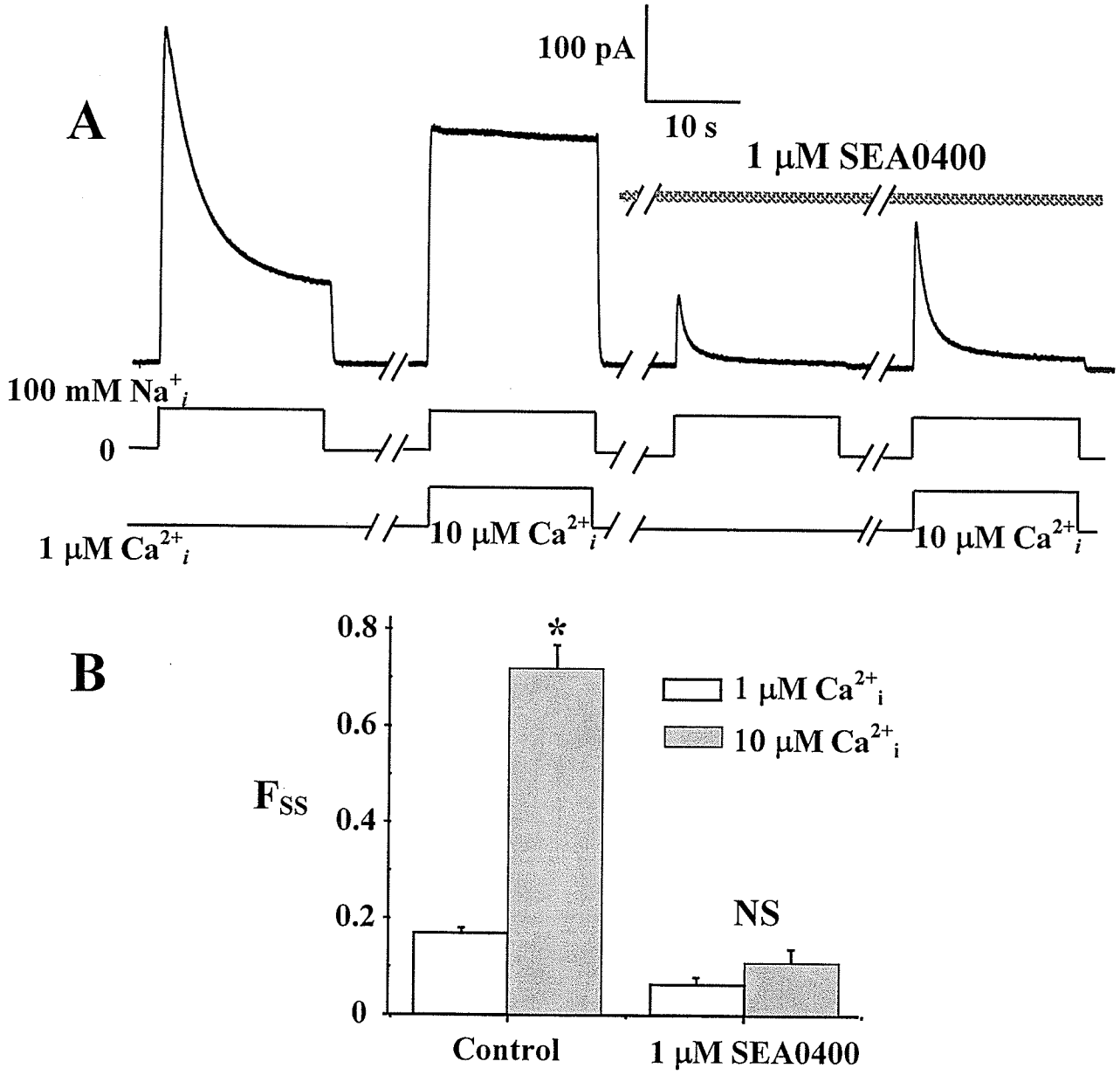

Figure 15. ***Effects of SEA0400 with Increasing Regulatory Ca^{2+} Concentrations.*** Panel A (*top*) shows the effects of regulatory Ca^{2+} on typical outward Na^+-Ca^{2+} exchange currents before and after treatment with 1 μM SEA0400. Currents were initiated by applying 100 mM Na^+ to the cytoplasmic surface of the patch with either 1 or 10 μM regulatory Ca^{2+} present. Panel B (*bottom*) shows pooled data (mean ± S.E., n = 3-43 patches) illustrating the effect of regulatory Ca^{2+} on F_{SS} (ratio of steady state to peak current) for control and SEA0400 treated patches.

4. SEA0400 and Exchanger Recovery

To examine the hypothesis that SEA0400 interacts with Na^+-dependent inactivation (I_1), paired-pulse experiments were performed to determine exchanger rate of recovery from I_1. Outward currents were initiated through the cytoplasmic application of 100 mM Na^+ with 1 μM Ca^{2+}. Following exchanger activation, an inter-pulse was initiated 6.4 seconds into the recovery period, thereby stimulating outward exchange (Figure 16A). The paired-pulse experiments were conducted in the presence and absence of 0.1 μM SEA0400, over a range of time intervals and regulatory Ca^{2+} concentrations. Figure 16B demonstrates SEA0400's ability to reduce the rate of recovery for peak outward currents at an increased regulatory Ca^{2+} level of 3 μM. In addition, recovery rates measured over a wide range of regulatory Ca^{2+} values supports the contention that SEA0400 can interfere with exchanger recovery from I_1, as is shown in Figure 16C. In Na^+-Ca^{2+} exchangers with full regulatory function, increased regulatory Ca^{2+} significantly augmented the rate of recovery from I_1. This recovery is strongly attenuated by the presence of SEA0400. These results suggest that SEA0400 essentially stabilizes or promotes the entry of the exchanger into its Na^+-dependent inactive state (I_1).

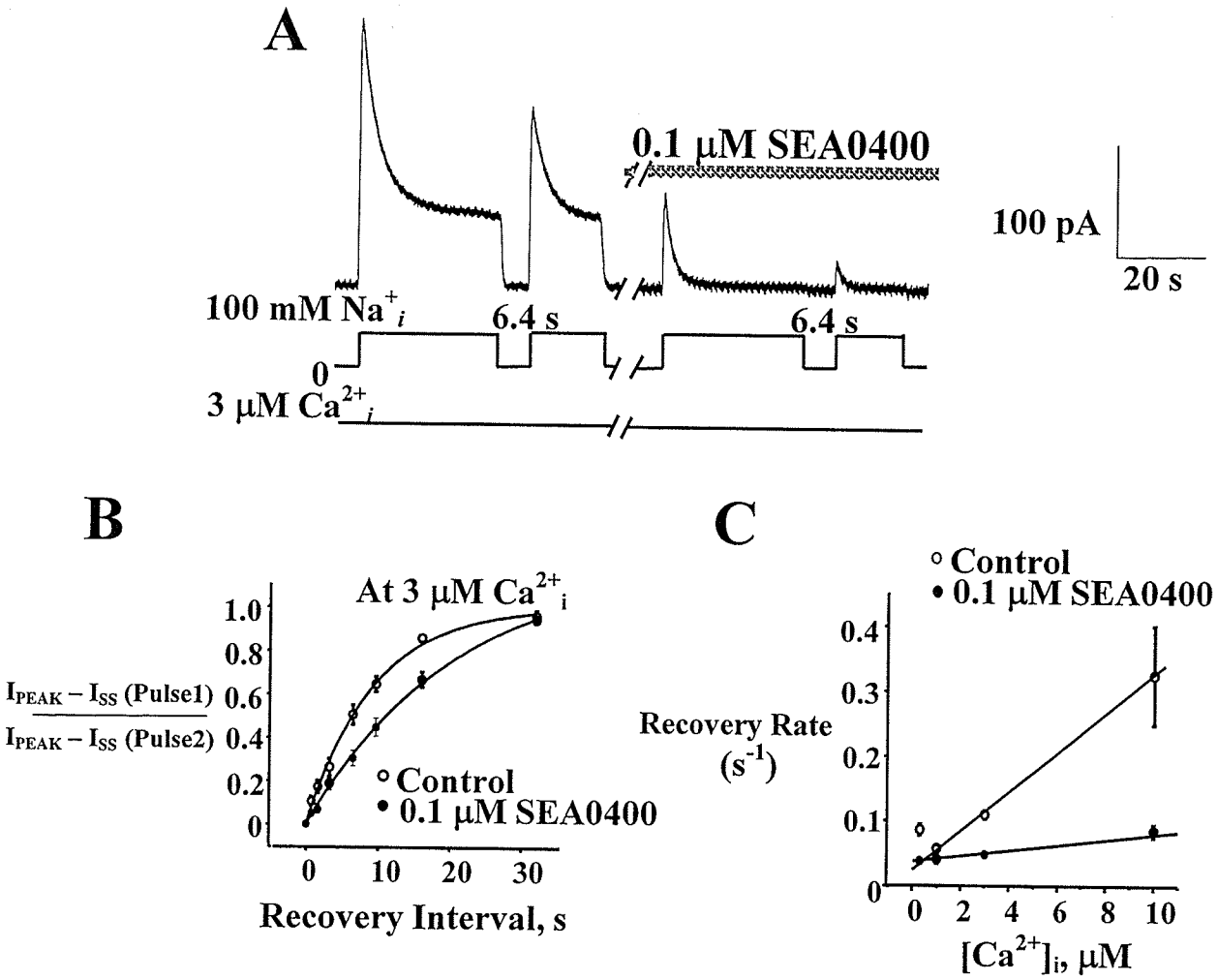

Figure 16. ***Effects of SEA0400 on Exchanger Recovery.*** Panel A (*top*) shows the effects of SEA0400 on representative paired-pulse recovery experiments where an inter-pulse interval of 6.4 sec is given. Outward Na^+-Ca^{2+} exchange currents were initiated by applying 100 mM Na^+ and 1 μM regulatory Ca^{2+} to the cytoplasmic surface of the patch. Pooled data are shown in panel B (*bottom left*) for results obtained from 6-7 patches (means ± S.E.) over a range of interpulse intervals (0.7-32 sec) to determine recovery rates. This data was used to generate panel C (*bottom right*), which shows recovery rates over a range of Ca^{2+} concentrations, in the presence and absence of 0.1 μM SEA0400. Points in panel C (*bottom right*) represents pooled data from 3-10 patches.

5. Effect of SEA0400 on Inward Na^+-Ca^{2+} Exchange

To further analyze SEA0400's mechanism of action, the compound was applied to intact and deregulated (1 mg/ml α-chymotrypsin) Na^+-Ca^{2+} exchangers and inward currents were measured (Figure 17A). Inward currents were initiated by applying 100 mM Li^+ with 10 μM Ca^{2+} to the cytoplasmic membrane surface, in exchange for 100 mM Na^+ (pipette). The inhibitory potency of SEA0400 on intact exchangers exhibiting forward mode exchange (inward current) is substantially less than that of reverse mode exchange (outward current). Consequently, the inhibitory efficacy of SEA0400 was further attenuated in deregulated exchangers (even at 3 μM SEA0400). As mentioned previously, SEA0400 demonstrated poor solubility at higher concentrations (> 1 μM); therefore it was difficult to assess an IC_{50} value for inward current. However an IC_{50} of ~ 8 μM was estimated for inward Na^+-Ca^{2+} current in intact patches.

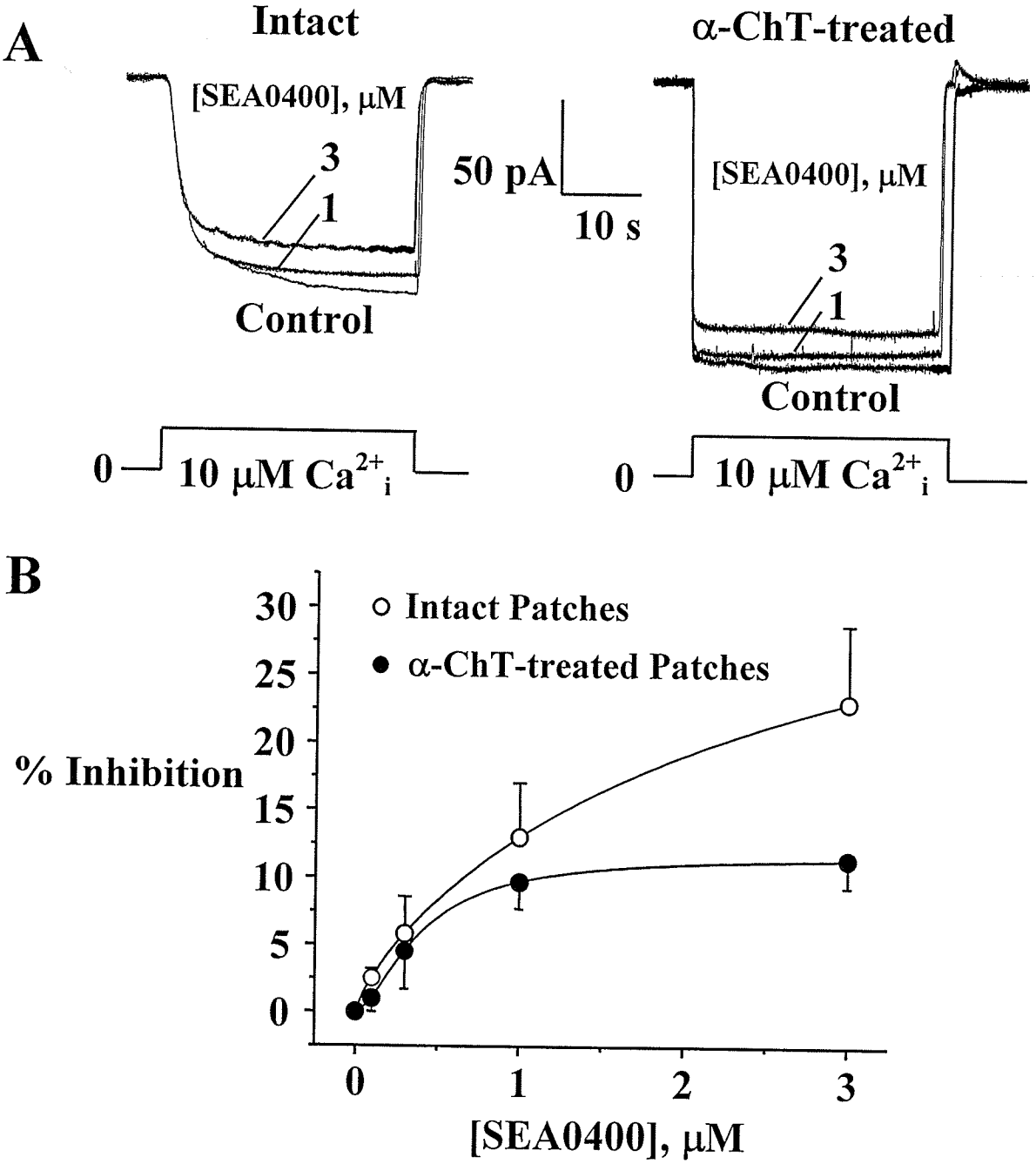

Figure 17. ***Effects of SEA0400 on Inward Exchange Currents After Proteolytic Treatment.*** Panel A (*top*) shows the effects of SEA0400 for typical inward Na^+-Ca^{2+} exchange currents before and after limited patch proteolysis with 1 mg/ml α-chymotrypsin, which deregulates the exchanger. In panel B (*bottom*), pooled data show mean values ± S.E. obtained from 3-15 patches.

6. NCX1.1 Mutant Exchangers

To test the hypothesis that SEA0400 stabilizes or facilitates entry of the exchanger into I_1, the effects of SEA0400 were tested on mutant exchangers exhibiting altered I_1 and I_2 regulatory characteristics. These three distinctive mutant exchanger groups, shown in Figures 18A, 18B and 18C, were previously characterized by the Philipson group in 1997 (209). Figure 18A illustrates Group 1 mutants (F223E and K225Q). Both of these mutants exhibited an accelerated rate of inactivation for outward current, which is measured as λ (discussed later) but differed in their extents of I_1. The extent of I_1 is measured by a ratio of steady state to peak current and is known as an F_{ss} value. The F223E mutant displayed an increase in I_1, whereas K225Q demonstrated a decrease in the extent of I_1, as compared to wild-type NCX1.1. In the Group 2 mutants (K229Q and Δ229-232), the extent of I_1 inactivation is greatly diminished compared to wild-type NCX1.1. Figure 18B shows outward currents of both Δ229-232 and K229Q, which display square waveforms, suggesting a lack of Na^+-dependent inactivation (I_1). The last mutant group, Group 3, contains the Δ680-685 mutation shown in Figure 18C. This mutant appears to have a greatly reduced I_2 regulatory mechanism. Illustrated in Figure 18C, are the resulting outward currents at 1 and 10 μM regulatory Ca^{2+}, that suggest a relative absence of both ionic regulatory mechanisms (I_1 and I_2). For the Δ680-685 mutant, there appears to be a decrease in current magnitude at 10 μM regulatory Ca^{2+}. This is most likely due to competition between intracellular Na^+ and Ca^{2+} for the exchanger transport sites as a result of the higher Ca^{2+} concentration.

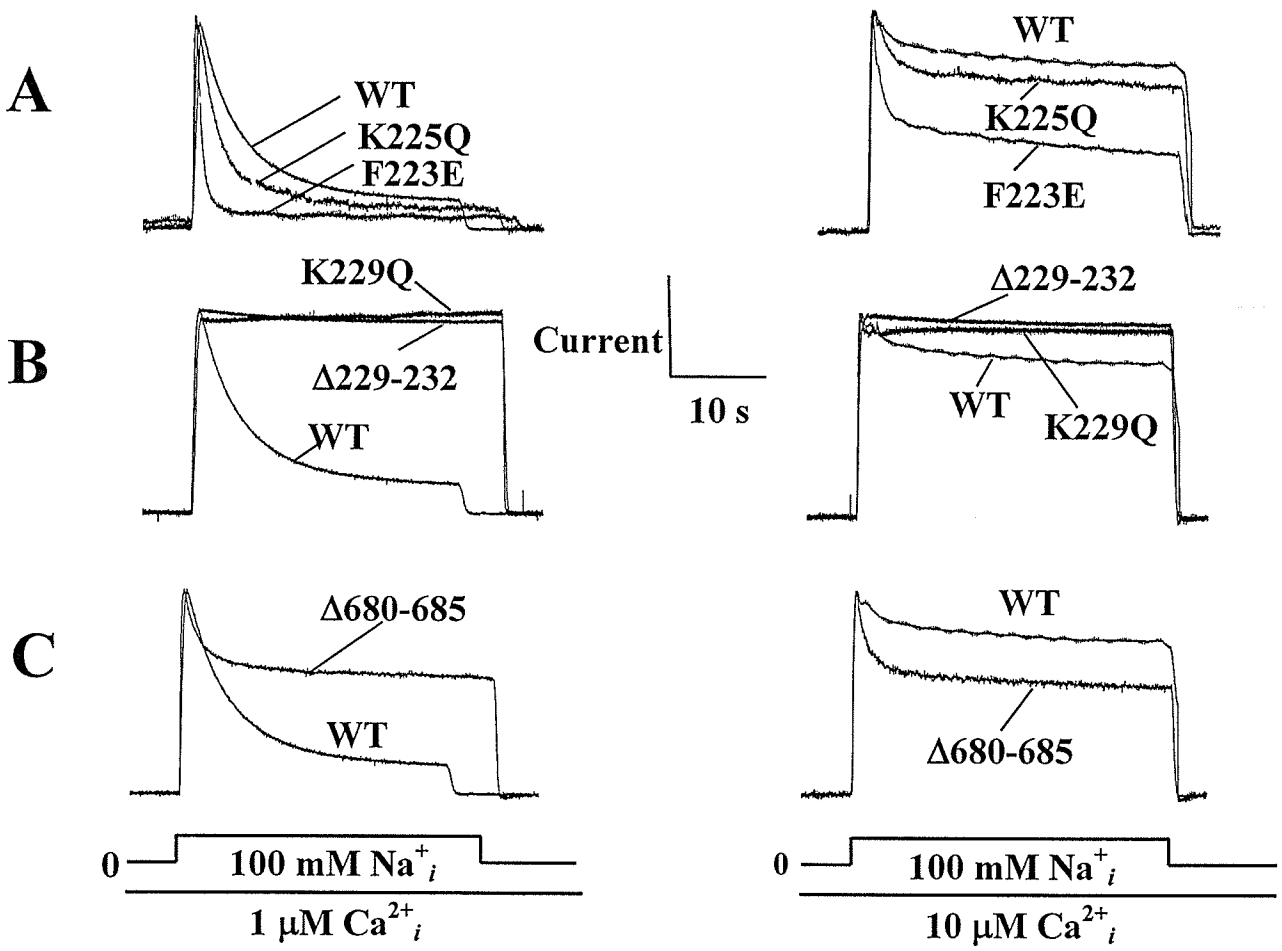

Figure 18. ***Electrophysiological Profiles of Wild-Type and NCX1.1 Mutants.*** This figure illustrates the three distinct groups of mutant NCX1.1 exchangers used to investigate the inhibitory mechanism of SEA0400 at 1 and 10 μM Ca^{2+}. Panel A (*top*) displays two mutant exchangers with increased Na^{+}_{i}-dependent inactivation (I_1). Panel B (*middle*) displays two mutants that have suppressed Na^{+}_{i}-dependent inactivation (I_1). Lastly, Panel C (*bottom*) displays a single mutant with altered Ca^{2+}_{i}-dependent regulation (I_2). Currents were initiated by the application of 100 mM Na^{+} with either 1 or 10 μM regulatory Ca^{2+}.

7. Group 1 NCX1.1 Mutants (Outward Current)

From previous results, it was suggested that SEA0400 interacts with the Na^+-dependent inactivation mechanism, either by stabilizing I_1 in the presence of high Ca^{2+}, or by promoting the entry of the exchanger into an inactive state. Furthermore, SEA0400 only exerted it effects strongly when I_1 was present (*i.e.,* reverse mode). However, in a deregulated setting (*i.e.,* α-chymotrypsin), where I_1 is absent, SEA0400 shows greatly reduced effects. Furthermore, for inward currents (forward mode), I_1 is absent and so is the inhibitory effect of SEA0400. These results suggested an interaction between SEA0400 and the exchanger's ionic regulatory mechanisms. Mutants displaying increased Na^+-dependent inactivation were tested in the presence of SEA0400. If a SEA0400-I_1 interaction existed, then perhaps SEA0400 could inhibit to a greater degree, when the extent of I_1 was increased. Figure 19A shows the effect of 0.1 μM SEA0400 on outward Na^+-Ca^{2+} exchange currents for mutant K225Q, where the rate of inactivation was increased, but the extent of I_1 inactivation (F_{ss}) was decreased or comparable to wild-type values. In this mutant, the inhibitory effects of SEA0400 on peak and steady state outward currents were similar to that of wild-type at both 1 and 10 μM regulatory Ca^{2+} and in the presence or absence of SEA0400 (Table 3). Demonstrated in Figure 19B, however, is the second Group 1 mutant, F223E. Prior to SEA0400 application, this mutant displays a clearly accelerated current decay, coupled with an increase in the extent of I_1. Table 2 shows that the extent of I_1 inactivation (F_{ss}) is greater at 1 μM Ca^{2+} than at 10 μM Ca^{2+}. Upon SEA0400 application, there was a further increase in the extent of I_1, bringing steady state current levels near baseline. This however, made the calculation of

percent inhibition and F_{ss} more difficult. In the presence of 1 and 10 μM Ca^{2+}, SEA0400 inhibited steady state currents by ~ 100 % and 56 ± 4 %, respectively. Peak currents for F223E were less affected by SEA0400's presence. Compared to F223E, results of K225Q with or without SEA0400 may be a consequence of being a more subtle mutation than that of F223E.

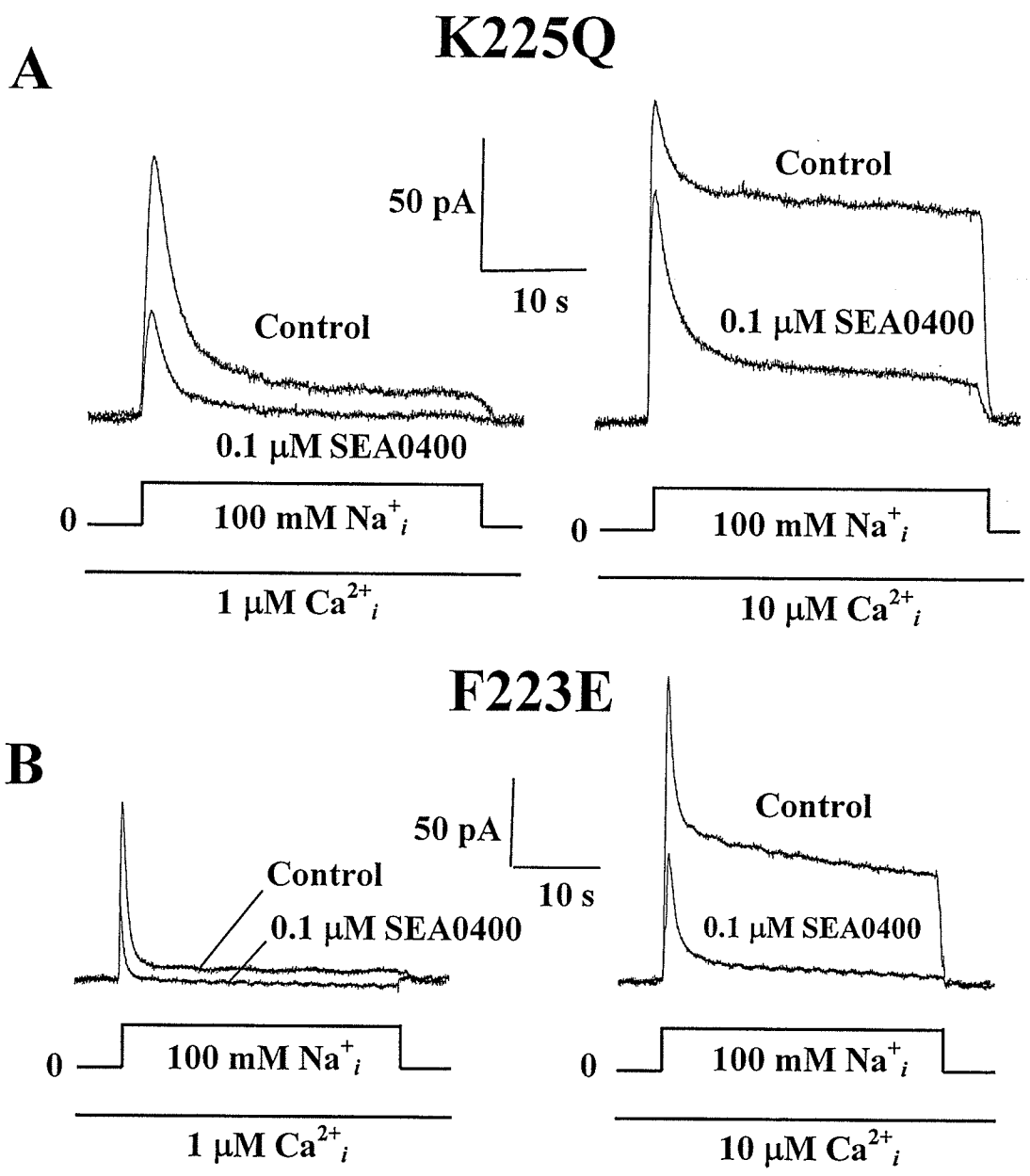

Figure 19. ***Effects of SEA0400 on Outward Na^+-Ca^{2+} Exchange Currents of Mutant NCX1.1 Exchangers Exhibiting Enhanced I_1 Inactivation.*** Panels A (*top*) and B (*bottom*) illustrate the effects of 0.1 μM SEA0400 on exchange currents from K225Q (A) and F223E (B), in the presence of 1 and 10 μM regulatory Ca^{2+}_i, respectively. Outward currents were initiated by applying 100 mM Na^+ to the cytoplasmic surface of the patch with 1 or 10 μM Ca^{2+}.

8. Group 2 NCX1.1 Mutants (Outward Current)

Experiments were conducted on mutants lacking Na^+-dependent inactivation to address the hypothesis that SEA0400 and I_1 interact If SEA0400 interacted as suggested, inhibition should be suppressed in these mutants (lacking Na^+-dependent inactivation (I_1)). The Group 2 mutants, K229Q and Δ229-232 both exhibited square current waveforms, indicating the absence of I_1. However, Figure 20A shows prominent inhibition of both peak and steady state current (at 1 μM regulatory Ca^{2+}) upon application of 0.1 μM SEA0400 on K229Q outward exchange currents. Furthermore, as shown in the right panel (Figure 20A), the inhibitory effects of SEA0400 were attenuated upon switching to a higher regulatory Ca^{2+} value (*i.e.,* 10 μM). As peak current inhibition at 1 and 10 μM Ca^{2+} remains relatively the same (26 ± 6 % and 22 ± 6 %, respectively), steady state current inhibition was significantly attenuated in the presence of 10 μM Ca^{2+}. SEA0400 may induce I_1-like behaviour in K229Q, which can be alleviated by increasing regulatory Ca^{2+} concentrations. In addition, this indicates that the I_1-like inactivation induced by SEA0400 behaves in a similar manner to the native I_1 inactivation process (with respect to regulatory Ca^{2+}), even though K229Q apparently lacks this form of regulation in SEA0400's absence. The second Group 2 mutant, Δ229-232 also shows a lack of I_1 in the absence of SEA0400. However, unlike K229Q, outward exchange current from Δ229-232 is minimally affected by 0.1 μM SEA0400 (Figure 20B). This slight inhibitory effect of SEA0400 was recorded at both high and low regulatory Ca^{2+} concentrations (*i.e.,* 1 and 10 μM). These differences, may be a result of Δ229-232 being a deletion mutant starting at the same point as K229Q. This

gross mutation (Δ229-232) may remove an entire portion of the XIP region involved in I_1 formation. These results continue to support the hypothesis that SEA0400 interacts with I_1; because when I_1 is absent, SEA0400 is almost without effect.

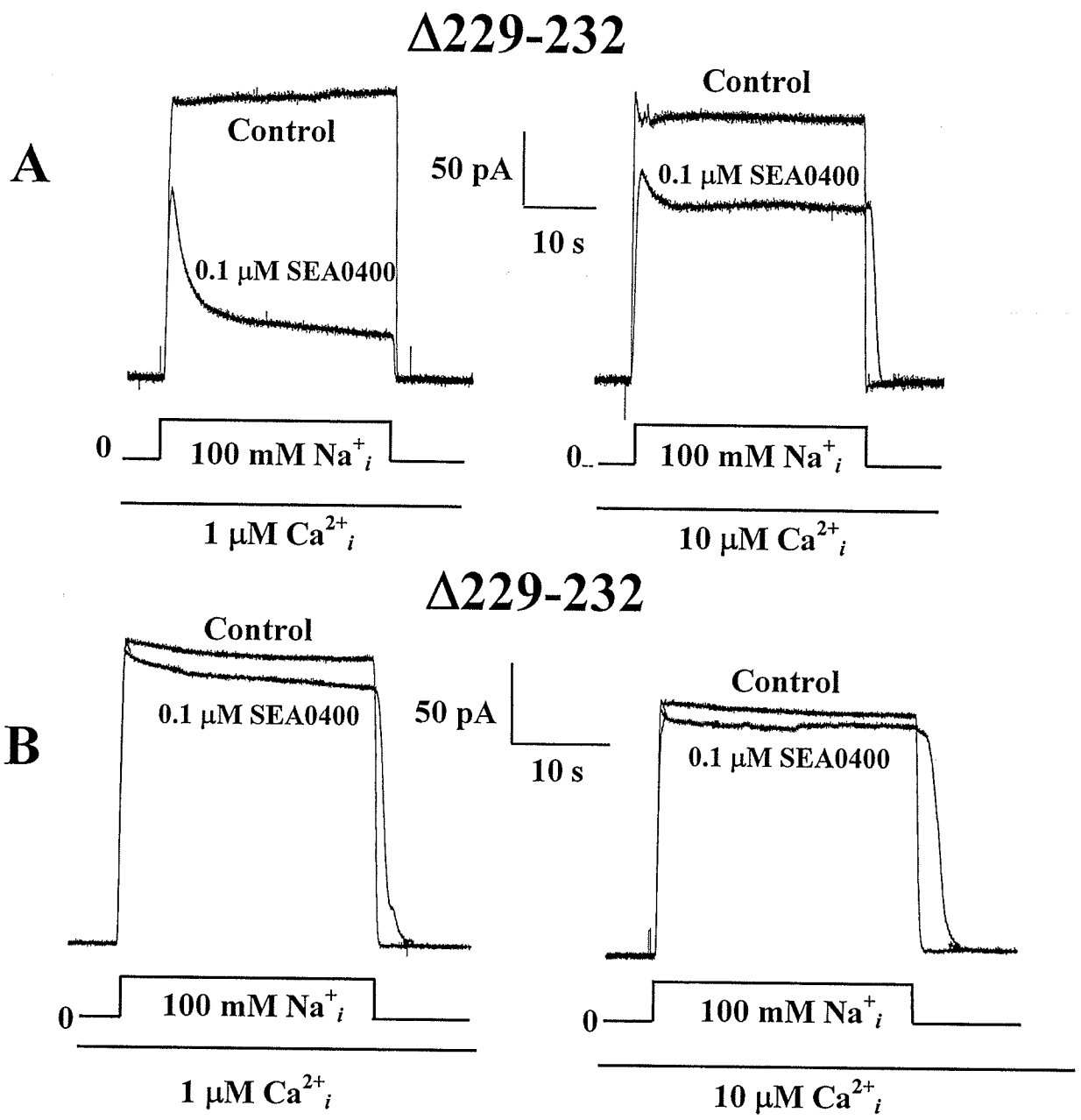

Figure 20. ***Effects of SEA0400 on Outward Na^+-Ca^{2+} Exchange Currents of Mutant NCX1.1 Exchangers Exhibiting Suppressed I_1 Inactivation.*** Panels A (*top*) and B (*bottom*) illustrate the effects of 0.1 μM SEA0400 on outward exchange currents mediated by Δ229-232 (A) and K229Q (B) in the presence of 1 μM (*left*) and 10 μM (*right*) regulatory Ca^{2+}. Outward currents were initiated by rapidly applying 100 mM Na^+ to the cytoplasmic surface of the patch with either 1 or 10 μM regulatory Ca^{2+}.

9. Group 3 NCX1.1 Mutants (Outward Current)

The last category of NCX1.1 mutants consisted of only one member, Δ680-685. This non-XIP mutant (created in the COOH-terminal of the intracellular loop) demonstrated suppressed Ca^{2+}-dependent regulation (I_2) (212). Represented in Figure 21 are the effects of 0.1 μM SEA0400 on outward Δ680-685 exchange currents in the presence of 0, 1, and 10 μM regulatory Ca^{2+}. Ca^{2+}-dependent regulation (I_2) is lacking in Δ680-685, for this mutant exchanger is fully active in the absence of regulatory Ca^{2+} (*i.e.*, 0 μM). Consecutive increases in regulatory Ca^{2+} for control currents show no alteration in effect, save for a small decrease in peak current at 10 μM Ca^{2+}. This can be explained as transport-ion competition. However, regardless that the exchanger lacks I_2, inhibition with SEA0400 mirrors that of wild-type. Table 1 shows that for Δ680-685, % peak inhibition was 32 ± 8 and 31 ± 6, while the wild-type was 57 ± 6 and 31 ± 8 at 1 and 10 μM regulatory Ca^{2+}, respectively. These results suggest that SEA0400 does not interact with and/or require Ca^{2+}-dependent regulation (I_2) for proper inhibition.

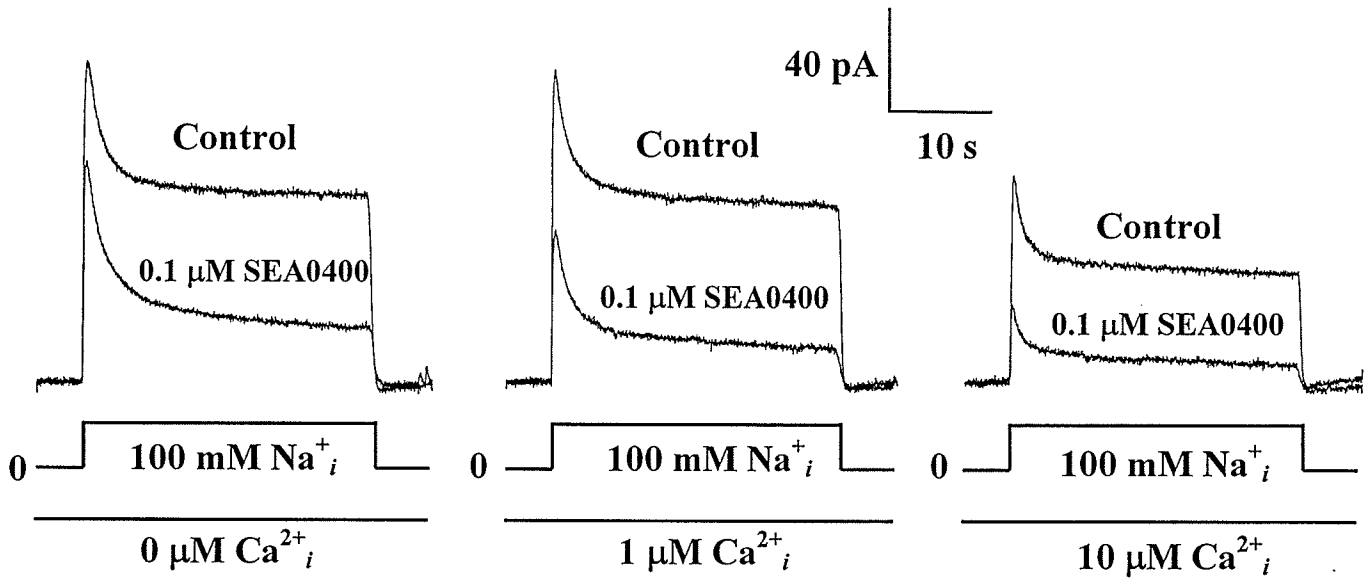

Figure 21. ***Effects of SEA0400 on Outward Na^+-Ca^{2+} Exchange Currents of a Mutant NCX1.1 Exchanger Exhibiting Altered I_1 and I_2 Regulation.*** This figure demonstrates the effects of 0.1 μM SEA0400 on Δ680-685 exchange currents in the presence of 0 (*left*), 1 (*middle*) and 10 (*right*) μM regulatory Ca^{2+}. Outward exchange currents were initiated by applying 100 mM Na^+ to the cytoplasmic surface of the patch with 0, 1 or 10 μM regulatory Ca^{2+}.

10. F_{ss} and λ

Tables 3 and 4 summarize the F_{ss} and λ results for NCX1.1 exchangers and all three mutant groups, in the absence and presence of 0.1 μM SEA0400. As stated by Hilgemann *et al.*, F_{ss} values are the ratio of steady state to peak outward currents (121; 181). A high F_{ss} value represents a lower extent of Na^+-dependent (I_1) inactivation and vice versa. F_{ss} values also represent the fraction of active exchangers producing current at steady state (121). The parameter, λ, is a measured rate constant for outward current inactivation. Furthermore, λ is indicative of I_1 development represented by the formula: $\lambda = \alpha E_{3ni} + \beta$. Here, α is a rate constant for the transition of exchangers in the cytoplasmic $\mathbf{E_{3ni}}$ state into the I_1 inactivation state. Basically, $\mathbf{E_{3ni}}$ represents the fraction of 3 Na^+-loaded exchangers with an intracellular orientation, while β is a rate constant for the recovery of exchangers from I_1 to the E_{3ni} state. In short, λ is a measure of the rate of I_1 inactivation, whereas F_{ss} measures the level or extent of I_1 inactivation.

Interpreting F_{ss} and λ data in Tables 3 and 4 further strengthens the argument for an involvement of SEA0400 with the I_1 process. Both K225Q and Δ680-685 had similar F_{ss} values to that of NCX1.1 wild-type at both 1 and 10 μM regulatory Ca^{2+}, and in the absence and presence of SEA0400. This suggests that either the fine mutation or the lack of I_2 does not affect the inhibitory function of SEA0400. Both Δ229-232 and K229Q, mutants lacking I_1, show an increase in F_{ss} values in the absence or presence of SEA0400, and without regard for regulatory Ca^{2+} concentrations. These results parallel those of α-chymotrypsin treated patches, lacking regulatory mechanisms I_1 and I_2. Here SEA0400 was without effect, leaving the deregulated exchanger with an F_{ss} value nearing ~ 1.

Conversely, the opposite occurs for the Group 1 mutant, F223E, which displays an accelerated and enhanced I_1. In this case, F_{ss} was reduced and λ was increased under control conditions, while an additional increase was observed following the addition of SEA0400. Results post-SEA0400 application on F223E (enhanced I_1) and Δ229-232 (suppressed I_1) mutants are in agreement with the belief that SEA0400 exerts its inhibitory effects through interactions involving the I_1 inactivation regulatory process.

11. Group 1 NCX1.1 Mutants (Inward Exchange)

To measure SEA0400's inhibitory action in an exchanger mode lacking Na^+-dependent inactivation (I_1), all mutant inward exchange currents were tested in the absence and presence of SEA0400. I_1 inactivation is imperceptible for inward currents as Na^+ is lacking in the bath solution. All inward Na^+-Ca^{2+} exchange currents (forward mode) were initiated by switching from a "Na^+ and Ca^{2+} free" (but Li^+ containing) bath solution to one containing 3 or 10 μM regulatory Ca^{2+}. The pipette contained 100 mM Na^+ and was "Ca^{2+}-free". Figure 22 illustrates a representative inward current of wild-type NCX1.1 in the absence and presence of 0.1 μM SEA0400. Here, SEA0400 is without effect on inward exchange currents at both 3 and 10 μM Ca^{2+}, as is expected.

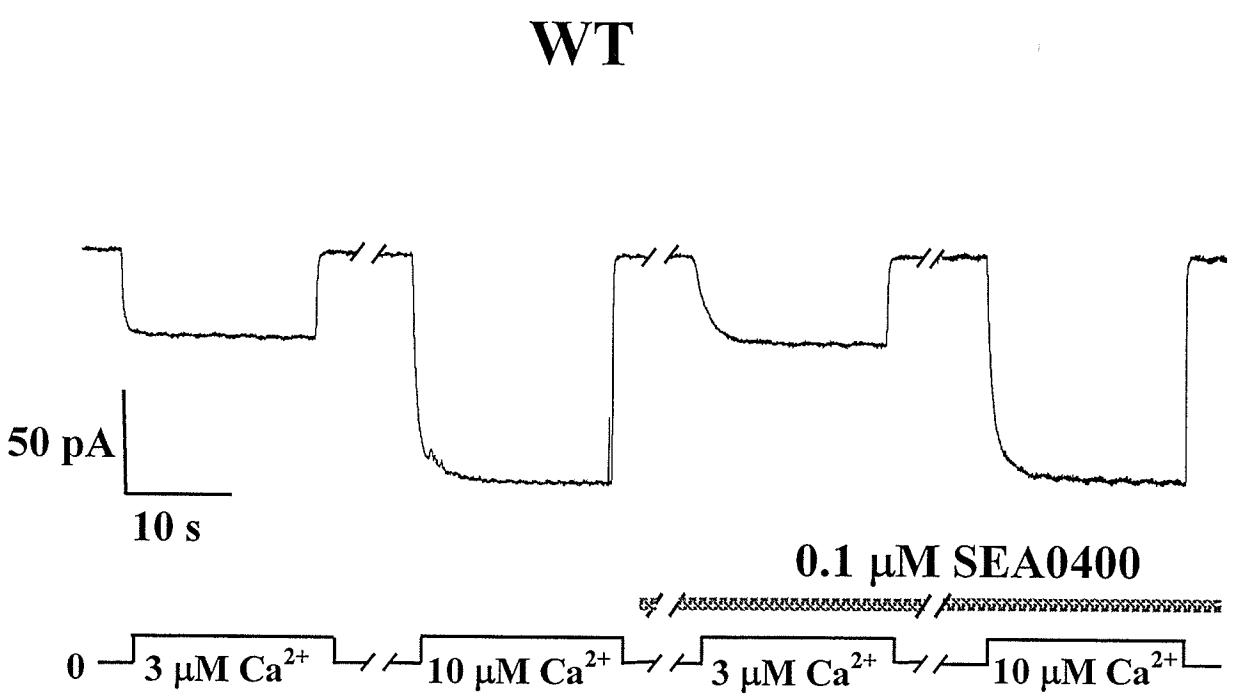

Figure 22. ***Effects of SEA0400 on Inward Na^+-Ca^{2+} Exchange Currents of Wild-Type NCX1.1 Exchangers.*** This figure demonstrates a representative inward, NCX1.1-mediated exchange current, in the absence (Control) and presence of 0.1 μM SEA0400, are shown. Inward Na^+-Ca^{2+} exchange currents were initiated by rapidly applying either 3 or 10 μM Ca^{2+} to the cytoplasmic surface of the patch. The pipette solution contained 100 mM Na^+.

Following the same order, Group 1 mutants (K225Q, F223E) were subjected to 0.1 μM SEA0400 during inward exchange current generation at both 3 and 10 μM regulatory Ca^{2+}. As is seen in Figure 23A, K225Q is somewhat inhibited by SEA0400 at both regulatory Ca^{2+} concentrations (3 and 10 μM). Whereas, inward current of the second group 2 mutant F223E (exhibited in Figure 23B), is strongly inhibited by SEA0400 (% inhibition of steady state ~ 54 ± 6). These results suggest that SEA0400 maintains its inhibitory function in mutants displaying significantly increased I_1, even under ionic conditions where I_1 is absent. All percent inhibitions for inward exchange are summarized in Table 5.

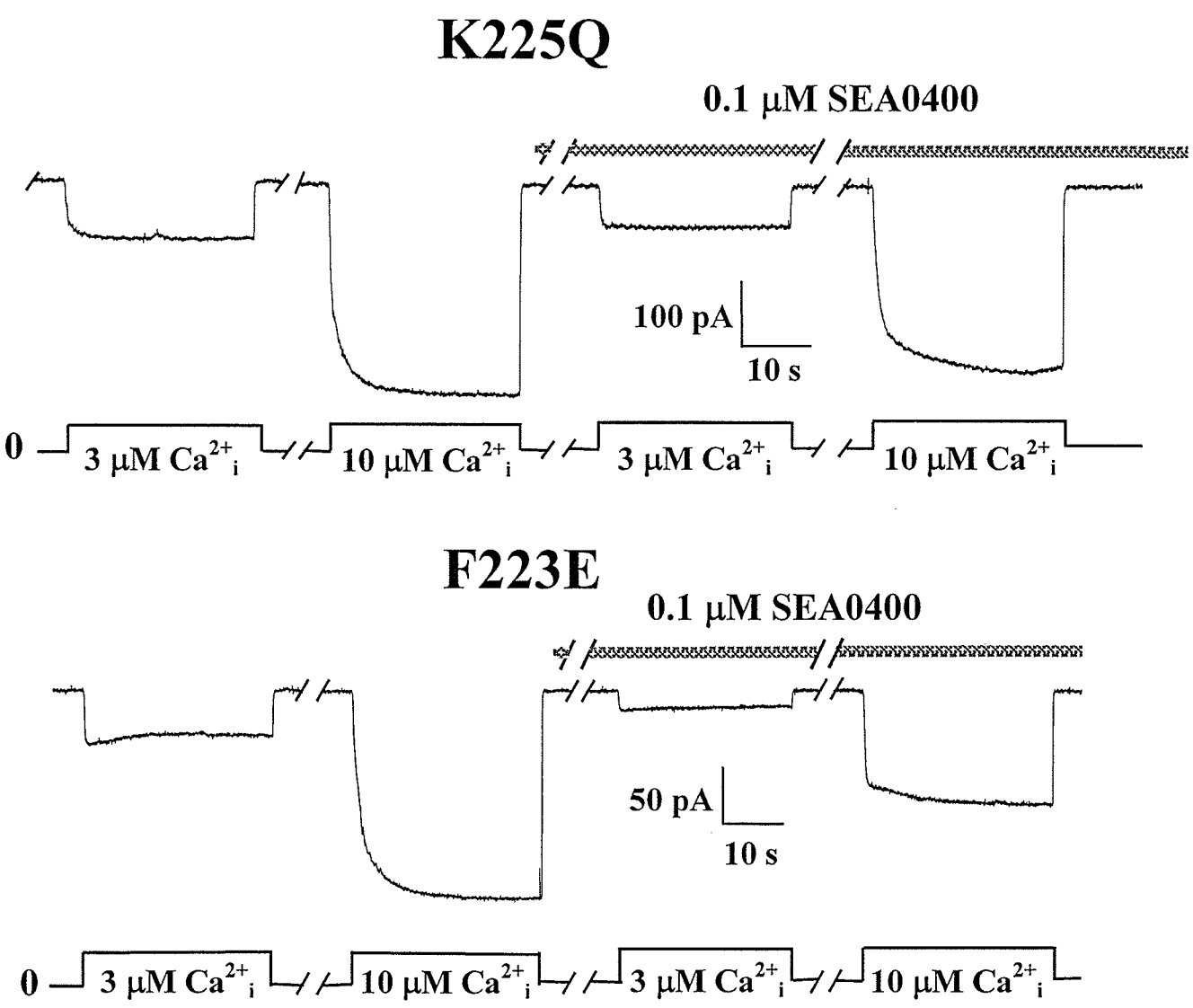

Figure 23. ***Effects of SEA0400 on Inward Na^+-Ca^{2+} Exchange Currents of Mutant NCX1.1 Exchangers Exhibiting Enhanced I_1 Inactivation.*** Panels A (*top*) and B (*bottom*), show the effects of 0.1 μM SEA0400 on inward exchange currents from K225Q (A) and F223E (B), respectively in the absence (*left*) and presence (*right*) of 0.1 μM SEA0400. Inward Na^+-Ca^{2+} exchange currents were initiated by rapidly applying either 3 or 10 μM Ca^{2+} to the cytoplasmic surface of the patch in exchange for 100 mM pipette Na^+.

12. Group 2 and 3 Mutant Inward Exchange

When inward exchange currents for Group 2 mutants (K229Q, Δ229-232) were examined, it was observed in Figure 24, that both mutants were relatively unaffected by SEA0400, resulting in a % inhibitory range of 3 ± 1 to 13 ± 3. As expected, these I_1-suppressed mutants were similarly insensitive to SEA0400 on inward exchange currents, as they were on outward exchange currents. Lastly, inward exchange current for the sole Group 3 mutant, Δ680-685, was recorded. Shown in Figure 25, SEA0400 allows moderate inhibition of inward current at both regulatory Ca^{2+} concentrations.

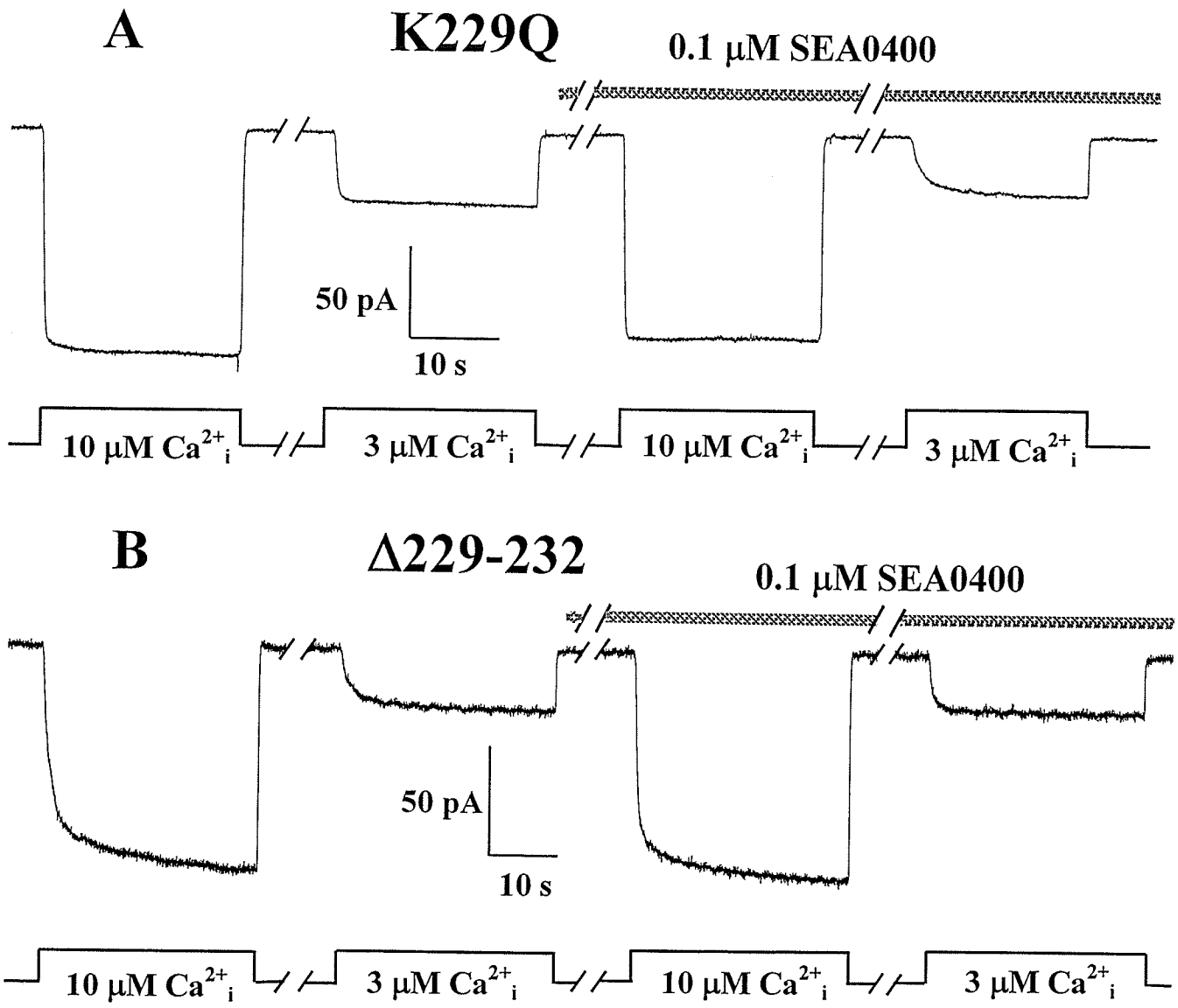

Figure 24. ***Effects of SEA0400 on Inward Na^+-Ca^{2+} Exchange Currents of Mutant NCX1.1 Exchangers Exhibiting Suppressed I_1 Inactivation.*** Panels A (*top*) and B (*bottom*) show representative tracings from K229Q (A), Δ229-232 (B) in the absence (*left*) and presence (*right*) of 0.1 μM SEA0400. Inward Na^+-Ca^{2+} exchange currents were generated by rapidly applying either 3 or 10 μM Ca^{2+} to the cytoplasmic surface of the patch in exchange for 100 mM pipette Na^+.

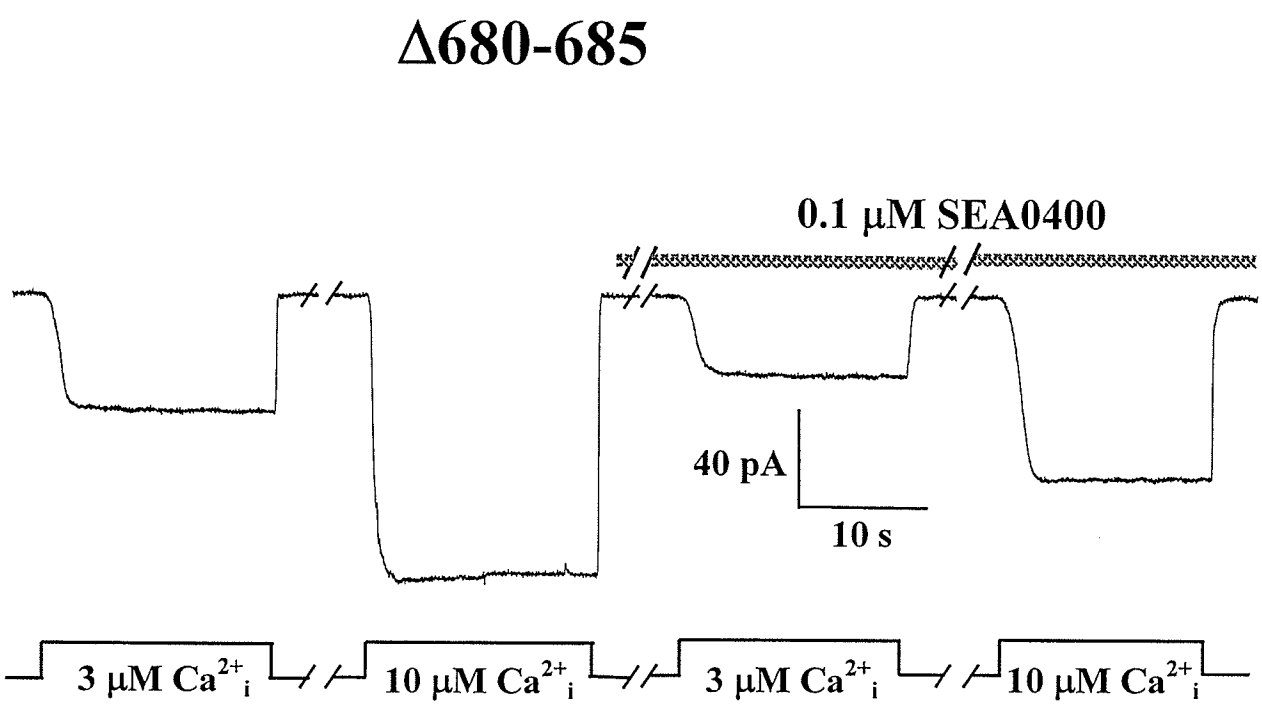

Figure 25. ***Effects of SEA0400 on Inward Na^+-Ca^{2+} Exchange Current of a Mutant NCX1.1 Exchangers Exhibiting Altered I_1 and I_2 Regulation.*** This figure represents inward exchange current of Δ680-685 in the absence (*left*) and presence (*right*) of 0.1 μM SEA0400. Inward Na^+-Ca^{2+} exchange currents were initiated by rapidly applying either 3 or 10 μM Ca^{2+} to the cytoplasmic surface of the patch in exchange for 100 mM pipette Na^+.

Table 2. *Effects of 0.1 μM SEA0400 on Peak and Steady State Outward Current in NCX1.1 and Mutant Na^+-Ca^{2+} Exchangers.*

Mutant	I_{peak} (% Inhibition)	*n*	I_{ss} (% Inhibition)	*n*
1 μM Ca^{2+}				
WT	57 ± 6	12	88 ± 5	10
F223E	54 ± 4	12	100‡	11
K225Q	54 ± 8	7	73 ± 9	8
Δ229-232	7 ± 3*	11	20 ± 5*	11
K229Q	22 ± 4*	14	64 ± 6*	14
Δ680-685	32 ± 8*	8	78 ± 3	8
10 μM Ca^{2+}				
WT	31 ± 8	8	71 ± 7	8
F223E	57 ± 6*	10	87 ± 3*	10
K225Q	25 ± 4	7	71 ± 4	7
Δ229-232	9 ± 3*	8	21 ± 10*	8
K229Q	14 ± 5	13	36 ± 3*	13
Δ680-685	31 ± 6	14	65 ± 5	14

I_{peak}: peak outward current; I_{ss}: steady-state outward current; WT: wild-type NCX.1; *: $P<0.05$ compared to WT; ‡: block is to zero current level (see text for details).

Table 3. *Effects of 0.1 μM SEA0400 on F_{ss} in NCX1.1 and Mutant Na^+-Ca^{2+} Exchangers.*

Mutant	Control		SEA0400	
	F_{ss}	*n*	F_{ss}	*n*
1 μM Ca^{2+}				
WT	0.17 ± 0.01	43	0.10 ± 0.03	9
F223E	0.07 ± 0.02*	18	0.06 ± 0.02	11
K225Q	0.24 ± 0.02*	13	0.16 ± 0.04	7
Δ229-232	0.82 ± 0.05*	12	0.69 ± 0.06*	11
K229Q	0.90 ± 0.03*	28	0.38 ± 0.05*	14
Δ680-685	0.63 ± 0.05*	13	0.20 ± 0.04	8
10 μM Ca^{2+}				
WT	0.72 ± 0.05	13	0.27 ± 0.03	12
F223E	0.34 ± 0.04*	17	0.11 ± 0.03*	10
K225Q	0.83 ± 0.03	11	0.37 ± 0.06	7
Δ229-232	0.94 ± 0.02*	17	0.89 ± 0.04*	9
K229Q	0.94 ± 0.02*	20	0.72 ± 0.03*	12
Δ680-685	0.62 ± 0.05	17	0.32 ± 0.04	13

F_{ss}: I_{ss}/I_{peak}; WT: wild-type NCX.1; *: $P<0.05$ compared to WT.

Table 4. ***Effects of 0.1 μM SEA0400 on λ in NCX1.1 and Mutant Na^+-Ca^{2+} Exchangers.***

Mutant	Control		SEA0400	
	λ	*n*	λ	*n*
1 μM Ca^{2+}				
WT	0.20 ± 0.02	43	0.35 ± 0.05	9
F223E	1.53 ± 0.06*	18	1.78 ± 0.09*	12
K225Q	0.33 ± 0.03*	13	0.56 ± 0.07	7
Δ229-232	1.07 ± 0.24*	10	1.32 ± 0.22*	9
K229Q	0.51 ± 0.08*	15	0.41 ± 0.04	10
Δ680-685	0.34 ± 0.04*	13	0.41 ± 0.02	8
10 μM Ca^{2+}				
WT	0.86 ± 0.22	12	0.20 ± 0.03	12
F223E	1.47 ± 0.15*	17	1.86 ± 0.37*	10
K225Q	1.13 ± 0.25	8	0.49 ± 0.03*	6
Δ229-232	1.57 ± 0.33	11	2.53 ± 0.56*	7
K229Q	0.68 ± 0.32	9	0.51 ± 0.14*	9
Δ680-685	0.32 ± 0.04*	17	0.28 ± 0.04	13

λ: rate of current inactivation s^{-1}; WT: wild-type NCX.1; *: $P<0.05$ compared to WT.

Table 5. ***Effects of 0.1 μM SEA0400 on Steady State Inward Current in NCX1.1 and Mutant Na^+-Ca^{2+} Exchangers.***

Mutant	I_{ss} (% Inhibition)	*n*
3 μM Ca^{2+}		
WT	3 ± 1	6
F223E	52 ± 4*	6
K225Q	15 ± 5	10
Δ229-232	13 ± 3*	4
K229Q	5 ± 2	12
10 μM Ca^{2+}		
WT	3 ± 1	15
F223E	28 ± 5*	10
K225Q	10 ± 5	8
Δ229-232	2 ± 1	8
K229Q	7 ± 2	10

I_{ss}: steady-state outward current; WT: wild-type NCX.1; *: $P<0.05$ compared to WT.

V. DISCUSSION

1. Transport Mode Selectivity

The primary aim was to examine the inhibitory effects of SEA0400, a novel Na^+-Ca^{2+} exchange inhibitor and provide insight into its inhibitory mechanism(s). Using NCX1.1 (canine cardiac Na^+-Ca^{2+} exchanger), expressed in *Xenopus laevis* oocytes, we applied the giant, excised patch clamp technique. We wished to investigate SEA0400's mode selectivity on NCX1.1, if any. Previous results indicate that SEA0400 may exhibit reverse mode (*i.e.,* outward) selectivity in both neural cells (204) and cardiomyocytes (310; 311) but in some instances it was not selective for the Na^+-Ca^{2+}exchanger itself (274). However, under bi-directional conditions, inward and outward currents were measured using the same population of exchangers (*i.e.,* same patch) and indicated inhibition of outward exchange current by SEA0400 to a greater degree than for inward current. Under these conditions, 0.3 μM SEA0400 reduced outward current by ~ 90 % but only affected inward currents by ~ 30 %. With pooled data in Figure 12B, it is apparent that SEA0400 inhibits steady state outward currents to a greater extent that peak outward currents. SEA0400 was also tested under unidirectional conditions that measure outward and inward exchange currents separately. Even under unidirectional conditions, as Figures 13A illustrates, SEA0400 still exerts its potent effects on outward current, while Figure 17A shows SEA0400 to be virtually without effect on inward currents at concentrations up to 3 μM SEA0400. An IC_{50} value for outward exchange inhibition was placed at ~ 23 nM (0.023 μM), whereas an IC_{50} value for inward exchange currents could

not be obtained due to SEA0400's poor solubility at higher concentrations. As mentioned previously, the effects of SEA0400 on inward current at higher concentrations (*i.e.*, > 3 μM) could not be tested due to solubility issues. Although an accurate IC_{50} could not be isolated, an estimated value of ~ 8 μM was suggested. Despite the tendency for SEA0400 to precipitate out of solution it is quite evident under both conditions, SEA0400 is reverse mode selective. This parallels results from previous studies (204; 310). However, there are reports of SEA0400 functioning with equal potency for both forward and reverse mode. In a study by Tanaka *et al.*, both SEA0400 and KB-R7943 were applied to guinea pig ventricular myocytes, and resulted in an equipotent inhibition of both outward and inward Na^+-Ca^{2+} exchange currents (IC_{50} ~ 32 and 40 nM, respectively) (311). Results for KB-R7943 provided a similar trend, however with higher IC_{50} values (311). It was suggested that mode-selective drug binding occurs through the preferential recognition of certain exchanger conformations. Thus, binding to these positions would render the exchanger inactive. Nevertheless, under certain ionic conditions (favouring forward or reverse mode), the exchangers position themselves according to their preferred mode of exchange. This adjusts the relative percentage of exchangers displaying certain conformational forms. This implies that there are a different percentage of exchanger conformations under unidirectional and bi-directional conditions. Therefore, under unidirectional conditions, exchangers will be in one of two conformations (facing cytoplasmically or extracellularly). As the drug binds, it chooses a favourable conformation and this renders the exchanger temporarily inactive. The drug will affect both modes differently, for they each contain different conformations. However, in the bi-directional setting, the possibility for either exchange mode to occur

exists and so does the potential for both conformational positions. Therefore, in certain circumstances, equipotent inhibition is observed (311). Conversely, Takahashi *et al.* reported that in canine sarcolemmal vesicles and rat myocytes, SEA0400 inhibits reverse mode exchange, with IC_{50} values of 90 nM and 92 nM, respectively (310). Iwamoto *et al.* also reported mode selective inhibition for both SEA0400 and KB-R7943, while measuring Na^+-dependent Ca^{2+} uptake (204). Placing these mode preference discrepancies aside, our results suggest that SEA0400 does exert reverse mode selectivity.

2. SEA0400 and Ionic Regulatory Mechanisms

In an attempt to reveal a mechanism(s) for SEA0400 inhibition, the exchanger was removed of its ionic regulatory processes. Using α-chymotrypsin, both significant ionic regulatory mechanisms, I_1 and I_2, were eliminated, leaving the exchanger in a deregulated state. Both of these mechanisms have been suggested to play important roles in maintaining exchanger function, under various ionic conditions (116; 121; 123). As mentioned previously, I_1 is known as Na^+-dependent inactivation. As a result of cytoplasmic Na^+ application during outward Na^+-Ca^{2+} exchange current, the exchanger is stimulated to a peak current level, upon which rapid current decay begins, levelling off to a steady state. However, I_2 or Ca^{2+}-dependent regulation refers to the requirement of cytoplasmic (regulatory) Ca^{2+} for both outward and inward exchange current to occur. In the absence of cytoplasmic Ca^{2+}, no exchange activity is observed, whereas by gradually increasing regulatory Ca^{2+}, exchange current increases as the regulatory binding site

becomes saturated ($K_d \sim 0.3$ μM). This increase, however, results in the removal of the I_1 mechanism, leaving a square waveform. At higher regulatory Ca^{2+} levels (> 10 μM Ca^{2+}), current values begin to decrease as this probably reflects a competition between transported Na^+ and Ca^{2+} ions. As a note, regardless of favourable ionic conditions, Na^+-Ca^{2+} exchangers devoid of regulatory Ca^{2+} will not exhibit exchange. As Figure 14A demonstrates, SEA0400 appears to have a decreased inhibitory effect on outward exchange current in deregulated exchangers (lacking I_1 and I_2). This result that when regulatory mechanisms are absent or disrupted, SEA0400 cannot fully exert its inhibitory action. This predicates a requirement or utilization of either or both I_1 and I_2. However, inward exchange currents were also measured after proteolysis, and SEA0400 was found to be without effect even at 3 μM SEA0400. Nevertheless, α-chymotrypsin's site(s) of proteolysis is unknown, and may very well interact with certain exchanger regions specific for SEA0400 binding and inhibition. Therefore, although SEA0400 appears to require intact ionic regulatory mechanisms, the potential for an alternate binding site cannot be completely ruled out.

It is understood that both I_1 and I_2 interact (121; 123). It has been shown that for outward exchange, upon increasing regulatory Ca^{2+} levels, there is an alleviation of I_1. Figure 15A clearly shows that switching from 1 to 10 μM regulatory Ca^{2+} strongly attenuates Na^+-dependent inactivation (I_1). Therefore, to further investigate the involvement of regulatory mechanisms in SEA0400's mode of inhibition, experiments were performed at 1 and 10 μM Ca^{2+}. SEA0400 was, however, able to prevent the alleviation of I_1 in the presence of high regulatory Ca^{2+} concentrations (*i.e.*, 10 μM). It would appears that SEA0400 is able to promote entry or maintain the exchanger's I_1

mechanism, such that Na^+-dependent inactivation is present under conditions where it is normally absent. In addition, SEA0400 minimally inhibits inward exchange current (Figure 12), where Na^+-dependent inactivation is absent. This result implicated I_1 involvement for inhibition through SEA0400.

When comparing the results of SEA0400 inhibition, current decay rate (λ) was greatly increased in comparison to control (decay) rates. Thus, the rate at which I_1 entry occurred upon SEA0400 application is increased (Table 2). Further supporting the involvement of I_1, were the results stemming from paired-pulse experiments. Data from measured recovery rate (β) in the presence and absence of 0.1 μM SEA0400 revealed that under the same conditions, β was for the most part unchanged (Figure 16C). With increasing regulatory Ca^{2+} concentrations, SEA0400 appears to prevent the alleviation of I_1 normally associated with such increased Ca^{2+} levels. It appears that SEA0400 assists the entry into I_1 during lower regulatory Ca^{2+} levels (*i.e.*, 1 μM) and does not affect the rate of recovery from I_1. Upon increased regulatory Ca^{2+} levels, SEA0400 stabilizes I_1 with minimal alleviation, even at high Ca^{2+} values (*i.e.*, 10 μM) (Figure 16C). These results strongly implicated the involvement of ionic regulatory mechanisms in the process of SEA0400 inhibition, with a tendency towards favouring I_1. The next rational measure was to test the effects of SEA0400 on mutants displaying distinct altered ionic regulatory phenotypes.

3. SEA0400 and Mutant Na^+-Ca^{2+} Exchangers

Prior mutant exchanger experiments, we suggested that SEA0400 was reverse mode selective and required intact regulatory mechanisms for proper inhibition. Considering that forward mode exchange lacks I_1 and that following exchanger deregulation, SEA0400's potency was greatly reduced, it was suggested that the I_1 regulatory mechanism was involved. Changing regulatory Ca^{2+} values showed SEA0400 to interact with I_1 and maintain this inhibitory state, even at excessively high Ca^{2+} levels. The primary purpose for implementing mutated Na^+-Ca^{2+} exchangers with altered ionic regulatory properties was to further determine the requirement of Na^+-dependent inactivation (I_1) for SEA0400 inhibition. Subsequent to Na^+-Ca^{2+} exchanger cloning (227), the XIP region was identified and proposed to contribute to exchanger autoregulation (193). Therefore, the XIP region was a target for mutation for the exploration of exchange regulation. In addition, the small 20 amino acid sequence (219-238) XIP region, was shown to be involved in ionic regulation when Matsuoka *et al.* created both point and deletion mutants, resulting in exchangers displaying altered ionic regulation (209; 211). Therefore, we chose to study these defined mutants in conjunction with SEA0400 analysis. The mutants were grouped according to their regulatory phenotype. In short, there were mutants with increased I_1, lacking I_1 and lacking I_2. Our results were most convincing with mutants with accelerated I_1 and those lacking I_1.

4. Mutant Na^+-Ca^{2+} Exchangers with Altered I_1 (Outward Exchange)

We found that the K225Q mutant had similar I_1 levels to that of wild-type, whereas F223E had significantly increased I_1 levels. Inhibition by SEA0400 on K225Q was nearly identical to that of wild-type. However, in the F233E mutant, carrying a ~ 2 fold increase in the rate and level of I_1, the degree of inhibition by SEA0400 was appreciably increased, bringing steady state current levels near baseline. Such inhibition made it difficult to quantify values for % inhibition (peak and steady state) and F_{ss} values. In the Group 2 mutants (K229Q, Δ229-232), both displayed suppressed I_1, resulting in square waveforms. When the first mutant, K229Q, was tested, SEA0400 appeared to induce I_1-like inactivation. Furthermore, increasing regulatory Ca^{2+} alleviated this I_1-like inactive state, just as Ca^{2+} does with wild-type. This suggested that the observed result was in fact, genuine I_1 being formed. The second Group 2 mutant, Δ229-232, displayed a more definitive effect, showing minimal inhibition with SEA0400. Therefore, both F223E and Δ229-232 complement one another; such that when I_1 is augmented, so is SEA0400's ability to inhibit and when I_1 is absent, so is SEA0400's ability to inhibit. However, the effects of SEA0400 on both K225Q and K229Q should not be dismissed. The resulting "lack of effect" of SEA0400 on K225Q may be due to its more subtle mutation compared to F223E. Furthermore, K225Q, in the absence of SEA0400, does not have significantly increased I_1. Thus, following the hypothesis that SEA0400 requires I_1, this may explain why SEA0400 inhibits to the same degree as wild-type. Conversely, K229Q initially appears to lack functional I_1. However, SEA0400 application produces an I_1-like inactivation that is alleviated by increasing regulatory

Ca^{2+} levels. Perhaps this ability of SEA0400 to form I_1 may reside in the position and severity of the mutation. Both group 2 mutants begin at amino acid 229. While K229Q is only a point mutation, Δ229-232 is a large deletion of 4 amino acids. It may be that the K229Q point mutation only alters a portion of the region governing I_1 entry, whereas Δ229-232 removes the entire segment. This could allow K229Q to retain the ability to enter the I_1 inactive state from the cytoplasmic E_{3ni} state. However, it may be that the potential of entry into I_1 exists; yet it may be less stable and therefore less favourable. We have previously suggested that SEA0400 may promote entry into I_1 or stabilize this inactive state. Therefore, in the case of K229Q, SEA0400 may stabilize the I_1 state and subsequently allow its accumulation. Lastly, this I_1-like state is alleviated by increasing regulatory Ca^{2+} concentrations, which follows the same convention of wild-type I_1. Due to the use of varied mutants, results with SEA0400 would most likely be mutant specific. Therefore, results found with SEA0400 on both K229Q and Δ229-232 do not detract from results indicating direct interaction with I_1, but complement them. However, we cannot unequivocally state that these explanations comprise the actual mechanism(s) of action for SEA0400.

5. Mutant Na^+-Ca^{2+} exchangers with altered I_2 (Outward exchange)

The last mutant, Δ680-685, belongs to Group 3 and displays suppressed Ca^{2+}-dependent regulation (I_2). As described previously, cytoplasmic Ca^{2+} regulates the exchanger, such that if it is not present, exchanger activation does not occur. We refer to this requirement of Ca^{2+} to activate the exchanger and to stimulate outward exchange

current with increasing levels, as Ca^{2+}-dependent regulation. However, at very low cytoplasmic Ca^{2+} levels, exchangers remain inactive or exhibit decreased exchange. This inactive state is referred to as I_2 inactivation. By this convention, we can say that both I_1 and I_2 inactivation depend on Ca^{2+}. Since both of these regulatory mechanisms are Ca^{2+}-dependent, we decided to examine a mutant Na^+-Ca^{2+} exchanger exhibiting altered I_2, previously described by Maxwell *et al.* (212). Our results in Figure 21, displaying outward exchange currents, demonstrate that in the presence of SEA0400, inhibition was equal to that of wild-type for peak and steady state currents (Table 3). However, this suggests that I_2 does not play an important role for SEA0400 inhibition, yet results have varied in the extent of I_1 production between Δ680-685 mutants. Therefore, I_2 cannot be wholly excluded as a potential mechanism of SEA0400 action.

6. Inward Mutant Na^+-Ca^{2+} Exchange (Group 1-3)

We continued to test inward Na^+-Ca^{2+} exchange currents, known to lack I_1, in hopes of further establishing I_1 as the dominant mechanism for SEA0400 inhibition. The I_1 inactive state arises from E_{3ni}, which is more likely to occur during outward exchange currents, where cytoplasmic $[Na^+]_i$ is high. Conversely, during inward exchange current, Na^+ translocates from the extracellular side to a virtually "Na^+-free" side, where unbinding is most favourable. Therefore, E_{3ni} is less likely to accumulate here and enter the I_1 state. This is the primary reason for its absence during inward exchange. As we expected, most inward exchange currents were insensitive to SEA0400, except for that of F223E. The Group 1 mutant displayed moderate inhibition with SEA0400 exposure. A

potential explanation may be that F223E shows greatly increased I_1 for outward current but may form a small amount of I_1 during inward exchange currents, which is further acted upon by SEA0400 (which uses I_1 to exert its inhibitory effects).

7. Peak vs. Steady State Current Inhibition

As Table 2 indicates, during outward exchange current, SEA0400 inhibits steady state current to a greater extent than peak current. However, peak current is thought to be independent of Na^+-dependent inactivation. Therefore, if we suggest that SEA0400 inhibits through I_1, and we see a resulting inhibition of peak current, SEA0400 may have an alternate site of interaction. It remains difficult to determine whether the resulting peak current is due to SEA0400, for peak current represents the net outcome between developing current and that of I_1 entry. At present, we lack the temporal resolution to distinguish between these two possibilities.

8. Pathophysiological Implications

As previously discussed, the primary physiological role of the Na^+-Ca^{2+} exchanger is to maintain Ca^{2+} homeostasis by directly removing the proportional amount of Ca^{2+} that enters through L-type Ca^{2+} channels. If this coupling is not met, the cell can become either Ca^{2+} overloaded or depleted. In addition, the exchanger can function bi-directionally, as its mode of action depends on both electrical and concentration gradients. Therefore, under various pathophysiological conditions, reverse mode (Ca^{2+}

influx) exchange can occur, leading to not only a reduction in the removal of Ca^{2+} but an increased Ca^{2+} influx. This can be severely detrimental to the cell and can quickly result in Ca^{2+} overload (with associated dysfunctions) and cell death. In cases such as ischemia-reperfusion injury (either surgically induced or naturally occurring) and arrhythmogenesis, where reverse mode Na^{+}-Ca^{2+} exchange is considered to be a prime contributor, having a reverse mode selective inhibitor would be invaluable. A selective Na^{+}-Ca^{2+} inhibitor that preferentially blocks Ca^{2+} entry but leaves Ca^{2+} efflux unaltered could play a crucial role in the therapeutic treatment of cardiac ailments. Even more appealing would be an inhibitor that selectively targeted reverse mode exchange with a very high potency, thus requiring low doses for treatment. Until recently, KB-R7943 showed promise, as it appeared significantly more potent and reverse mode selective than any other available inhibitor (145; 327). However, results on KB-R7943's selectivity (both mode and cellular protein) and potency were varied, and in some cases investigators discounted KB-R7943 as a potentially useful clinical inhibitor.

In summary, we have shown SEA0400 to be a potent, reverse mode selective inhibitor and suggest that it or its analogue derivatives could serve as potential therapeutic agents (cardiac disease/injury, renal disease/injury and cerebral disease/injury). Understanding SEA0400's mechanism(s) of action could give insight into the Na^{+}-Ca^{2+} exchanger's properties and lead to the rational approach in future pharmacological design. The exchanger has been shown to have a crucial physiological role in maintaining proper cardiac function and, however, has been implicated in several cardiac injuries, namely ischemia-reperfusion injury. It is essential to fully understand the mechanism(s) of Na^{+}-Ca^{2+} exchange function in order to develop specific tools

directly targeting this membrane transporter. Therefore, we must examine SEA0400 and identify its inhibitory mechanism(s) and mode(s) of action. If fully understood, SEA0400 or putative derivatives could be applied to various diseases/injuries. For example, during periods of induced ischemia-reperfusion injury (*i.e.,* cardiac surgery), preceding drug administration would be most desirable. Here, the majority of damage is a result of reperfusing the recently operated heart. With SEA0400, we could give the drug before inflicting unavoidable damage (reperfusion) and hopefully improve patient recovery. Furthermore, access to a viable reverse mode selective Na^+-Ca^{2+} exchange inhibitor would allow for prophylactic treatment. Theoretically, an ideal inhibitor would exert its effects only during reverse mode exchange, leaving forward mode exchange unaltered. The population who would benefit most, are those with a history of heart disease and/or are at risk for cardiac injury (via obesity, diabetes, high cholesterol, smoking and genetic predisposition). If the heart becomes ischemic, it is essential that blood flow be re-established. Although reperfusion is imperative (without it,.the tissue will die), it is this very act that induces the most serious and irreversible damage. Therefore, having the inhibitor present *prior to* the insult, would provide the most effective protection against the necessary reperfusion. To conclude, SEA0400, in conjunction with effective reperfusion therapy could greatly increase a patient's prospect for recovery following a cardiac insult.

As cardiac disease and injury are reaching epidemic proportion in North America alone, further study of cardiac Na^+-Ca^{2+} exchange and its pharmacology will play a vital role in both the treatment of pre-existing cardiac disease and its prophylactic utilization.

Reference List

1. **Aceto JF, Condrescu M, Kroupis C, Nelson H, Nelson N, Nicoll D, Philipson KD and Reeves JP**. Cloning and expression of the bovine cardiac sodium-calcium exchanger. *Arch Biochem Biophys* 298: 553-560, 1992.

2. **Altschul SF, Madden TL, Schaffer AA, Zhang J, Zhang Z, Miller W and Lipman DJ**. Gapped BLAST and PSI-BLAST: a new generation of protein database search programs. *Nucleic Acids Res* 25: 3389-3402, 1997.

3. **Anderson SE, Cala PM, Steenbergen C, London RE and Murphy E**. Effects of hypoxia and acidification on myocardial Na and Ca. Role of Na-H and Na-Ca exchange. *Ann N Y Acad Sci* 639: 453-455, 1991.

4. **Arakawa N, Sakaue M, Yokoyama I, Hashimoto H, Koyama Y, Baba A and Matsuda T**. KB-R7943 Inhibits Store-Operated Ca^{2+} Entry in Cultured Neurons and Astrocytes. *Biochem Biophys Res Commun* 279: 354-357, 2000.

5. **Armoundas AA, Hobai IA, Tomaselli GF, Winslow RL and O'Rourke B**. Role of sodium-calcium exchanger in modulating the action potential of ventricular myocytes from normal and failing hearts. *Circ Res* 93: 46-53, 2003.

6. **Baker DL, Hashimoto K, Grupp IL, Ji Y, Reed T, Loukianov E, Grupp G, Bhagwhat A, Hoit B, Walsh R, Marban E and Periasamy M**. Targeted

overexpression of the sarcoplasmic reticulum Ca2+-ATPase increases cardiac contractility in transgenic mouse hearts. *Circ Res* 83: 1205-1214, 1998.

7. **Baker PF, Blaustein MP, Hodgkin AL and Steinhardt RA**. The influence of calcium on sodium efflux in squid axons. *J Physiol (Lond)* 200: 431-458, 1969.

8. **Ballard C, Mozaffari M and Schaffer S**. Signal transduction mechanism for the stimulation of the sarcolemmal Na^+-Ca^{2+} exchanger by insulin. *Mol Cell Biochem* 135: 113-119, 1994.

9. **Ballard C and Schaffer S**. Stimulation of the Na^+/Ca^{2+} exchanger by phenylephrine, angiotensin II and endothelin 1. *J Mol Cell Cardiol* 28: 11-17, 1996.

10. **Barnes KV, Cheng G, Dawson MM and Menick DR**. Cloning of cardiac, kidney, and brain promoters of the feline ncx1 gene. *J Biol Chem* 272: 11510-11517, 1997.

11. **Barry WH and Bridge JH**. Intracellular calcium homeostasis in cardiac myocytes. *Circulation* 87: 1806-1815, 1993.

12. **Barry WH, Hasin Y and Smith TW**. Sodium pump inhibition, enhanced calcium influx via sodium- calcium exchange, and positive inotropic response in cultured heart cells. *Circ Res* 56: 231-241, 1985.

13. **Bassani JW, Bassani RA and Bers DM**. Relaxation in rabbit and rat cardiac cells: species-dependent differences in cellular mechanisms. *J Physiol (Lond)* 476: 279-293, 1994.

14. **Bassani RA, Bassani JW and Bers DM**. Relaxation in ferret ventricular myocytes: role of the sarcolemmal Ca ATPase. *Pflugers Arch* 430: 573-578, 1995.

15. **Bell PD, Mashburn N and Unlap MT**. Renal sodium/calcium exchange; a vasodilator that is defective in salt-sensitive hypertension. *Acta Physiol Scand* 168: 209-214, 2000.

16. **Bers DM**. Ca influx and sarcoplasmic reticulum Ca release in cardiac muscle activation during postrest recovery. *Am J Physiol* 248: H366-H381, 1985.

17. **Bers DM**. Mechanisms contributing to the cardiac inotropic effect of Na pump inhibition and reduction of extracellular Na. *J Gen Physiol* 90: 479-504, 1987.

18. **Bers DM**. Species differences and the role of sodium-calcium exchange in cardiac muscle relaxation. *Ann N Y Acad Sci* 639: 375-385, 1991.

19. **Bers DM**. Calcium fluxes involved in control of cardiac myocyte contraction. *Circ Res* 87: 275-281, 2000.

20. **Bers DM**. *Excitation-contraction coupling and cardiac contractile force*. London, UK: Kluwer Academic Publications, 2001.

21. **Bers DM**. Regulation of Cellular Calcium in Cardiac Myocytes. In: Handbook of Physiology. Section 2: The Cardiovascular System. V. 1: The Heart, edited by Page.E., Fozzard HA and Solaro RJ. Oxford: Oxford University Press, 2002, p. 335-387.

22. **Bers DM and Bridge JH**. Relaxation of rabbit ventricular muscle by Na-Ca exchange and sarcoplasmic reticulum calcium pump. Ryanodine and voltage sensitivity. *Circ Res* 65: 334-342, 1989.

23. **Bers DM, Bridge JH and Spitzer KW**. Intracellular Ca^{2+} transients during rapid cooling contractures in guinea-pig ventricular myocytes. *J Physiol (Lond)* 417: 537-553, 1989.

24. **Bers DM, Christensen DM and Nguyen TX**. Can Ca entry via Na-Ca exchange directly activate cardiac muscle contraction? *J Mol Cell Cardiol* 20: 405-414, 1988.

25. **Bers DM, Patton CW and Nuccitelli R**. A practical guide to the preparation of Ca^{2+} buffers. *Methods Cell Biol* 40: 3-29, 1994.

26. **Bers DM and Perez-Reyes E.** Ca channels in cardiac myocytes: structure and function in Ca influx and intracellular Ca release. *Cardiovasc Res* 42: 339-360, 1999.

27. **Bers DM, Philipson KD and Nishimoto AY.** Sodium-calcium exchange and sidedness of isolated cardiac sarcolemmal vesicles. *Biochim Biophys Acta* 601: 358-371, 1980.

28. **Beuckelmann DJ, Nabauer M and Erdmann E.** Intracellular calcium handling in isolated ventricular myocytes from patients with terminal heart failure. *Circulation* 85: 1046-1055, 1992.

29. **Beuckelmann DJ and Wier WG.** Mechanism of release of calcium from sarcoplasmic reticulum of guinea- pig cardiac cells. *J Physiol (Lond)* 405: 233-255, 1988.

30. **Beuckelmann DJ and Wier WG.** Sodium-calcium exchange in guinea-pig cardiac cells: exchange current and changes in intracellular Ca^{2+}. *J Physiol (Lond)* 414: 499-520, 1989.

31. **Bielefeld DR, Hadley RW, Vassilev PM and Hume JR.** Membrane electrical properties of vesicular Na-Ca exchange inhibitors in single atrial myocytes. *Circ Res* 59: 381-389, 1986.

32. **Billman GE**. KB-R7943. Kanebo. *Curr Opin Investig Drugs* 2: 1740-1745, 2001.

33. **Blaustein MP**. Relative roles of sodium/calcium exchange and ATP-fueled calcium transport in the control of cell calcium. *Ann N Y Acad Sci* 402: 457-458, 1982.

34. **Blaustein MP**. The cellular basis of cardiotonic steroid action. *Trends Pharmacol Sci* 6: 289-292, 1985.

35. **Blaustein MP**. Physiological effects of endogenous ouabain: control of intracellular Ca^{2+} stores and cell responsiveness. *Am J Physiol* 264: C1367-C1387, 1993.

36. **Blaustein MP and Lederer WJ**. Sodium/calcium exchange: its physiological implications. *Physiol Rev* 79: 763-854, 1999.

37. **Blaustein MP and Santiago EM**. Effects of internal and external cations and of ATP on sodium-calcium and calcium-calcium exchange in squid axons. *Biophys J* 20: 79-111, 1977.

38. **Boerth SR, Zimmer DB and Artman M**. Steady-state mRNA levels of the sarcolemmal Na^{+}-Ca^{2+} exchanger peak near birth in developing rabbit and rat hearts. *Circ Res* 74: 354-359, 1994.

39. **Bouchard RA, Clark RB and Giles WR**. Role of sodium-calcium exchange in activation of contraction in rat ventricle. *J Physiol (Lond)* 472: 391-413, 1993.

40. **Bridge JH**. Relationships between the sarcoplasmic reticulum and sarcolemmal calcium transport revealed by rapidly cooling rabbit ventricular muscle. *J Gen Physiol* 88: 437-473, 1986.

41. **Bridge JH, Smolley JR and Spitzer KW**. The relationship between charge movements associated with I_{Ca} and I_{Na-Ca} in cardiac myocytes. *Science* 248: 376-378, 1990.

42. **Bridge JH, Spitzer KW and Ershler PR**. Relaxation of isolated ventricular cardiomyocytes by a voltage- dependent process. *Science* 241: 823-825, 1988.

43. **Callewaert G, Cleemann L and Morad M**. Epinephrine enhances Ca^{2+} current-regulated Ca^{2+} release and Ca^{2+} reuptake in rat ventricular myocytes. *Proc Natl Acad Sci U S A* 85: 2009-2013, 1988.

44. **Cannell MB**. Contribution of sodium-calcium exchange to calcium regulation in cardiac muscle. *Ann N Y Acad Sci* 639: 428-443, 1991.

45. **Cannell MB, Grantham CJ, Main MJ and Evans AM**. The roles of the sodium and calcium current in triggering calcium release from the sarcoplasmic reticulum. *Ann N Y Acad Sci* 779: 443-450, 1996.

46. **Carafoli E**. The homeostasis of calcium in heart cells. *J Mol Cell Cardiol* 17: 203-212, 1985.

47. **Caroni P, Reinlib L and Carafoli E**. Charge movements during the Na^+-Ca^{2+} exchange in heart sarcolemmal vesicles. *Proc Natl Acad Sci U S A* 77: 6354-6358, 1980.

48. **Chen F, Mottino G, Klitzner TS, Philipson KD and Frank JS**. Distribution of the Na^+/Ca^{2+} exchange protein in developing rabbit myocytes. *Am J Physiol* 268: C1126-C1132, 1995.

49. **Cheng G, Hagen TP, Dawson ML, Barnes KV and Menick DR**. The role of GATA, CArG, E-box, and a novel element in the regulation of cardiac expression of the Na^+-Ca^{2+} exchanger gene. *J Biol Chem* 274: 12819-12826, 1999.

50. **Cheng H, Lederer MR, Lederer WJ and Cannell MB**. Calcium sparks and $[Ca^{2+}]_i$ waves in cardiac myocytes. *Am J Physiol* 270: C148-C159, 1996.

51. **Cheng H, Lederer MR, Xiao RP, Gomez AM, Zhou YY, Ziman B, Spurgeon H, Lakatta EG and Lederer WJ**. Excitation-contraction coupling in heart: new insights from Ca^{2+} sparks. *Cell Calcium* 20: 129-140, 1996.

52. **Chernaya G, Vazquez M and Reeves JP**. Sodium-calcium exchange and store-dependent calcium influx in transfected Chinese hamster ovary cells expressing

the bovine cardiac sodium-calcium exchanger. Acceleration of exchange activity in thapsigargin-treated cells. *J Biol Chem* 271: 5378-5385, 1996.

53. **Chin TK, Spitzer KW, Philipson KD and Bridge JH.** The effect of exchanger inhibitory peptide (XIP) on sodium-calcium exchange current in guinea pig ventricular cells. *Circ Res* 72: 497-503, 1993.

54. **Choi HS and Eisner DA.** The effects of inhibition of the sarcolemmal Ca-ATPase on systolic calcium fluxes and intracellular calcium concentration in rat ventricular myocytes. *Pflugers Arch* 437: 966-971, 1999.

55. **Cleemann L and Morad M.** Role of Ca^{2+} channel in cardiac excitation-contraction coupling in the rat: evidence from Ca^{2+} transients and contraction. *J Physiol (Lond)* 432: 283-312, 1991.

56. **Collins A and Hilgemann DW.** A novel method for direct application of phospholipids to giant excised membrane patches in the study of sodium-calcium exchange and sodium channel currents. *Pflugers Arch* 423: 347-355, 1993.

57. **Collins A, Somlyo AV and Hilgemann DW.** The giant cardiac membrane patch method: stimulation of outward Na^{+}- Ca^{2+} exchange current by MgATP. *J Physiol (Lond)* 454: 27-57, 1992.

58. **Condrescu M, Chernaya G, Kalaria V and Reeves JP**. Barium influx mediated by the cardiac sodium-calcium exchanger in transfected Chinese hamster ovary cells. *J Gen Physiol* 109: 41-51, 1997.

59. **Condrescu M, Hantash BM, Fang Y and Reeves JP**. Mode-specific inhibition of sodium-calcium exchange during protein phosphatase blockade. *J Biol Chem* 274: 33279-33286, 1999.

60. **Convery MK, Levi AJ, Khananshvili D and Hancox JC**. Actions of myristyl-FRCRCFa, a cell-permeant blocker of the cardiac sarcolemmal Na-Ca exchanger, tested in rabbit ventricular myocytes. *Pflugers Arch* 436: 581-590, 1998.

61. **Cook O, Low W and Rahamimoff H**. Membrane topology of the rat brain Na^+-Ca^{2+} exchanger. *Biochim Biophys Acta* 1371: 40-52, 1998.

62. **Crespo LM, Grantham CJ and Cannell MB**. Kinetics, stoichiometry and role of the Na-Ca exchange mechanism in isolated cardiac myocytes. *Nature* 345: 618-621, 1990.

63. **Cunningham KW and Fink GR**. Calcineurin inhibits VCX1-dependent H^+/Ca^{2+} exchange and induces Ca^{2+} ATPases in *Saccharomyces cerevisiae*. *Mol Cell Biol* 16: 2226-2237, 1996.

64. **Dhalla NS, Dixon IM, Rupp H and Barwinsky J.** Experimental congestive heart failure due to myocardial infarction: sarcolemmal receptors and cation transporters. *Basic Res Cardiol* 86 Suppl 3: 13-23, 1991.

65. **Dipla K, Mattiello JA, Margulies KB, Jeevanandam V and Houser SR.** The sarcoplasmic reticulum and the Na^+/Ca^{2+} exchanger both contribute to the Ca^{2+} transient of failing human ventricular myocytes. *Circ Res* 84: 435-444, 1999.

66. **DiPolo R.** Characterization of the ATP-dependent calcium efflux in dialyzed squid giant axons. *J Gen Physiol* 69: 795-813, 1977.

67. **DiPolo R.** Calcium influx in internally dialyzed squid giant axons. *J Gen Physiol* 73: 91-113, 1979.

68. **DiPolo R and Beauge L.** The effect of pH on Ca^{2+} extrusion mechanisms in dialyzed squid axons. *Biochim Biophys Acta* 688: 237-245, 1982.

69. **DiPolo R and Beauge L.** In squid axons, ATP modulates Na^+-Ca^{2+} exchange by a $Ca^{2+}{}_i$-dependent phosphorylation. *Biochim Biophys Acta* 897: 347-354, 1987.

70. **DiPolo R and Beauge L.** Regulation of Na-Ca exchange. An overview. *Ann N Y Acad Sci* 639: 100-111, 1991.

71. **DiPolo R and Beauge L**. Cardiac sarcolemmal Na/Ca-inhibiting peptides XIP and FMRF-amide also inhibit Na/Ca exchange in squid axons. *Am J Physiol* 267: C307-C311, 1994.

72. **DiPolo R and Beauge L**. Metabolic pathways in the regulation of invertebrate and vertebrate Na^+/Ca^{2+} exchange. *Biochim Biophys Acta* 1422: 57-71, 1999.

73. **DiPolo R, Berberian G, Delgado D, Rojas H and Beauge L**. A novel 13 kDa cytoplasmic soluble protein is required for the nucleotide (MgATP) modulation of the Na/Ca exchange in squid nerve fibers. *FEBS Lett* 401: 6-10, 1997.

74. **Dixon IM, Hata T and Dhalla NS**. Sarcolemmal calcium transport in congestive heart failure due to myocardial infarction in rats. *Am J Physiol* 262: H1387-H1394, 1992.

75. **Doering AE, Eisner DA and Lederer WJ**. Cardiac Na-Ca exchange and pH. *Ann N Y Acad Sci* 779: 182-198, 1996.

76. **Doering AE and Lederer WJ**. The mechanism by which cytoplasmic protons inhibit the sodium-calcium exchanger in guinea-pig heart cells. *J Physiol (Lond)* 466: 481-499, 1993.

77. **Doering AE and Lederer WJ**. The action of Na^+ as a cofactor in the inhibition by cytoplasmic protons of the cardiac Na^+-Ca^{2+} exchanger in the guinea-pig. *J Physiol (Lond)* 480: 9-20, 1994.

78. **Doering AE, Nicoll DA, Lu Y, Lu L, Weiss JN and Philipson KD**. Topology of a functionally important region of the cardiac Na^+/Ca^{2+} exchanger. *J Biol Chem* 273: 778-783, 1998.

79. **Dong H, Dunn J and Lytton J**. Stoichiometry of the Cardiac Na^+/Ca^{2+} Exchanger NCX1.1 Measured in Transfected HEK Cells. *Biophys J* 82: 1943-1952, 2002.

80. **Donnadieu E and Trautmann A**. Is there a Na^+/Ca^{2+} exchanger in macrophages and in lymphocytes? *Pflugers Arch* 424: 448-455, 1993.

81. **Durkin JT, Ahrens DC, Pan YC and Reeves JP**. Purification and amino-terminal sequence of the bovine cardiac sodium- calcium exchanger: evidence for the presence of a signal sequence. *Arch Biochem Biophys* 290: 369-375, 1991.

82. **Dyck C, Maxwell K, Buchko J, Trac M, Omelchenko A, Hnatowich M and Hryshko LV**. Structure-function analysis of CALX1.1, a Na^+-Ca^{2+} exchanger from *Drosophila*. Mutagenesis of ionic regulatory sites. *J Biol Chem* 273: 12981-12987, 1998.

83. **Dyck C, Omelchenko A, Elias CL, Quednau BD, Philipson KD, Hnatowich M and Hryshko L.** Ionic regulatory properties of brain and kidney splice variants of the NCX1 Na^+-Ca^{2+} exchanger. *J Gen Physiol* 114: 701-711, 1999.

84. **Egger M, Ruknudin A, Lipp P, Kofuji P, Lederer WJ, Schulze DH and Niggli E.** Functional expression of the human cardiac Na^+/Ca^{2+} exchanger in Sf9 cells: rapid and specific Ni^{2+} transport. *Cell Calcium* 25: 9-17, 1999.

85. **Egger M, Ruknudin A, Niggli E, Lederer WJ and Schulze DH.** Ni^{2+} transport by the human Na^+/Ca^{2+} exchanger expressed in Sf9 cells. *Am J Physiol* 276: C1184-C1192, 1999.

86. **Ehara T, Matsuoka S and Noma A.** Measurement of reversal potential of Na^+-Ca^{2+} exchange current in single guinea-pig ventricular cells. *J Physiol (Lond)* 410: 227-249, 1989.

87. **Eisner DA and Lederer WJ.** Na-Ca exchange: stoichiometry and electrogenicity. *Am J Physiol* 248: C189-C202, 1985.

88. **Elias CL, Lukas A, Shurraw S, Scott J, Omelchenko A, Gross GJ, Hnatowich M and Hryshko LV.** Inhibition of Na^+/Ca^{2+} exchange by KB-R7943: transport mode selectivity and antiarrhythmic consequences. *Am J Physiol Heart Circ Physiol* 281: H1334-H1345, 2001.

89. **Enyedi A and Penniston JT**. Autoinhibitory domains of various Ca^{2+} transporters cross-react. *J Biol Chem* 268: 17120-17125, 1993.

90. **Evans AM and Cannell MB**. The role of L-type Ca^{2+} current and Na^{+} current-stimulated Na/Ca exchange in triggering SR calcium release in guinea-pig cardiac ventricular myocytes. *Cardiovasc Res* 35: 294-302, 1997.

91. **Fabiato A**. Calcium release in skinned cardiac cells: variations with species, tissues, and development. *Fed Proc* 41: 2238-2244, 1982.

92. **Fabiato A**. Time and calcium dependence of activation and inactivation of calcium- induced release of calcium from the sarcoplasmic reticulum of a skinned canine cardiac Purkinje cell. *J Gen Physiol* 85: 247-289, 1985.

93. **Fang Y, Condrescu M and Reeves JP**. Regulation of Na^{+}/Ca^{2+} exchange activity by cytosolic Ca^{2+} in transfected Chinese hamster ovary cells. *Am J Physiol* 275: C50-C55, 1998.

94. **Fedida D, Noble D, Shimoni Y and Spindler AJ**. Inward current related to contraction in guinea-pig ventricular myocytes. *J Physiol (Lond)* 385: 565-589, 1987.

95. **Flesch M, Schwinger RH, Schiffer F, Frank K, Sudkamp M, Kuhn-Regnier F, Arnold G and Bohm M**. Evidence for functional relevance of an enhanced

expression of the Na^+-Ca^{2+} exchanger in failing human myocardium. *Circulation* 94: 992-1002, 1996.

96. **Frank JS, Mottino G, Reid D, Molday RS and Philipson KD**. Distribution of the Na^+-Ca^{2+} exchange protein in mammalian cardiac myocytes: an immunofluorescence and immunocolloidal gold- labeling study. *J Cell Biol* 117: 337-345, 1992.

97. **Fujioka Y, Hiroe K and Matsuoka S**. Regulation kinetics of Na^+-Ca^{2+} exchange current in guinea-pig ventricular myocytes. *J Physiol* 529: 611-623, 2000.

98. **Fujioka Y, Komeda M and Matsuoka S**. Stoichiometry of Na^+-Ca^{2+} exchange in inside-out patches excised from guinea-pig ventricular myocytes. *J Physiol (Lond)* 523 Pt 2: 339-351, 2000.

99. **Furman I, Cook O, Kasir J, Low W and Rahamimoff H**. The putative amino-terminal signal peptide of the cloned rat brain Na^+-Ca^{2+} exchanger gene (RBE-1) is not mandatory for functional expression. *J Biol Chem* 270: 19120-19127, 1995.

100. **Furman I, Cook O, Kasir J and Rahamimoff H**. Cloning of two isoforms of the rat brain Na^+-Ca^{2+} exchanger gene and their functional expression in HeLa cells. *FEBS Lett* 319: 105-109, 1993.

101. **Gabellini N, Zatti A, Rispoli G, Navangione A and Carafoli E.** Expression of an active Na^+/Ca^{2+} exchanger isoform lacking the six C- terminal transmembrane segments. *Eur J Biochem* 239: 897-904, 1996.

102. **Golden KL, Ren J, O'Connor J, Dean A, DiCarlo SE and Marsh JD.** In vivo regulation of Na/Ca exchanger expression by adrenergic effectors. *Am J Physiol Heart Circ Physiol* 280: H1376-H1382, 2001.

103. **Gomez AM, Valdivia HH, Cheng H, Lederer MR, Santana LF, Cannell MB, McCune SA, Altschuld RA and Lederer WJ.** Defective excitation-contraction coupling in experimental cardiac hypertrophy and heart failure. *Science* 276: 800-806, 1997.

104. **Haigney MC, Miyata H, Lakatta EG, Stern MD and Silverman HS.** Dependence of hypoxic cellular calcium loading on Na^+-Ca^{2+} exchange. *Circ Res* 71: 547-557, 1992.

105. **Hale CC, Slaughter RS, Ahrens DC and Reeves JP.** Identification and partial purification of the cardiac sodium-calcium exchange protein. *Proc Natl Acad Sci USA* 81: 6569-6573, 1984.

106. **Hammes A, Oberdorf-Maass S, Rother T, Nething K, Gollnick F, Linz KW, Meyer R, Hu K, Han H, Gaudron P, Ertl G, Hoffmann S, Ganten U, Vetter R, Schuh K, Benkwitz C, Zimmer HG and Neyses L.** Overexpression of the

sarcolemmal calcium pump in the myocardium of transgenic rats. *Circ Res* 83: 877-888, 1998.

107. **Hasenfuss G, Meyer M, Schillinger W, Preuss M, Pieske B and Just H.** Calcium handling proteins in the failing human heart. *Basic Res Cardiol* 92 Suppl 1: 87-93, 1997.

108. **Hasenfuss G, Reinecke H, Studer R, Pieske B, Meyer M, Drexler H and Just H.** Calcium cycling proteins and force-frequency relationship in heart failure. *Basic Res Cardiol* 91 Suppl 2: 17-22, 1996.

109. **Hasenfuss G, Schillinger W, Lehnart SE, Preuss M, Pieske B, Maier LS, Prestle J, Minami K and Just H.** Relationship between Na^+-Ca^{2+}-exchanger protein levels and diastolic function of failing human myocardium. *Circulation* 99: 641-648, 1999.

110. **Haug-Collet K, Pearson B, Webel R, Szerencsei RT, Winkfein RJ, Schnetkamp PP and Colley NJ.** Cloning and characterization of a potassium-dependent sodium/calcium exchanger in *Drosophila*. *J Cell Biol* 147: 659-670, 1999.

111. **He S, Ruknudin A, Bambrick LL, Lederer WJ and Schulze DH.** Isoform-specific regulation of the Na^+/Ca^{2+} exchanger in rat astrocytes and neurons by PKA. *J Neurosci* 18: 4833-4841, 1998.

112. **He Z, Feng S, Tong Q, Hilgemann DW and Philipson KD**. Interaction of PIP_2 with the XIP region of the cardiac Na/Ca exchanger. *Am J Physiol* 278: C661-C666, 2000.

113. **He Z, Petesch N, Voges K, Roben W and Philipson KD**. Identification of important amino acid residues of the Na^+-Ca^{2+} exchanger inhibitory peptide, XIP. *J Membr Biol* 156: 149-156, 1997.

114. **He Z, Tong Q, Quednau BD, Philipson KD and Hilgemann DW**. Cloning, expression, and characterization of the squid Na^+-Ca^{2+} exchanger (NCX-SQ1). *J Gen Physiol* 111: 857-873, 1998.

115. **Hilgemann DW**. Giant excised cardiac sarcolemmal membrane patches: sodium and sodium-calcium exchange currents. *Pflugers Arch* 415: 247-249, 1989.

116. **Hilgemann DW**. Regulation and deregulation of cardiac Na^+-Ca^{2+} exchange in giant excised sarcolemmal membrane patches. *Nature* 344: 242-245, 1990.

117. **Hilgemann DW**. The cardiac Na-Ca exchanger in giant membrane patches. *Ann N Y Acad Sci* 779: 136-158, 1996.

118. **Hilgemann DW**. Unitary cardiac Na^+, Ca^{2+} exchange current magnitudes determined from channel-like noise and charge movements of ion transport. *Biophys J* 71: 759-768, 1996.

119. **Hilgemann DW and Ball R**. Regulation of cardiac Na^+-Ca^{2+} exchange and K_{ATP} potassium channels by PIP_2. *Science* 273: 956-959, 1996.

120. **Hilgemann DW and Collins A**. Mechanism of cardiac Na^+-Ca^{2+} exchange current stimulation by MgATP: possible involvement of aminophospholipid translocase. *J Physiol (Lond)* 454: 59-82, 1992.

121. **Hilgemann DW, Collins A and Matsuoka S**. Steady-state and dynamic properties of cardiac sodium-calcium exchange. Secondary modulation by cytoplasmic calcium and ATP. *J Gen Physiol* 100: 933-961, 1992.

122. **Hilgemann DW and Lu CC**. Giant membrane patches: improvements and applications. *Methods Enzymol* 293: 267-280, 1998.

123. **Hilgemann DW, Matsuoka S, Nagel GA and Collins A**. Steady-state and dynamic properties of cardiac sodium-calcium exchange. Sodium-dependent inactivation. *J Gen Physiol* 100: 905-932, 1992.

124. **Hilgemann DW, Nicoll DA and Philipson KD**. Charge movement during Na^+ translocation by native and cloned cardiac Na^+/Ca^{2+} exchanger. *Nature* 352: 715-718, 1991.

125. **Hinata M, Yamamura H, Li L, Watanabe Y, Watano T, Imaizumi Y and Kimura J**. Stoichiometry of Na^+-Ca^{2+} exchange is 3:1 in guinea-pig ventricular myocytes. *J Physiol* 545: 453-461, 2002.

126. **Hirschi KD, Zhen RG, Cunningham KW, Rea PA and Fink GR**. CAX1, an H^+/Ca^{2+} antiporter from *Arabidopsis*. *Proc Natl Acad Sci U S A* 93: 8782-8786, 1996.

127. **Hobai IA, Khananshvili D and Levi AJ**. The peptide "FRCRCFa", dialysed intracellularly, inhibits the Na/Ca exchange in rabbit ventricular myocytes with high affinity. *Pflugers Arch* 433: 455-463, 1997.

128. **Horackova M and Vassort G**. Sodium-calcium exchange in regulation of cardiac contraction. *Recent Adv Stud Cardiac Struct Metab* 11: 137-141, 1976.

129. **Horackova M and Vassort G**. Sodium-calcium exchange in regulation of cardiac contractility. Evidence for an electrogenic, voltage-dependent mechanism. *J Gen Physiol* 73: 403-424, 1979.

130. **Hryshko LV**. The cardiac Na^+-Ca^{2+} exchanger. In: Handbook of Physiology. Section 2: The Cardiovascular System. V. 1: The Heart, edited by Page.E., Fozzard HA and Solaro RJ. Oxford: Oxford University Press, 2002, p. 388-419.

131. **Hryshko LV, Matsuoka S, Nicoll DA, Weiss JN, Schwarz EM, Benzer S and Philipson KD**. Anomalous regulation of the *Drosophila* Na^+-Ca^{2+} exchanger by Ca^{2+}. *J Gen Physiol* 108: 67-74, 1996.

132. **Hryshko LV, Nicoll DA, Weiss JN and Philipson KD**. Biosynthesis and initial processing of the cardiac sarcolemmal Na^+-Ca^{2+} exchanger. *Biochim Biophys Acta* 1151: 35-42, 1993.

133. **Hryshko LV, Stiffel V and Bers DM**. Rapid cooling contractures as an index of sarcoplasmic reticulum calcium content in rabbit ventricular myocytes. *Am J Physiol* 257: H1369-H1377, 1989.

134. **Ikari A, Sakai H and Takeguchi N**. Protein kinase C-mediated up-regulation of Na^+/Ca^{2+}-exchanger in rat hepatocytes determined by a new Na^+/Ca^{2+}-exchanger inhibitor, KB-R7943. *Eur J Pharmacol* 360: 91-98, 1998.

135. **Ikemoto N**. Structure and function of the calcium pump protein of sarcoplasmic reticulum. *Annu Rev Physiol* 44: 297-317, 1982.

136. **Ivey DM, Guffanti AA, Zemsky J, Pinner E, Karpel R, Padan E, Schuldiner S and Krulwich TA**. Cloning and characterization of a putative Ca^{2+}/H^+ antiporter gene from *Escherichia coli* upon functional complementation of Na^+/H^+ antiporter-deficient strains by the overexpressed gene. *J Biol Chem* 268: 11296-11303, 1993.

137. **Iwamoto T, Kita S and Shigekawa M.** [Functional analysis of Na^+/Ca^{2+} exchanger using novel drugs and genetically engineered mice]. *Nippon Yakurigaku Zasshi* 120: 91P-93P, 2002.

138. **Iwamoto T, Kita S, Uehara A, Inoue Y, Taniguchi Y, Imanaga I and Shigekawa M.** Structural Domains Influencing Sensitivity to Isothiourea Derivative Inhibitor KB-R7943 in Cardiac Na+-Ca2+ Exchanger. *Mol Pharmacol* 59: 524-531, 2001.

139. **Iwamoto T, Nakamura TY, Pan Y, Uehara A, Imanaga I and Shigekawa M.** Unique topology of the internal repeats in the cardiac Na^+/Ca^{2+} exchanger. *FEBS Lett* 446: 264-268, 1999.

140. **Iwamoto T, Pan Y, Nakamura TY, Wakabayashi S and Shigekawa M.** Protein kinase C-dependent regulation of Na^+/Ca^{2+} exchanger isoforms NCX1 and NCX3 does not require their direct phosphorylation. *Biochemistry* 37: 17230-17238, 1998.

141. **Iwamoto T, Pan Y, Wakabayashi S, Imagawa T, Yamanaka HI and Shigekawa M.** Phosphorylation-dependent regulation of cardiac Na^+/Ca^{2+} exchanger via protein kinase C. *J Biol Chem* 271: 13609-13615, 1996.

142. **Iwamoto T and Shigekawa M.** Differential inhibition of Na^+/Ca^{2+} exchanger isoforms by divalent cations and isothiourea derivative. *Am J Physiol* 275: C423-C430, 1998.

143. **Iwamoto T, Uehara A, Nakamura TY, Imanaga I and Shigekawa M.** Chimeric analysis of Na^+/Ca^{2+} exchangers NCX1 and NCX3 reveals structural domains important for differential sensitivity to external Ni^{2+} or Li^+. *J Biol Chem* 274: 23094-23102, 1999.

144. **Iwamoto T, Wakabayashi S and Shigekawa M.** Growth factor-induced phosphorylation and activation of aortic smooth muscle Na^+/Ca^{2+} exchanger. *J Biol Chem* 270: 8996-9001, 1995.

145. **Iwamoto T, Watano T and Shigekawa M.** A novel isothiourea derivative selectively inhibits the reverse mode of Na^+/Ca^{2+} exchange in cells expressing NCX1. *J Biol Chem* 271: 22391-22397, 1996.

146. **Iwata T, Kraev A, Guerini D and Carafoli E.** A new splicing variant in the frog heart sarcolemmal Na-Ca exchanger creates a putative ATP-binding site. *Ann N Y Acad Sci* 779: 37-45, 1996.

147. **Kaczorowski GJ, Barros F, Dethmers JK, Trumble MJ and Cragoe EJ, Jr.** Inhibition of Na^+/Ca^{2+} exchange in pituitary plasma membrane vesicles by analogues of amiloride. *Biochemistry* 24: 1394-1403, 1985.

148. **Kaczorowski GJ, Slaughter RS, Garcia ML and King VF**. Block of cardiac sodium-calcium exchange by mechanism-based inhibitors. *Prog Clin Biol Res* 252: 261-266, 1988.

149. **Kaczorowski GJ, Slaughter RS, King VF and Garcia ML**. Inhibitors of sodium-calcium exchange: identification and development of probes of transport activity. *Biochim Biophys Acta* 988: 287-302, 1989.

150. **Kappl M and Hartung K**. Kinetics of Na-Ca exchange current after a Ca^{2+} concentration jump. *Ann N Y Acad Sci* 779: 290-292, 1996.

151. **Kappl M and Hartung K**. Rapid charge translocation by the cardiac Na^{+}-Ca^{2+} exchanger after a Ca^{2+} concentration jump. *Biophys J* 71: 2473-2485, 1996.

152. **Kass RS and Davies MP**. The roles of ion channels in an inherited heart disease: molecular genetics of the long QT syndrome. *Cardiovasc Res* 32: 443-454, 1996.

153. **Kass RS, Lederer WJ, Tsien RW and Weingart R**. Role of calcium ions in transient inward currents and aftercontractions induced by strophanthidin in cardiac Purkinje fibres. *J Physiol* 281: 187-208, 1978.

154. **Kass RS, Tsien RW and Weingart R**. Ionic basis of transient inward current induced by strophanthidin in cardiac Purkinje fibres. *J Physiol* 281: 209-226, 1978.

155. **Khananshvili D**. Distinction between the two basic mechanisms of cation transport in the cardiac Na^+-Ca^{2+} exchange system. *Biochemistry* 29: 2437-2442, 1990.

156. **Khananshvili D, Price DC, Greenberg MJ and Sarne Y**. Phe-Met-Arg-Phe-NH_2 (FMRFa)-related peptides inhibit Na^+-Ca^{2+} exchange in cardiac sarcolemma vesicles. *J Biol Chem* 268: 200-205, 1993.

157. **Khananshvili D and Sarne Y**. The effect of opiate agonists and antagonists on Na^+-Ca^{2+} exchange in cardiac sarcolemma vesicles. *Life Sci* 51: 275-283, 1992.

158. **Khananshvili D, Shaulov G, Weil-Maslansky E and Baazov D**. Positively charged cyclic hexapeptides, novel blockers for the cardiac sarcolemma Na^+-Ca^{2+} exchanger. *J Biol Chem* 270: 16182-16188, 1995.

159. **Khananshvili D and Weil-Maslansky E**. The cardiac Na^+-Ca^{2+} exchanger: relative rates of calcium and sodium movements and their modulation by protonation-deprotonation of the carrier. *Biochemistry* 33: 312-319, 1994.

160. **Kieval RS, Bloch RJ, Lindenmayer GE, Ambesi A and Lederer WJ**. Immunofluorescence localization of the Na-Ca exchanger in heart cells. *Am J Physiol* 263: C545-C550, 1992.

161. **Kihara Y, Sasayama S, Inoko M and Morgan JP**. Sodium/calcium exchange modulates intracellular calcium overload during posthypoxic reoxygenation in mammalian working myocardium. Evidence from aequorin-loaded ferret ventricular muscles. *J Clin Invest* 93: 1275-1284, 1994.

162. **Kim I, Koh GY and Lee CO**. Identification of alternatively spliced Na^+-Ca^{2+} exchanger isoforms expressed in the heart. *Comp Biochem Physiol B Biochem Mol Biol* 119: 157-161, 1998.

163. **Kim I and Lee CO**. Cloning of the mouse cardiac Na^+-Ca^{2+} exchanger and functional expression in *Xenopus* oocytes. *Ann N Y Acad Sci* 779: 126-128, 1996.

164. **Kimura J, Miyamae S and Noma A**. Identification of sodium-calcium exchange current in single ventricular cells of guinea-pig. *J Physiol (Lond)* 384: 199-222, 1987.

165. **Kimura J, Noma A and Irisawa H**. Na-Ca exchange current in mammalian heart cells. *Nature* 319: 596-597, 1986.

166. **Kimura J, Watano T, Kawahara M, Sakai E and Yatabe J**. Direction-independent block of bi-directional Na^+/Ca^{2+} exchange current by KB-R7943 in guinea-pig cardiac myocytes. *Br J Pharmacol* 128: 969-974, 1999.

167. **Kimura J, Watano T and Watanabe Y**. Electropharmacology of Na^+/Ca^{2+} exchange inhibitors. *Jpn J Pharmacol* 79: 22P, 1999.

168. **Kofuji P, Hadley RW, Kieval RS, Lederer WJ and Schulze DH**. Expression of the Na-Ca exchanger in diverse tissues: a study using the cloned human cardiac Na-Ca exchanger. *Am J Physiol* 263: C1241-C1249, 1992.

169. **Kofuji P, Lederer WJ and Schulze DH**. Mutually exclusive and cassette exons underlie alternatively spliced isoforms of the Na/Ca exchanger. *J Biol Chem* 269: 5145-5149, 1994.

170. **Komuro I, Wenninger KE, Philipson KD and Izumo S**. Molecular cloning and characterization of the human cardiac Na^+/Ca^{2+} exchanger cDNA. *Proc Natl Acad Sci U S A* 89: 4769-4773, 1992.

171. **Kozak M**. The scanning model for translation: an update. *J Cell Biol* 108: 229-241, 1989.

172. **Kraev A, Chumakov I and Carafoli E**. Molecular biological studies of the cardiac sodium-calcium exchanger. *Ann N Y Acad Sci* 779: 103-109, 1996.

173. **Kraev A, Chumakov I and Carafoli E**. The organization of the human gene NCX1 encoding the sodium-calcium exchanger. *Genomics* 37: 105-112, 1996.

174. **Kraev A, Quednau BD, Leach S, Li XF, Dong H, Winkfein R, Perizzolo M, Cai X, Yang R, Philipson KD and Lytton J**. Molecular cloning of a third member of the potassium-dependent sodium-calcium exchanger gene family, NCKX3. *J Biol Chem* 276: 23161-23172, 2001.

175. **Kuro T, Kobayashi Y, Takaoka M and Matsumura Y**. Protective effect of KB-R7943, a novel Na^+/Ca^{2+} exchange inhibitor, on ischemic acute renal failure in rats. *Jpn J Pharmacol* 81: 247-251, 1999.

176. **Kutryk MJ, Maddaford TG, Ramjiawan B and Pierce GN**. Oxidation of membrane cholesterol alters active and passive transsarcolemmal calcium movement. *Circ Res* 68: 18-26, 1991.

177. **Kutryk MJ and Pierce GN**. Stimulation of sodium-calcium exchange by cholesterol incorporation into isolated cardiac sarcolemmal vesicles. *J Biol Chem* 263: 13167-13172, 1988.

178. **Ladilov Y, Haffner S, Balser-Schafer C, Maxeiner H and Piper HM**. Cardioprotective effects of KB-R7943: a novel inhibitor of the reverse mode of Na^+/Ca^{2+} exchanger. *Am J Physiol* 276: H1868-H1876, 1999.

179. **Lauger P**. Voltage dependence of sodium-calcium exchange: predictions from kinetic models. *J Membr Biol* 99: 1-11, 1987.

180. **Lazdunski M, Frelin C and Vigne P**. The sodium/hydrogen exchange system in cardiac cells: its biochemical and pharmacological properties and its role in regulating internal concentrations of sodium and internal pH. *J Mol Cell Cardiol* 17: 1029-1042, 1985.

181. **Leblanc N and Hume JR**. Sodium current-induced release of calcium from cardiac sarcoplasmic reticulum. *Science* 248: 372-376, 1990.

182. **Ledvora RF and Hegyvary C**. Dependence of Na^+-Ca^{2+} exchange and Ca^{2+}-Ca^{2+} exchange on monovalent cations. *Biochim Biophys Acta* 729: 123-136, 1983.

183. **Lee CO, Uhm DY and Dresdner K**. Sodium-calcium exchange in rabbit heart muscle cells: direct measurement of sarcoplasmic Ca^{2+} activity. *Science* 209: 699-701, 1980.

184. **Lee SL, Yu AS and Lytton J**. Tissue-specific expression of Na^+-Ca^{2+} exchanger isoforms. *J Biol Chem* 269: 14849-14852, 1994.

185. **Levesque PC, Leblanc N and Hume JR**. Role of reverse-mode Na^+-Ca^{2+} exchange in excitation- contraction coupling in the heart. *Ann N Y Acad Sci* 639: 386-397, 1991.

186. **Levesque PC, Leblanc N and Hume JR**. Release of calcium from guinea pig cardiac sarcoplasmic reticulum induced by sodium-calcium exchange. *Cardiovasc Res* 28: 370-378, 1994.

187. **Levi AJ, Boyett MR and Lee CO**. The cellular actions of digitalis glycosides on the heart. *Prog Biophys Mol Biol* 62: 1-54, 1994.

188. **Levitsky DO, Nicoll DA and Philipson KD**. Identification of the high affinity Ca^{2+}-binding domain of the cardiac Na^{+}-Ca^{2+} exchanger. *J Biol Chem* 269: 22847-22852, 1994.

189. **Li JM and Kimura J**. Translocation mechanism of Na-Ca exchange in single cardiac cells of guinea pig. *J Gen Physiol* 96: 777-788, 1990.

190. **Li JM and Kimura J**. Translocation mechanism of cardiac Na-Ca exchange. *Ann N Y Acad Sci* 639: 48-60, 1991.

191. **Li XF and Lytton J**. A circularized sodium-calcium exchanger exon 2 transcript. *J Biol Chem* 274: 8153-8160, 1999.

192. **Li Z, Matsuoka S, Hryshko LV, Nicoll DA, Bersohn MM, Burke EP, Lifton RP and Philipson KD**. Cloning of the NCX2 isoform of the plasma membrane Na^{+}-Ca^{2+} exchanger. *J Biol Chem* 269: 17434-17439, 1994.

193. **Li Z, Nicoll DA, Collins A, Hilgemann DW, Filoteo AG, Penniston JT, Weiss JN, Tomich JM and Philipson KD**. Identification of a peptide inhibitor of the cardiac sarcolemmal Na^+-Ca^{2+} exchanger. *J Biol Chem* 266: 1014-1020, 1991.

194. **Linck B, Qiu Z, He Z, Tong Q, Hilgemann DW and Philipson KD**. Functional comparison of the three isoforms of the Na^+/Ca^{2+} exchanger (NCX1, NCX2, NCX3). *Am J Physiol* 274: C415-C423, 1998.

195. **Lipp P and Pott L**. Transient inward current in guinea-pig atrial myocytes reflects a change of sodium-calcium exchange current. *J Physiol (Lond)* 397: 601-630, 1988.

196. **Lipp P and Pott L**. Voltage dependence of sodium-calcium exchange current in guinea-pig atrial myocytes determined by means of an inhibitor. *J Physiol (Lond)* 403: 355-366, 1988.

197. **Litwin SE and Bridge JH**. Enhanced Na^+-Ca^{2+} exchange in the infarcted heart. Implications for excitation-contraction coupling. *Circ Res* 81: 1083-1093, 1997.

198. **Litwin SE, Li J and Bridge JH**. Na-Ca exchange and the trigger for sarcoplasmic reticulum Ca release: studies in adult rabbit ventricular myocytes. *Biophys J* 75: 359-371, 1998.

199. **Longoni S and Carafoli E.** Identification of the Na^+/Ca^{2+} exchanger of calf heart sarcolemma with the help of specific antibodies. *Biochem Biophys Res Commun* 145: 1059-1063, 1987.

200. **Lopez-Lopez JR, Shacklock PS, Balke CW and Wier WG.** Local calcium transients triggered by single L-type calcium channel currents in cardiac cells. *Science* 268: 1042-1045, 1995.

201. **Lu HR, Yang P, Remeysen P, Saels A, Dai DZ and De Clerck F.** Ischemia/reperfusion-induced arrhythmias in anaesthetized rats: a role of Na^+ and Ca^{2+} influx. *Eur J Pharmacol* 365: 233-239, 1999.

202. **Luther PW, Yip RK, Bloch RJ, Ambesi A, Lindenmayer GE and Blaustein MP.** Presynaptic localization of sodium/calcium exchangers in neuromuscular preparations. *J Neurosci* 12: 4898-4904, 1992.

203. **Magee WP, Deshmukh G, DeNinno MP, Sutt JC, Chapman JG and Tracey WR.** Differing cardioprotective efficacy of the Na^+-Ca^{2+} exchanger inhibitors, SEA0400 and KB-R7943. *Am J Physiol Heart Circ Physiol* 284: H903-H910, 2003.

204. **Matsuda T, Arakawa N, Takuma K, Kishida Y, Kawasaki Y, Sakaue M, Takahashi K, Takahashi T, Suzuki T, Ota T, Hamano-Takahashi A, Onishi M, Tanaka Y, Kameo K and Baba A.** SEA0400, a novel and selective inhibitor

of the Na^+-Ca^{2+} exchanger, attenuates reperfusion injury in the in vitro and in vivo cerebral ischemic models. *J Pharmacol Exp Ther* 298: 249-256, 2001.

205. **Matsuoka S, Ehara T and Noma A**. Reversal potential of the Na-Ca exchange current in the cardiac myocyte of the guinea pig. *Bimedical Research* 9: 149-152, 1988.

206. **Matsuoka S, Fujioka Y and Noma A**. Reversal potential of the Na+-Ca2+ exchange suggests 4:1 stoichiometry in "macro" patch from guinea-pig ventricular cells. *Biophys J* 76: A252, 1999.

207. **Matsuoka S and Hilgemann DW**. Steady-state and dynamic properties of cardiac sodium-calcium exchange. Ion and voltage dependencies of the transport cycle. *J Gen Physiol* 100: 963-1001, 1992.

208. **Matsuoka S and Hilgemann DW**. Inactivation of outward Na^+-Ca^{2+} exchange current in guinea- pig ventricular myocytes. *J Physiol (Lond)* 476: 443-458, 1994.

209. **Matsuoka S, Nicoll DA, He Z and Philipson KD**. Regulation of cardiac Na^+-Ca^{2+} exchanger by the endogenous XIP region. *J Gen Physiol* 109: 273-286, 1997.

210. **Matsuoka S, Nicoll DA, Hryshko LV, Levitsky DO, Weiss JN and Philipson KD**. Regulation of the cardiac Na^+-Ca^{2+} exchanger by Ca^{2+}. Mutational analysis of the Ca^{2+}-binding domain. *J Gen Physiol* 105: 403-420, 1995.

211. **Matsuoka S, Nicoll DA, Reilly RF, Hilgemann DW and Philipson KD**. Initial localization of regulatory regions of the cardiac sarcolemmal Na^+-Ca^{2+} exchanger. *Proc Natl Acad Sci U S A* 90: 3870-3874, 1993.

212. **Maxwell K, Scott J, Omelchenko A, Lukas A, Lu L, Lu Y, Hnatowich M, Philipson KD and Hryshko LV**. Functional role of ionic regulation of Na^+/Ca^{2+} exchange assessed in transgenic mouse hearts. *Am J Physiol* 277: H2212-H2221, 1999.

213. **Mene P, Pugliese F, Faraggiana T and Cinotti GA**. Identification and characteristics of a Na^+/Ca^{2+} exchanger in cultured human mesangial cells. *Kidney Int* 38: 1199-1205, 1990.

214. **Milanick MA and Frame MD**. Kinetic models of Na-Ca exchange in ferret red blood cells. Interaction of intracellular Na, extracellular Ca, Cd, and Mn. *Ann N Y Acad Sci* 639: 604-615, 1991.

215. **Miura Y and Kimura J**. Sodium-calcium exchange current. Dependence on internal Ca and Na and competitive binding of external Na and Ca. *J Gen Physiol* 93: 1129-1145, 1989.

216. **Miyamoto S, Zhu BM, Kamiya K, Nagasawa Y and Hashimoto K.** KB-R7943, a Na^+/Ca^{2+} exchange inhibitor, does not suppress ischemia/reperfusion arrhythmias nor digitalis arrhythmias in dogs. *Jpn J Pharmacol* 90: 229-235, 2002.

217. **Miyata A, Zipes DP, Hall S and Rubart M.** KB-R7943 prevents acute, atrial fibrillation-induced shortening of atrial refractoriness in anesthetized dogs. *Circulation* 106: 1410-1419, 2002.

218. **Mukai M, Terada H, Sugiyama S, Satoh H and Hayashi H.** Effects of a selective inhibitor of Na^+/Ca^{2+} exchange, KB-R7943, on reoxygenation-induced injuries in guinea pig papillary muscles. *J Cardiovasc Pharmacol* 35: 121-128, 2000.

219. **Mullins LJ.** A mechanism for Na/Ca transport. *J Gen Physiol* 70: 681-695, 1977.

220. **Murphy E, Perlman M, London RE and Steenbergen C.** Amiloride delays the ischemia-induced rise in cytosolic free calcium. *Circ Res* 68: 1250-1258, 1991.

221. **Nabauer M, Callewaert G, Cleemann L and Morad M.** Regulation of calcium release is gated by calcium current, not gating charge, in cardiac myocytes. *Science* 244: 800-803, 1989.

222. **Nakamura A, Harada K, Sugimoto H, Nakajima F and Nishimura N**. Effects of KB-R7943, a novel Na^+/Ca^{2+} exchange inhibitor, on myocardial ischemia/reperfusion injury. *Nippon Yakurigaku Zasshi* 111: 105-115, 1998.

223. **Neary P, Duncan AM, Cobbe SM and Smith GL**. Assessment of sarcoplasmic reticulum Ca^{2+} flux pathways in cardiomyocytes from rabbits with infarct-induced left-ventricular dysfunction. *Pflugers Arch* 444: 360-371, 2002.

224. **Nicholas SB and Philipson KD**. Cardiac expression of the Na^+/Ca^{2+} exchanger NCX1 is GATA factor dependent. *Am J Physiol* 277: H324-H330, 1999.

225. **Nicoll DA, Hryshko LV, Matsuoka S, Frank JS and Philipson KD**. Mutagenesis studies of the cardiac Na^+-Ca^{2+} exchanger. *Ann N Y Acad Sci* 779: 86-92, 1996.

226. **Nicoll DA, Hryshko LV, Matsuoka S, Frank JS and Philipson KD**. Mutation of amino acid residues in the putative transmembrane segments of the cardiac sarcolemmal Na^+-Ca^{2+} exchanger. *J Biol Chem* 271: 13385-13391, 1996.

227. **Nicoll DA, Longoni S and Philipson KD**. Molecular cloning and functional expression of the cardiac sarcolemmal Na^+-Ca^{2+} exchanger. *Science* 250: 562-565, 1990.

228. **Nicoll DA, Ottolia M, Lu L, Lu Y and Philipson KD**. A new topological model of the cardiac sarcolemmal Na^+-Ca^{2+} exchanger. *J Biol Chem* 274: 910-917, 1999.

229. **Nicoll DA and Philipson KD**. Molecular studies of the cardiac sarcolemmal sodium-calcium exchanger. *Ann N Y Acad Sci* 639: 181-188, 1991.

230. **Nicoll DA, Quednau BD, Qui Z, Xia YR, Lusis AJ and Philipson KD**. Cloning of a third mammalian Na^+-Ca^{2+} exchanger, NCX3. *J Biol Chem* 271: 24914-24921, 1996.

231. **Niggli E**. Strontium-induced creep currents associated with tonic contractions in cardiac myocytes isolated from guinea-pigs. *J Physiol (Lond)* 414: 549-568, 1989.

232. **Niggli E and Lederer WJ**. Molecular operations of the sodium-calcium exchanger revealed by conformation currents. *Nature* 349: 621-624, 1991.

233. **Niggli E and Lederer WJ**. Activation of Na-Ca exchange current by photolysis of "caged calcium". *Biophys J* 65: 882-891, 1993.

234. **Nishida M, Urushidani T, Sakamoto K and Nagao T**. L-*cis* diltiazem attenuates intracellular Ca^{2+} overload by metabolic inhibition in guinea pig myocytes. *Eur J Pharmacol* 385: 225-230, 1999.

235. **Noble D, LeGuennec JY and Winslow R.** Functional roles of sodium-calcium exchange in normal and abnormal cardiac rhythm. *Ann N Y Acad Sci* 779: 480-488, 1996.

236. **Nuss HB, Kaab S, Kass DA, Tomaselli GF and Marban E.** Cellular basis of ventricular arrhythmias and abnormal automaticity in heart failure. *Am J Physiol* 277: H80-H91, 1999.

237. **O'Neill SC, Valdeolmillos M, Lamont C, Donoso P and Eisner DA.** The contribution of Na-Ca exchange to relaxation in mammalian cardiac muscle. *Ann N Y Acad Sci* 639: 444-452, 1991.

238. **O'Rourke B, Kass DA, Tomaselli GF, Kaab S, Tunin R and Marban E.** Mechanisms of altered excitation-contraction coupling in canine tachycardia-induced heart failure, I: experimental studies. *Circ Res* 84: 562-570, 1999.

239. **Ogata M, Iwamoto T, Tazawa N, Nishikawa M, Yamashita J, Takaoka M and Matsumura Y.** A novel and selective Na^+/Ca^{2+} exchange inhibitor, SEA0400, improves ischemia/reperfusion-induced renal injury. *Eur J Pharmacol* 478: 187-198, 2003.

240. **Omelchenko A, Dyck C, Hnatowich M, Buchko J, Nicoll DA, Philipson KD and Hryshko LV.** Functional differences in ionic regulation between

alternatively spliced isoforms of the Na^+-Ca^{2+} exchanger from *Drosophila melanogaster*. *J Gen Physiol* 111: 691-702, 1998.

241. **Omelchenko A, Elias CL, Hnatowich M and Hryshko LV**. A unique form of $Ca^{2+}{}_i$-dependent regulation of the kidney Na^+-Ca^{2+} exchanger, NCX1.3. *Biophys J* 78: 54A, 2000.

242. **Omelchenko A and Hryshko LV**. Current-voltage relations and steady-state characteristics of Na^+-Ca^{2+} exchange: characterization of the eight-state consecutive transport model. *Biophys J* 71: 1751-1763, 1996.

243. **Ottolia M, John S, Qiu Z and Philipson KD**. Split Na^+-Ca^{2+} exchangers. Implications for function and expression. *J Biol Chem* 276: 19603-19609, 2001.

244. **Pan Y, Iwamoto T, Uehara A, Nakamura TY, Imanaga I and Shigekawa M**. Physiological functions of the regulatory domains of the cardiac Na^+/Ca^{2+} exchanger NCX1. *Am J Physiol Cell Physiol* 279: C393-C402, 2000.

245. **Periasamy M, Reed TD, Liu LH, Ji Y, Loukianov E, Paul RJ, Nieman ML, Riddle T, Duffy JJ, Doetschman T, Lorenz JN and Shull GE**. Impaired cardiac performance in heterozygous mice with a null mutation in the sarco(endo)plasmic reticulum Ca^{2+}-ATPase isoform 2 (SERCA2) gene. *J Biol Chem* 274: 2556-2562, 1999.

246. **Peterson BZ, DeMaria CD, Adelman JP and Yue DT**. Calmodulin is the Ca^{2+} sensor for Ca^{2+}-dependent inactivation of L-type calcium channels. *Neuron* 22: 549-558, 1999.

247. **Philipson KD, Bersohn MM and Nishimoto AY**. Effects of pH on Na^{+}-Ca^{2+} exchange in canine cardiac sarcolemmal vesicles. *Circ Res* 50: 287-293, 1982.

248. **Philipson KD, Frank JS and Nishimoto AY**. Effects of phospholipase C on the Na^{+}-Ca^{2+} exchange and Ca^{2+} permeability of cardiac sarcolemmal vesicles. *J Biol Chem* 258: 5905-5910, 1983.

249. **Philipson KD, Longoni S and Ward R**. Purification of the cardiac Na^{+}-Ca^{2+} exchange protein. *Biochim Biophys Acta* 945: 298-306, 1988.

250. **Philipson KD and Nicoll DA**. Sodium-calcium exchange: a molecular perspective. *Annu Rev Physiol* 62: 111-133, 2000.

251. **Philipson KD and Nishimoto AY**. Stimulation of Na^{+}-Ca^{2+} exchange in cardiac sarcolemmal vesicles by phospholipase D. *J Biol Chem* 259: 16-19, 1984.

252. **Philipson KD and Ward R**. Effects of fatty acids on Na^{+}-Ca^{2+} exchange and Ca^{2+} permeability of cardiac sarcolemmal vesicles. *J Biol Chem* 260: 9666-9671, 1985.

253. **Philipson KD and Ward R.** Modulation of Na^+-Ca^{2+} exchange and Ca^{2+} permeability in cardiac sarcolemmal vesicles by doxylstearic acids. *Biochim Biophys Acta* 897: 152-158, 1987.

254. **Pierce GN and Panagia V.** Role of phosphatidylinositol in cardiac sarcolemmal membrane sodium- calcium exchange. *J Biol Chem* 264: 15344-15350, 1989.

255. **Pilitsis JG, Diaz FG, O'Regan MH and Phillis JW.** Inhibition of Na^+/Ca^{2+} exchange by KB-R7943, a novel selective antagonist, attenuates phosphoethanolamine and free fatty acid efflux in rat cerebral cortex during ischemia-reperfusion injury. *Brain Res* 916: 192-198, 2001.

256. **Pintado AJ, Herrero CJ, Garcia AG and Montiel C.** The novel Na^+/Ca^{2+} exchange inhibitor KB-R7943 also blocks native and expressed neuronal nicotinic receptors. *Br J Pharmacol* 130: 1893-1902, 2000.

257. **Pitts BJ.** Stoichiometry of sodium-calcium exchange in cardiac sarcolemmal vesicles. Coupling to the sodium pump. *J Biol Chem* 254: 6232-6235, 1979.

258. **Pogwizd SM.** Nonreentrant mechanisms underlying spontaneous ventricular arrhythmias in a model of nonischemic heart failure in rabbits. *Circulation* 92: 1034-1048, 1995.

259. **Pogwizd SM, Qi M, Yuan W, Samarel AM and Bers DM.** Upregulation of Na^+/Ca^{2+} exchanger expression and function in an arrhythmogenic rabbit model of heart failure. *Circ Res* 85: 1009-1019, 1999.

260. **Pogwizd SM, Schlotthauer K, Li L, Yuan W and Bers DM.** Arrhythmogenesis and contractile dysfunction in heart failure: Roles of sodium-calcium exchange, inward rectifier potassium current, and residual β-adrenergic responsiveness. *Circ Res* 88: 1159-1167, 2001.

261. **Poon S, Leach S, Li XF, Tucker JE, Schnetkamp PP and Lytton J.** Alternatively spliced isoforms of the rat eye sodium/calcium-potassium exchanger NCKX1. *Am J Physiol Cell Physiol* 278: C651-C660, 2000.

262. **Powell T, Noma A, Shioya T and Kozlowski RZ.** Turnover rate of the cardiac Na^+-Ca^{2+} exchanger in guinea-pig ventricular myocytes. *J Physiol (Lond)* 472: 45-53, 1993.

263. **Pozos TC, Sekler I and Cyert MS.** The product of HUM1, a novel yeast gene, is required for vacuolar Ca^{2+}/H^+ exchange and is related to mammalian Na^+/Ca^{2+} exchangers. *Mol Cell Biol* 16: 3730-3741, 1996.

264. **Qiu Z, Nicoll DA and Philipson KD.** Helix packing of functionally important regions of the cardiac Na+-Ca2+ exchanger. *J Biol Chem* 276: 194-199, 2001.

265. **Quednau BD, Nicoll DA and Philipson KD.** Tissue specificity and alternative splicing of the Na^+/Ca^{2+} exchanger isoforms NCX1, NCX2, and NCX3 in rat. *Am J Physiol* 272: C1250-C1261, 1997.

266. **Quinn FR, Currie S, Duncan AM, Miller SL, Sayeed R, Cobbe SM and Smith GL.** Myocardial infarction causes increased expression but decreased activity of myocardial Na^+/Ca^{2+} exchanger in the rabbit. *J Physiol* .: 2003.

267. **Quist EE and Roufogalis BD.** Determination of the stoichiometry of the calcium pump in human erythrocytes using lanthanum as a selective inhibitor. *FEBS Lett* 50: 135-139, 1975.

268. **Reeves JP.** Na^+/Ca^{2+} exchange and cellular Ca^{2+} homeostasis. *J Bioenerg Biomembr* 30: 151-160, 1998.

269. **Reeves JP and Hale CC.** The stoichiometry of the cardiac sodium-calcium exchange system. *J Biol Chem* 259: 7733-7739, 1984.

270. **Reeves JP and Poronnik P.** Modulation of Na^+-Ca^{2+} exchange in sarcolemmal vesicles by intravesicular Ca^{2+}. *Am J Physiol* 252: C17-C23, 1987.

271. **Reeves JP and Sutko JL.** Sodium-calcium ion exchange in cardiac membrane vesicles. *Proc Natl Acad Sci U S A* 76: 590-594, 1979.

272. **Reeves JP and Sutko JL**. Sodium-calcium exchange activity generates a current in cardiac membrane vesicles. *Science* 208: 1461-1464, 1980.

273. **Reilander H, Achilles A, Friedel U, Maul G, Lottspeich F and Cook NJ**. Primary structure and functional expression of the Na/Ca,K- exchanger from bovine rod photoreceptors. *EMBO J* 11: 1689-1695, 1992.

274. **Reuter H, Henderson SA, Han T, Matsuda T, Baba A, Ross RS, Goldhaber JI and Philipson KD**. Knock-out mice for pharmacological screening: testing the specificity of Na+-Ca2+ exchange inhibitors. *Circ Res* 91: 90-92, 2002.

275. **Reuter H and Seitz N**. The dependence of calcium efflux from cardiac muscle on temperature and external ion composition. *J Physiol (Lond)* 195: 451-470, 1968.

276. **Ruknudin A, He S, Lederer WJ and Schulze DH**. Functional differences between cardiac and renal isoforms of the rat Na^+-Ca^{2+} exchanger NCX1 expressed in *Xenopus* oocytes. *J Physiol* 529: 599-610, 2000.

277. **Ruknudin A, Valdivia C, Kofuji P, Lederer WJ and Schulze DH**. Na^+/Ca^{2+} exchanger in *Drosophila*: cloning, expression, and transport differences. *Am J Physiol* 273: C257-C265, 1997.

278. **Sahin-Toth M, Nicoll DA, Frank JS, Philipson KD and Friedlander M**. The cleaved N-terminal signal sequence of the cardiac Na^+-Ca^{2+} exchanger is not

required for functional membrane integration. *Biochem Biophys Res Commun* 212: 968-974, 1995.

279. **Santana LF, Cheng H, Gomez AM, Cannell MB and Lederer WJ**. Relation between the sarcolemmal Ca^{2+} current and Ca^{2+} sparks and local control theories for cardiac excitation-contraction coupling. *Circ Res* 78: 166-171, 1996.

280. **Sarkadi B, Szasz I, Gerloczy A and Gardos G**. Transport parameters and stoichiometry of active calcium ion extrusion in intact human red cells. *Biochim Biophys Acta* 464: 93-107, 1977.

281. **Satoh H, Ginsburg KS, Qing K, Terada H, Hayashi H and Bers DM**. KB-R7943 block of Ca^{2+} influx via Na^{+}/Ca^{2+} exchange does not alter twitches or glycoside inotropy but prevents Ca^{2+} overload in rat ventricular myocytes. *Circulation* 101: 1441-1446, 2000.

282. **Schillinger W, Janssen PM, Emami S, Henderson SA, Ross RS, Teucher N, Zeitz O, Philipson KD, Prestle J and Hasenfuss G**. Impaired contractile performance of cultured rabbit ventricular myocytes after adenoviral gene transfer of Na^{+}-Ca^{2+} exchanger. *Circ Res* 87: 581-587, 2000.

283. **Schillinger W, Lehnart SE, Prestle J, Preuss M, Pieske B, Maier LS, Meyer M, Just H and Hasenfuss G**. Influence of SR Ca^{2+}-ATPase and Na^{+}-Ca^{2+}-

exchanger on the force- frequency relation. *Basic Res Cardiol* 93 Suppl 1: 38-45, 1998.

284. **Schlotthauer KOA, Pogwizd SM and Bers DM**. SR release triggers action potential (AP) through Na/Ca exchange current in myocytes from failing and non-failing rabbit and human. *Biophys J* 78: 55A, 2000.

285. **Schnetkamp PP, Basu DK and Szerencsei RT**. Na^+-Ca^{2+} exchange in bovine rod outer segments requires and transports K^+. *Am J Physiol* 257: C153-C157, 1989.

286. **Schnetkamp PP and Szerencsei RT**. Effect of potassium ions and membrane potential on the Na-Ca-K exchanger in isolated intact bovine rod outer segments. *J Biol Chem* 266: 189-197, 1991.

287. **Schnetkamp PP and Szerencsei RT**. Intracellular Ca^{2+} sequestration and release in intact bovine retinal rod outer segments. Role in inactivation of Na-Ca+K exchange. *J Biol Chem* 268: 12449-12457, 1993.

288. **Schnetkamp PP, Tucker JE and Szerencsei RT**. Ca^{2+} influx into bovine retinal rod outer segments mediated by $Na^+/Ca^{2+}/K^+$ exchange. *Am J Physiol* 269: C1153-C1159, 1995.

289. **Schroder UH, Breder J, Sabelhaus CF and Reymann KG**. The novel Na^+/Ca^{2+} exchange inhibitor KB-R7943 protects CA1 neurons in rat hippocampal slices against hypoxic/hypoglycemic injury. *Neuropharmacology* 38: 319-321, 1999.

290. **Schwarz EM and Benzer S**. *Calx*, a Na-Ca exchanger gene of *Drosophila melanogaster*. *Proc Natl Acad Sci U S A* 94: 10249-10254, 1997.

291. **Seki S, Taniguchi M, Takeda H, Nagai M, Taniguchi I and Mochizuki S**. Inhibition by KB-R7943 of the reverse mode of the Na^+/Ca^{2+} exchanger reduces Ca^{2+} overload in ischemic-reperfused rat hearts. *Circ J* 66: 390-396, 2002.

292. **Sham JS, Cleemann L and Morad M**. Gating of the cardiac Ca^{2+} release channel: the role of Na^+ current and Na^+-Ca^{2+} exchange. *Science* 255: 850-853, 1992.

293. **Sham JS, Cleemann L and Morad M**. Functional coupling of Ca^{2+} channels and ryanodine receptors in cardiac myocytes. *Proc Natl Acad Sci U S A* 92: 121-125, 1995.

294. **Shi S, Chang B and Brunnert SR**. Identification and cloning of a truncated isoform of the cardiac sodium- calcium exchanger in the BALB/c mouse heart. *Biochem Genet* 36: 119-135, 1998.

295. **Shieh BH, Xia Y, Sparkes RS, Klisak I, Lusis AJ, Nicoll DA and Philipson KD**. Mapping of the gene for the cardiac sarcolemmal Na^+-Ca^{2+} exchanger to human chromosome 2p21-p23. *Genomics* 12: 616-617, 1992.

296. **Shimizu H, Borin ML and Blaustein MP**. Use of La^{3+} to distinguish activity of the plasmalemmal Ca^{2+} pump from Na^+/Ca^{2+} exchange in arterial myocytes. *Cell Calcium* 21: 31-41, 1997.

297. **Siegl PK, Cragoe EJ, Jr., Trumble MJ and Kaczorowski GJ**. Inhibition of Na^+/Ca^{2+} exchange in membrane vesicle and papillary muscle preparations from guinea pig heart by analogs of amiloride. *Proc Natl Acad Sci U S A* 81: 3238-3242, 1984.

298. **Sipido KR**. Efficiency of L-type Ca^{2+} current compared to reverse mode Na/Ca exchange or T-type Ca^{2+} current as trigger for Ca^{2+} release from the sarcoplasmic reticulum. *Ann N Y Acad Sci* 853: 357-360, 1998.

299. **Sipido KR, Maes M and Van de Werf F**. Low efficiency of Ca^{2+} entry through the Na^+-Ca^{2+} exchanger as trigger for Ca^{2+} release from the sarcoplasmic reticulum. A comparison between L-type Ca^{2+} current and reverse-mode Na^+-Ca^{2+} exchange. *Circ Res* 81: 1034-1044, 1997.

300. **Slaughter RS, Garcia ML, Cragoe EJ, Jr., Reeves JP and Kaczorowski GJ**. Inhibition of sodium-calcium exchange in cardiac sarcolemmal membrane

vesicles. 1. Mechanism of inhibition by amiloride analogues. *Biochemistry* 27: 2403-2409, 1988.

301. **Smith JB, Cragoe EJ, Jr. and Smith L**. Na^+/Ca^{2+} antiport in cultured arterial smooth muscle cells. Inhibition by magnesium and other divalent cations. *J Biol Chem* 262: 11988-11994, 1987.

302. **Smith L, Porzig H, Lee HW and Smith JB**. Phorbol esters downregulate expression of the sodium/calcium exchanger in renal epithelial cells. *Am J Physiol* 269: C457-C463, 1995.

303. **Smith L and Smith JB**. Activation of adenylyl cyclase downregulates sodium/calcium exchanger of arterial myocytes. *Am J Physiol* 269: C1379-C1384, 1995.

304. **Stains JP and Gay CV**. Inhibition of Na^+/Ca^{2+} exchange with KB-R7943 or bepridil diminished mineral deposition by osteoblasts. *J Bone Miner Res* 16: 1434-1443, 2001.

305. **Stengl M, Mubagwa K, Carmeliet E and Flameng W**. Phenylephrine-induced stimulation of Na^+/Ca^{2+} exchange in rat ventricular myocytes. *Cardiovasc Res* 38: 703-710, 1998.

306. **Stern MD**. Theory of excitation-contraction coupling in cardiac muscle. *Biophys J* 63: 497-517, 1992.

307. **Studer R, Reinecke H, Bilger J, Eschenhagen T, Bohm M, Hasenfuss G, Just H, Holtz J and Drexler H**. Gene expression of the cardiac Na^+-Ca^{2+} exchanger in end-stage human heart failure. *Circ Res* 75: 443-453, 1994.

308. **Szabo B, Sweidan R, Rajagopalan CV and Lazzara R**. Role of Na^+:Ca^{2+} exchange current in Cs^+-induced early afterdepolarizations in Purkinje fibers. *J Cardiovasc Electrophysiol* 5: 933-944, 1994.

309. **Szerencsei RT, Prinsen CF and Schnetkamp PP**. Stoichiometry of the retinal cone Na/Ca-K exchanger heterologously expressed in insect cells: comparison with the bovine heart Na/Ca exchanger. *Biochemistry* 40: 6009-6015, 2001.

310. **Takahashi K, Takahashi T, Suzuki T, Onishi M, Tanaka Y, Hamano-Takahashi A, Ota T, Kameo K, Matsuda T and Baba A**. Protective effects of SEA0400, a novel and selective inhibitor of the Na^+/Ca^{2+} exchanger, on myocardial ischemia-reperfusion injuries. *Eur J Pharmacol* 458: 155-162, 2003.

311. **Tanaka H, Nishimaru K, Aikawa T, Hirayama W, Tanaka Y and Shigenobu K**. Effect of SEA0400, a novel inhibitor of sodium-calcium exchanger, on myocardial ionic currents. *Br J Pharmacol* 135: 1096-1100, 2002.

312. **Tani M and Neely JR.** Na^+ accumulation increases Ca^{2+} overload and impairs function in anoxic rat heart. *J Mol Cell Cardiol* 22: 57-72, 1990.

313. **Thomas MJ, Sjaastad I, Andersen K, Helm PJ, Wasserstrom JA, Sejersted OM and Ottersen OP.** Localization and function of the Na^+/Ca^{2+}-exchanger in normal and detubulated rat cardiomyocytes. *J Mol Cell Cardiol* 35: 1325-1337, 2003.

314. **Trac M, Dyck C, Hnatowich M, Omelchenko A and Hryshko LV.** Transport and regulation of the cardiac Na^+-Ca^{2+} exchanger, NCX1. Comparison between Ca^{2+} and Ba^{2+}. *J Gen Physiol* 109: 361-369, 1997.

315. **Trosper TL and Philipson KD.** Effects of divalent and trivalent cations on Na^+-Ca^{2+} exchange in cardiac sarcolemmal vesicles. *Biochim Biophys Acta* 731: 63-68, 1983.

316. **Tsoi M, Rhee KH, Bungard D, Li XF, Lee SL, Auer RN and Lytton J.** Molecular cloning of a novel potassium-dependent sodium-calcium exchanger from rat brain. *J Biol Chem* 273: 4155-4162, 1998.

317. **Tsuruya Y, Bersohn MM, Li Z, Nicoll DA and Philipson KD.** Molecular cloning and functional expression of the guinea pig cardiac Na^+-Ca^{2+} exchanger. *Biochim Biophys Acta* 1196: 97-99, 1994.

318. **Uetani T, Matsubara TA, Nomura H, Murohara TA and Nakayama S.** Ca^{2+}-dependent modulation of intracellular Mg^{2+} concentration with amiloride and KB-R7943 in pig carotid artery. *J Biol Chem* .: 2003.

319. **Van Eylen F, Gourlet P, Vandermeers A, Lebrun P and Herchuelz A.** Phe-Met-Arg-Phe-NH2 (FMRFa)-related peptides inhibit Na/Ca exchange in pancreatic B cells. *Adv Exp Med Biol* 426: 223-225, 1997.

320. **Varro A, Negretti N, Hester SB and Eisner DA.** An estimate of the calcium content of the sarcoplasmic reticulum in rat ventricular myocytes. *Pflugers Arch* 423: 158-160, 1993.

321. **Vemuri R and Philipson KD.** Phospholipid composition modulates the Na^{+}-Ca^{2+} exchange activity of cardiac sarcolemma in reconstituted vesicles. *Biochim Biophys Acta* 937: 258-268, 1988.

322. **Vemuri R and Philipson KD.** Influence of sterols and phospholipids on sarcolemmal and sarcoplasmic reticular cation transporters. *J Biol Chem* 264: 8680-8685, 1989.

323. **Volders PG, Kulcsar A, Vos MA, Sipido KR, Wellens HJ, Lazzara R and Szabo B.** Similarities between early and delayed afterdepolarizations induced by isoproterenol in canine ventricular myocytes. *Cardiovasc Res* 34: 348-359, 1997.

324. **Wakimoto K, Kuro O, Yanaka N, Omori K, Komuro I, Imai Y and Nabeshima Y**. Isolation and characterization of Na^+/Ca^{2+} exchanger gene and splicing isoforms in mice. *DNA Seq* 11: 75-81, 2000.

325. **Watano T, Harada Y, Harada K and Nishimura N**. Effect of Na^+/Ca^{2+} exchange inhibitor, KB-R7943 on ouabain-induced arrhythmias in guinea-pigs. *Br J Pharmacol* 127: 1846-1850, 1999.

326. **Watano T and Kimura J**. Calcium-dependent inhibition of the sodium-calcium exchange current by KB-R7943. *Can J Cardiol* 14: 259-262, 1998.

327. **Watano T, Kimura J, Morita T and Nakanishi H**. A novel antagonist, No. 7943, of the Na^+/Ca^{2+} exchange current in guinea-pig cardiac ventricular cells. *Br J Pharmacol* 119: 555-563, 1996.

328. **Weber CR, Ginsburg KS and Bers DM**. Cardiac Submembrane $[Na^+]$ Transients Sensed by Na^+-Ca^{2+} Exchange Current. *Circ Res* .: 2003.

329. **Weber CR, Piacentino V, III, Ginsburg KS, Houser SR and Bers DM**. Na^+-Ca^{2+} exchange current and submembrane $[Ca^{2+}]$ during the cardiac action potential. *Circ Res* 90: 182-189, 2002.

330. **Wier WG**. Cytoplasmic Ca^{2+} in mammalian ventricle: dynamic control by cellular processes. *Annu Rev Physiol* 52: 467-485, 1990.

331. **Wilson R, Ainscough R, Anderson K, Baynes C, Berks M, Bonfield J, Burton J, Connell M, Copsey T, Cooper J and .** 2.2 Mb of contiguous nucleotide sequence from chromosome III of C. elegans. *Nature* 368: 32-38, 1994.

332. **Xu W, Denison H, Hale CC, Gatto C and Milanick MA.** Identification of critical positive charges in XIP, the Na/Ca exchange inhibitory peptide. *Arch Biochem Biophys* 341: 273-279, 1997.

333. **Xu W, Gatto C and Milanick MA.** Positive charge modifications alter the ability of XIP to inhibit the plasma membrane calcium pump. *Am J Physiol* 271: C736-C741, 1996.

334. **Yamashita J, Ogata M, Takaoka M and Matsumura Y.** KB-R7943, a selective Na^+/Ca^{2+} exchange inhibitor, protects against ischemic acute renal failure in mice by inhibiting renal endothelin-1 overproduction. *J Cardiovasc Pharmacol* 37: 271-279, 2001.

335. **Yao A, Su Z, Nonaka A, Zubair I, Lu L, Philipson KD, Bridge JH and Barry WH.** Effects of overexpression of the Na^+-Ca^{2+} exchanger on $[Ca^{2+}]_i$ transients in murine ventricular myocytes. *Circ Res* 82: 657-665, 1998.

336. **Zeitz O, Maass AE, Nguyen PV, Hensmann G, Kögler H, Möller K, Hasenfuss G and Janssen PML.** Hydroxyl radical-induced acute diastolic

dysfunction is due to calcium overload via reverse-mode Na^+-Ca^{2+} exchange. *Circ Res* 90: 988-995, 2002.

337. **Zygmunt AC, Goodrow RJ and Weigel CM.** I_{NaCa} and $I_{Cl(Ca)}$ contribute to isoproterenol-induced delayed afterdepolarizations in midmyocardial cells. *Am J Physiol* 275: H1979-H1992, 1998.